Tampere University

JOHANNA HAAVISTO

# Electricity Generation from Industrial Wastewaters in Bioelectrochemical Systems

Tampere University Dissertations 136

Tampere University Dissertations 136

JOHANNA HAAVISTO

# Electricity Generation from Industrial Wastewaters in Bioelectrochemical Systems

ACADEMIC DISSERTATION
To be presented, with the permission of
the Faculty of Engineering and Natural Sciences
of Tampere University,
for public discussion in the Auditorium TB109
of the Tietotalo building, Korkeakoulunkatu 1, Tampere,
on 4 October 2019, at 12 o'clock.

ACADEMIC DISSERTATION
Tampere University, Faculty of Engineering and Natural Sciences
Finland

| | | |
|---|---|---|
| *Responsible supervisor and Custos* | Professor<br>Jaakko Puhakka<br>Tampere University<br>Finland | |
| *Supervisors* | Assistant Professor<br>Marika Kokko<br>Tampere University<br>Finland | Assistant Professor<br>Aino-Maija Lakaniemi<br>Tampere University<br>Finland |
| *Pre-examiners* | Professor<br>Zhen He<br>Virginia Polytechnic Institute and State University<br>United States of America | Professor<br>Marja Tiirola<br>University of Jyväskylä<br>Finland |
| *Opponent* | Associate Professor<br>Federico Aulenta<br>Water Research Institute, National Research Council<br>Italy | |

The originality of this thesis has been checked using the Turnitin OriginalityCheck service.



Cover design: Roihu Inc.

ISBN 978-952-03-1263-3 (print)
ISBN 978-952-03-1264-0 (pdf)
ISSN 2489-9860 (print)
ISSN 2490-0028 (pdf)
http://urn.fi/URN:ISBN:978-952-03-1264-0

PunaMusta Oy – Yliopistopaino Tampere 2019

# PREFACE

This thesis is based on the work carried out at the Faculty of Engineering and Natural Sciences, Tampere University (formerly Laboratory of Chemistry and Bioengineering, Tampere University of Technology), Finland. The experimental work was conducted as a part of Bio-e-MAT -project, which was coordinated by the Academy of Finland (New Indigo ERA-Net Energy 2014; Project no 283013), and the work was finalized with the support of Maa- ja vesitekniikan tuki ry -foundation.

I would like to express my gratitude to my responsible supervisor Professor Jaakko Puhakka for valuable guidance, encouragement and enthusiastic support during my studies. I want to thank my supervisors Assistant Professor Aino-Maija Lakaniemi and Assistant Professor Marika Kokko for their great support in laboratory and writing process, not to mention all the numerous comments on the manuscripts for which they always found time wherever they were. I would also like to thank Dr. Mira Sulonen for the great travelling companion and help in the laboratory. I am grateful to the project partners for guidance and hospitality during my research exchanges in Yildiz Technical University (Istanbul, Turkey) and CSIR-Indian Institute of Chemical Technology (Hyderabad, India). I am grateful to Professor Zhen He and Professor Marja Tiirola for pre-reviewing this thesis and for their valuable comments.

I want to thank my co-workers for all the advices and refreshing lunch conversations, which brought happiness to my days. I would also like to thank the laboratory staff members Antti Nuottajärvi and Tarja Ylikaiste for their priceless help with the laboratory ware and instruments.

Finally, I want to thank my friends, family and relatives for their encouragement and support. Special thanks to my husband Jukka for the patience, support during these years and for sharing the happy everyday moments with me and our son.

# ABSTRACT

Brewing and pulp and paper making are water-intensive industries generating biodegradable wastewaters that need to be treated prior to discharge. These wastewaters are generally treated with conventional activated sludge process, producing good quality effluent. To avoid energy intensive aeration, anaerobic methods are another option for the treatment. In microbial fuel cells (MFCs), electrochemically active microorganisms degrade organic compounds with simultaneous electricity generation. Compared to more traditional methanogenic treatment, MFCs can be operated at lower temperatures and with less concentrated wastewaters.

The aim of this work was to study the applicability of MFCs for treatment and resource recovery from synthetic wastewaters and real brewery and thermomechanical (TMP) wastewaters. Varying wastewater flow rates and compositions are typical for industrial operations, but challenging for biological treatment processes. For this reason, as a preparation to possible process upsets, different start-up methods were studied to accelerate the start-up of bioelectrochemical treatment. In addition, stable operation was optimized by comparing different anode electrode materials and organic loading rates.

The start-up was studied in semi-continuously operated air-cathode and three-chamber MFCs, and process optimization in a continuously fed up-flow MFC. Among studied electrochemical methods, -200 mV vs. Ag/AgCl adjusted anode potential resulted in the highest average power density of 0.65 $Wm^{-3}$ after the start-up in brewery wastewater fed reactors. MFCs inoculated with stored (at +4 or -20 °C) anolyte demonstrated for the first time that power densities recovered after one month storing, but not after six months storing. Granular activated carbon was the most potential anode electrode material among the studied electrode materials. In xylose-fed up-flow MFC, organic loading rates of 0.31 and 0.53 $g_{COD}L^{-1}d^{-1}$ enabled the highest power densities.

This study demonstrates the applicability of brewery and for the first time TMP wastewaters for bioelectrochemical treatment in MFCs. Power densities can likely be further increased by optimizing MFC design and operation. Partial removal of degradable compounds in brewery and TMP wastewater indicated the need for e.g. aerobic post-treatment.

# TIIVISTELMÄ

Olutpanimot sekä sellu- ja paperitehtaat tuottavat suuria määriä jätevesiä, jotka täytyy puhdistaa ennen vesistöön laskemista. Perinteisesti panimo- ja metsäteollisuuden jätevesiä on käsitelty aktiivilieteprosessilla, jolla pystytään saavuttamaan hyvä puhdistustehokkuus. Energiaa kuluttavan ilmastuksen välttämiseksi myös anaerobisia menetelmiä on hyödynnetty näiden jätevesien käsittelyssä. Mikrobipolttokennoissa (MFC) elektrokemiallisesti aktiiviset mikrobit tuottavat hapettamistaan jäteveden orgaanisista yhdisteitä sähköä. Näiden etu perinteisempään biokaasuprosessiin verrattuna on tehokas toiminta myös suhteellisen alhaisissa lämpötiloissa ja laimeiden jätevesien käsittelyssä.

Tämän työn tavoitteena oli tutkia MFC:n soveltuvuutta teollisten jätevesien, kuten panimo- ja sellutehtaan jätevesien, käsittelyyn ja niiden sisältämän kemiallisen energian hyödyntämiseen sähköntuotannossa. Vaihtelut jäteveden koostumuksessa ja virtaamassa ovat tyypillisiä teollisissa prosesseissa ja aiheuttavat haasteita biologiselle jätevedenpuhdistusprosessille. Tämän vuoksi tässä työssä varauduttiin mahdollisiin prosessihäiriöihin tutkimalla erilaisia aloitusmenetelmiä bioelektrokemiallisten käsittelyprosessien käynnistämisen nopeuttamiseksi. Lisäksi puhdistusprosessin toimintaa optimoitiin vertaamalla erilaisia anodielektrodimateriaaleja ja orgaanista kuormitusta.

Aloitusmenetelmiä tutkittiin panostoimisissa ilmakatodi- ja kolmikammioreaktoreissa ja prosessioptimointia jatkuvatoimisessa ylösvirtausreaktorissa. Panimojätevedellä syötetyssä prosessissa suurimpaan tehontiheyteen (0.65 $Wm^{-3}$) aloitusvaiheen jälkeisessä vertailussa päästiin säätämällä aloitusvaiheen anodipotentiaaliksi -200 mV (Ag/AgCl referenssielektrodiin nähden). Säilytyskokeissa osoitettiin ensimmäistä kertaa, että kuukauden anolyytin säilyttämisen jälkeen (+4 tai -20 °C:ssa) tehon tiheys palautui lähes alkuperäisiin arvoihin, mutta kuuden kuukauden säilytyksen jälkeen tehon tiheys oli hyvin alhainen. Tutkituista anodimateriaaleista aktiivihiiligranulat osoittautuivat potentiaalisimmaksi anodielektrodimateriaaliksi. Ksyloosilla syötetyssä ylösvirtausreaktorissa suurimmat tehontiheydet saavutettiin 0.31 ja 0.53 $g_{COD}L^{-1}d^{-1}$ orgaanisilla kuormituksilla.

Tämän työn tulokset osoittavat, että panimo- ja TMP-jätevedet soveltuvat bioelektrokemialliseen käsittelyyn MFC:ssä, mutta jätevesi tarvitsee vielä

jatkokäsittelyn ennen vesistöön laskemista. Keskimääräisiä tehontiheyksiä pystytään todennäköisesti kasvattamaan optimoimalla MFC:n rakennetta ja operointia.

# CONTENTS

## *List of Figures*

## *List of Tables*

# ABBREVIATIONS

| | |
|---|---|
| AD | Anaerobic digestion |
| AEM | Anion exchange membrane |
| BOD | Biological oxygen demand |
| BES | Bioelectrochemical system |
| CE | Coulombic efficiency |
| CEM | Cation exchange membrane |
| COD | Chemical oxygen demand |
| CV | Cyclic voltammetry |
| DF | Dark fermentation |
| DNA | Deoxyribonucleic acid |
| GAC | Granular activated carbon |
| HRT | Hydraulic retention time |
| LSV | Linear sweep voltammetry |
| MFC | Microbial fuel cell |
| OLR | Organic loading rate |
| PBS | Phosphate-buffered saline |
| PCR-DGGE | Polymerase chain reaction denaturation gradient gel electrophoresis |
| PEM | Proton exchange membrane |
| SS | Stainless steel |
| TMP | Thermomechanical pulping |
| VFA | Volatile fatty acid |

# ORIGINAL PUBLICATIONS

Publication I Haavisto, J.M., Kokko, M.E., Lakaniemi A-M., Sulonen, M.L.K. & Puhakka, J.A. The effect of start-up on energy recovery and compositional changes in brewery wastewater in bioelectrochemical systems. Submitted.

Publication II Haavisto, J.M., Lakaniemi, A-M. & Puhakka, J.A. 2019. Storing of exoelectrogenic catholyte for efficient microbial fuel cell recovery. Environmental Technology 40, 11, pp. 1467-1475.

Publication III Haavisto, J.M., Dessì, P., Chatterjee, P., Honkanen, M.H., Noori, M.T., Kokko, M.E., Lakaniemi A-M, Lens, P.N.L., Puhakka, J.A. 2019. Effects of anode materials on electricity production from xylose and treatability of TMP wastewater in an up-flow microbial fuel cell. Chemical Engineering Journal, 372, pp. 141-150.

Publication IV Haavisto, J.M., Kokko, M.E. Lay, C-H. & Puhakka, J.A. 2017. Effect of hydraulic retention time on continuous electricity production from xylose in up-flow microbial fuel cell. International Journal of Hydrogen Energy, 42, pp. 27494-27501.

# AUTHOR'S CONTRIBUTION

Publication I Johanna Haavisto performed the experimental work, wrote the manuscript and is the corresponding author. Mira Sulonen performed microbial community analysis and measured sugar concentrations. Marika Kokko and Aino-Maija Lakaniemi assisted in planning of the experiments and interpretation of the results. All co-authors commented on the manuscript.

Publication II Johanna Haavisto performed the experimental work, wrote the manuscript and is the corresponding author. Aino-Maija Lakaniemi assisted in planning of the experiments and interpretation of the results. All co-authors commented on the manuscript.

Publication III Johanna Haavisto performed the experimental work related to anode material comparison and Paolo Dessí related to thermomechanical pulping wastewater treatment. Paolo Dessí is the corresponding author, but Johanna Haavisto and Paolo Dessí equally contributed to the manuscript. Thus, the first author status in the publication was practically shared. Aino-Maija Lakaniemi, Marika Kokko and Pritha Chatterjee assisted in planning of the experiments and interpretation of the results. Mari Honkanen performed SEM analyses and assisted in the interpretation of the SEM results. Md Tabish Noori assisted in interpretation of the EIS results. All co-authors commented on the manuscript.

Publication IV Johanna Haavisto performed the experimental work, wrote the manuscript and is the corresponding author. Chyi-How Lay designed and constructed the reactor. Marika Kokko assisted in planning of the experiments and interpretation of the results. All co-authors commented on the manuscript.

# 1 INTRODUCTION

Due to the scarcity of fresh water sources on a global level, efficient wastewater treatment is of importance to protect environment and secure the availability of safe water for human and animal consumption and recreational purposes. Many industries, such as brewing and pulping processes are highly water-intensive. Brewing industry produces on average 5.5 L of wastewater per 1 L of produced beer [1] and pulping and papermaking processes e.g. in Europe 9.4-156 L per 1 kg of pulp (9.4-20 L per 1 kg of mechanical pulp) [2]. With worldwide annual production of 180 Mt of beer (in 2014) and almost 180 Mt of pulp (from which 25 Mt was from mechanical pulping in 2017), breweries produced close to 1000 $Mm^3$ of wastewater, pulp and paper processes even more, and mechanical pulping approximately 200-500 $Mm^3$ [1–3].

Today these wastewaters are typically treated with activated sludge processes or anaerobically in a methanogenic wastewater treatment process [4,5]. Traditional activated sludge wastewater treatment removes efficiently (up to 98% from brewery wastewater) chemical oxygen demand (COD) and nutrients [5]. However, the drawbacks of the process are high energy demand due to aeration (0.24-0.38 $kWhkg^{-1}COD^{-1}$ being 43-60% of the total energy consumption of the wastewater treatment plant according to [6]) and generation of high volumes of excess sludge (0.22-0.37 $g_{volatile\ suspended\ solids}$ per $g_{removed\ COD}$), which needs further treatment [6]. Methanogenic wastewater treatment does not require energy for aeration, but temperatures over 30 °C and concentrated wastewaters (due to slow growth rate of methanogens) are needed for optimal performance [7].

The COD concentrations of brewery wastewater vary typically between 2000 and 6000 $mgL^{-1}$, while in pulping processes the concentrations can vary between 500 and 115,000 $mgL^{-1}$ [4,5]. Most of the COD load in brewery wastewater originates from mash and yeast surplus, and in mechanical pulping wastewater from wood fragments from the chip washing and fibre from the fibre line [2,8]. Methanogens of anaerobic wastewater treatment process are sensitive to pH variations and toxic compounds in wastewater [9]. High concentration of washing chemicals from the tank and bottle washing can cause challenges to methanogenic wastewater treatment of brewery

wastewaters [8]. Pulping wastewaters contain wood based antimicrobial compounds, recalcitrant lignin derivatives and potentially toxic compounds from chemical pulping process, which all are known to be detrimental to methanogens [4,10].

In addition to anaerobic methane production, some early studies have been conducted for hydrogen production using dark fermentation from brewery and pulping wastewaters [11,12]. Electricity production with microbial fuel cells (MFCs) is another anaerobic biological treatment method for brewery and pulping wastewaters. Compared to methanogenic wastewater treatment, MFCs can be operated at lower temperatures, are able to treat wastewaters with lower COD concentration, and are more tolerant to toxic compounds present in many wastewaters [13,14]. However, decreased material costs are required to make wastewater treatment in MFCs feasible [15].

So far, wastewater treatment in MFCs has been studied in laboratory and pilot-scale. These studies have shown that MFCs can be operated with significantly smaller energy consumption compared to activated sludge processes, and the bioelectricity production can be sufficient for covering the energy needed for pumping [13,16]. MFCs can also be installed as a part of operating wastewater treatment processes to decrease energy consumption and excess sludge volumes [14]. Most of the results have been obtained in laboratory-scale with reactor volumes varying from milliliters to liters. These small MFCs are useful for studying reactor materials and microbial behavior [17–19]. They are also easy to operate and the internal resistances are small due to the small distances between anode and cathode electrodes [20]. For practical applications, MFC operation needs optimization to enable high power densities also in larger scale [21].

In this work, anode electrode materials were compared in respect to electricity production and scalability of the electrode materials. Also organic loading rate (OLR), as an important parameter affecting electricity generation and wastewater treatment, was studied here by changing hydraulic retention time and analyzing microbial communities of the anolyte at different OLRs. Biological industrial wastewater treatment is challenging due to the varying wastewater flow rate and composition [8]. For this reason, this work also focused on different start-up strategies to enable rapid start-up and recovery of the process after possible process upsets. This is the first study to demonstrate the recovery of electrochemical activity of the microbial community in a MFC after storing anolyte at +4 or -20 °C for one month. Also bioelectrochemical treatment of thermomechanical (TMP) pulping wastewater was studied for the first time in a MFC.

# 2 BACKGROUND

## 2.1 Microbial fuel cells in industrial wastewater management

MFCs treat wastewaters, such as brewery wastewater and forest industry wastewaters, by degrading the organic compounds present in the wastewater with the help of anaerobic microorganisms simultaneously producing electrical current. In MFCs, electrochemically active bacteria transfer electrons from the oxidized substrates outside the cell membrane to a solid anode electrode while ions from the same degraded compounds are released to the surrounding solution [22]. The anode electrode is connected through an external resistance to a cathode electrode, where the electrons and ions from the oxidized compounds react with terminal electron acceptor (Figure 1).

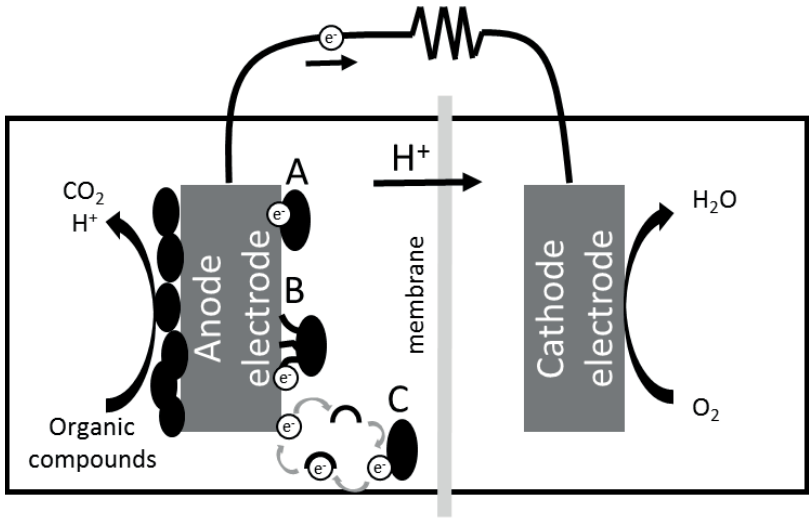


**Figure 1.** Schematic diagram of a membrane separated two-chamber microbial fuel cell with anode chamber on the left and cathode chamber on the right. In the anode chamber, microorganisms degrade organic compounds and transfer the electrons to a solid anode electrode with A) direct electron transfer via cytochromes, B) electron transfer via pilus, or C) via mediators. Electrons are transferred to cathode electrode through a resistor and the $H^+$ ions through the membrane. On the cathode electrode, the electrons and $H^+$ ions react with terminal electron acceptor (e.g. with $O_2$ to form water).

MFCs are electricity producing bioelectrochemical systems (BESs) [23]. In other BESs, the chemical energy from degraded compounds together with a small additional voltage can be used for producing e.g. hydrogen or other chemicals at the cathode [23]. All the BES types rely on the electrochemically active microorganisms capable of delivering electrons to the anode electrode or accepting electrons from the cathode electrode (in case of microbial electrosynthesis) [23]. These bacteria can form a biofilm on the electrode, or they can grow as a suspension [24,25]. From cell suspension, the electrons can be transferred to the electrode via mediators (compounds secreted by bacteria or added to the solution), such as neutral red, anthraquinone-2,6-disulfonate, and methylene blue [26,27]. In the biofilm, microorganisms can utilize cytochromes on the cell membrane or conductive pili for direct electron transfer (Figure 1). For example, a well-known electrochemically active species *Geobacter sulfurreducens* is often found from MFC biofilms, and is capable to transfer electrons efficiently both via cytochromes and conductive pili [24]. *Pseudomonas* sp. on the other hand is able to secrete mediators such as pyocyanin and pyoveridine for mediated electron transfer [25].

Mixed cultures consisting of several different microorganisms are favored for wastewater treatment to degrade diverse and often complex wastewater constituents and to avoid costs related to aseptic conditions required for pure culture operation [28]. Also the anodic biofilm is favored over the growth of suspended electrochemically active bacteria due to more efficient electron transfer mechanisms (via cytochromes or conductive pili) [29]. Some wastewaters, such as municipal wastewater, are rich sources of microorganisms capable of degrading the compounds in that specific wastewater, but also other sources of microorganisms can be used for starting up a new MFC including anaerobic digester sludge [9,30,31], rumen contents [32], sediments [32], and activated sludge [31]. If available, the use of an enrichment culture from a MFC with similar operating conditions and treating similar wastewater, is considered as the fastest method for starting up a new MFC [33].

Biological treatment of industrial wastewaters may suffer from changes in wastewater flow and composition. Brewing as batch process produces the highest wastewater organic loads at tank emptying and washing [34]. Pulping as continuous process produces more constant wastewater flow and composition, but occasional shutdowns and following start-ups cause fluctuation in wastewater flow [2]. These changes appear in treatment plant as cuts in wastewater flow (if wastewater is not stored in a large reservoir before feeding to the treatment process), overloads, and increased concentrations of washing detergents, which may damage the microbial

communities. To recover efficient wastewater treatment and electricity generation rapidly after severe disturbances without active enrichment culture, efficient start-up methods, or affordable storing methods for the electrochemically active community are needed to enrich new inoculum, or to start-up the system fast and efficiently with stored inoculum, respectively [25].

Enrichment of efficient, electricity producing, microbial culture can be enhanced e.g. by optimizing OLR (changing hydraulic retention time or diluting wastewater) and other operational parameters (temperature, pH, external resistance etc.), and by choosing reactor materials and configuration to promote biofilm formation on anode electrode and minimize losses in electricity production [25] (discussed in more detail in Sections 2.3.1-2.3.3). Also suppressing methanogenesis by e.g. starvation [35], inducing oxygen stress [9], or by adding 2-bromomethanesulfonate [9] have shown to support the enrichment of electrochemically active bacteria (for a review, see [36]). At the MFC start-up, enrichment can be speeded up with electrochemical methods including adjusted anode potential and different external resistances. However, the results of different research groups with different substrates and sources of microbial cultures are contradictory showing no consensus whether low or high external resistances or the more positive or more negative adjusted anode potentials speed-up electricity production the most [18,33,36–40].

## 2.2 Biological wastewater degradation in MFCs

In wastewater treating MFCs, various biological and (electro)chemical reactions take place in the degradation of complex substrates, such as cellulose. Some of the reactions (marked as green in Figure 2) increase the current production, while the others (marked as red) compete with electricity generating microorganisms for the substrate. These competing organisms include methanogens, denitrifiers and sulfate reducers [28].

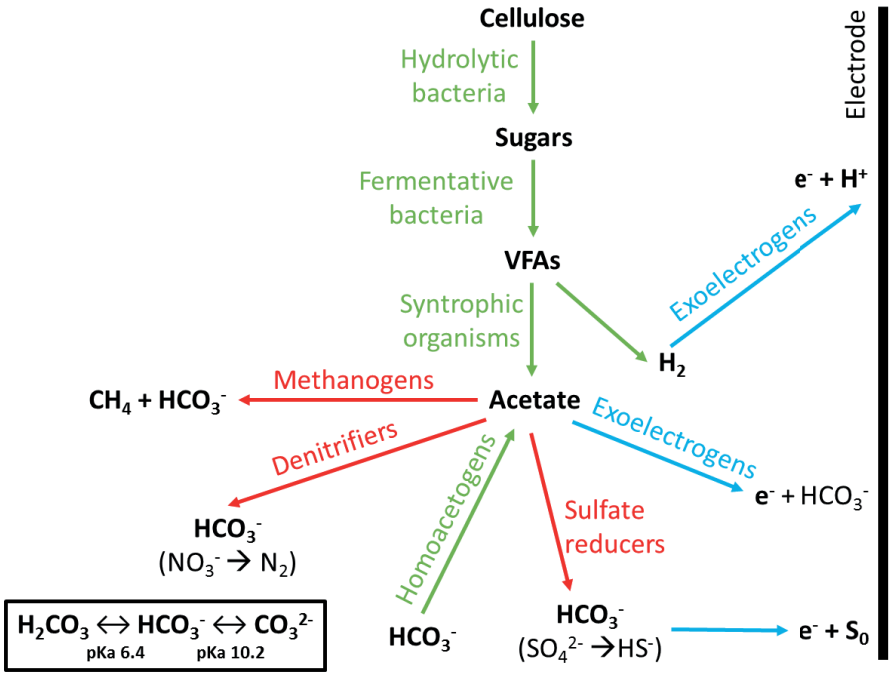


**Figure 2.** Anaerobic cellulose degradation by microorganisms present in a wastewater treating MFC. Green lines represent the reactions that can increase the electricity production by electrochemically active organisms (blue lines) and the red lines represent the competing reactions. Sulfides can be electrochemically oxidized to solid sulfur on electrode surface. The form of bicarbonate ($HCO_3^-$) depends on pH as shown in the figure. (modified from [28])

Syntrophic interactions of different organisms are needed for anaerobic degradation of complex wastewater compounds. The degradation of cellulose, hemicellulose, fats and proteins starts with hydrolysis by hydrolytic microorganisms (Figure 2). These bacteria degrade the polymeric compounds to monomeric sugars, fatty acids and amino acids. Hydrolysis is followed by fermentation to further metabolize the substrates into volatile fatty acids (VFAs), alcohols, $H_2$, and $CO_2$. Electrochemically active bacteria are able to utilize simple sugars, VFAs, and alcohols as substrate for electricity production [28]. For example, the well-known electrochemically active *Geobacter sulfurreducens* utilizes acetate and *Klebsiella* sp. glucose [24,41]. In addition to syntrophic interactions in degradation of complex polymeric compounds, some microorganisms are of assistance by maintaining optimal conditions for the others. For example, the oxygen consumption by facultative aerobic organisms is important in the reactor designs allowing oxygen penetration to anode, as these microorganisms help to maintain aerobic conditions [42]. These microorganisms

help to maintain anaerobic conditions at the anode. However, facultative aerobic organisms also compete with electricity production from the substrate decreasing the efficiency in which the chemical energy of the substrate is converted to electrical current also known as Coulombic efficiency (CE).

Methanogens metabolize acetate or $H_2$ and $CO_2$ to methane directing acetate away from electricity generation [43]. If nitrate is available, also denitrifiers decrease electricity generation by consuming acetate [28]. However, in absence of nitrate, denitrifiers, such as *Comamonas denitrificans*, can act as electrochemically active bacteria utilizing anode electrode as electron acceptor [44]. In the presence of sulfate, sulfate reducers can decrease electricity generation by consuming organics when reducing sulfate to sulfide [28]. Sulfide may be toxic to electrochemically active bacteria, but electrochemical oxidation of sulfide to elemental sulfur on the anode electrode generates current [45]. Sulfate reducing organisms contain also electrochemically active species such as *Desulfuromonas acetoxidans* [26]. Also the effect of homoacetogens, which metabolize $H_2$ and carbon dioxide to acetate, on electricity generation in a MFC is complicated [28]. The $H_2$ consumption by homoacetogens competes with electricity generation, but the produced acetate can be directed to electricity generation [46].

## 2.3 Reactor types

Several different reactor designs have been studied for electricity production in MFCs, but many of these systems have been designed for laboratory use only [22]. As the reactor design is one of the major issues in up-scaling of MFCs, effort has been invested increasingly on designing up-scalable reactors with low material costs.

The simplest laboratory scale reactors can be built by connecting two bottles with a salt bridge and electrical wires from electrodes through a resistance [47]. However, the internal resistance with this system is very high (almost 20000 Ω according to Min et al. [47]), and can be decreased to below 1300 Ω by changing the salt bridge to a tube connecting the anolyte and catholyte through a membrane (e.g. cation exchange membrane), which decreases the diffusion of substrate to cathode and oxygen to anode (Figure 3A) [47]. These simple reactors are called H-type MFCs [22]. As easily autoclavable systems, they are especially suitable for pure culture studies (Table 1) [48].

To further decrease the internal resistance, the membrane area can be increased and the electrodes brought closer to each other in cubic shaped MFCs [48] (Figure

3B). Also these reactors are very simple in structure, but varying the shape of the chambers brings different advantages. E.g. in flow-through MFCs, the reactors have high width to height ratio and horzontal liquid flow can be directed from one end to the other, while the chambers form flow channels to increase proton transfer from anode to cathode [49]. The liquid flow can also be directed upwards to enhance the mixing of anolyte without clogging the outlet tube with descending biomass, and the anode chamber can be positioned between two cathode chambers to increase membrane and cathode electrode area [30]. The cubic configuration also enables tight packing of reactors. Especially flat versions of the reactors (called flat plates) provide high membrane and electrode areas, short distance between the electrodes, and high packing density [50]. For these reasons flat plates are often used as stacks to combine several MFCs in a small space (Figure 4A).

Tubular MFC configurations also provide short distances between cylinder-shaped anode electrodes and cathodes. In these nested configurations, electrodes are separated with a membrane (or other separator material) [51] and the cathodes can be wrapped around the anode chamber [52] (Figure 3C), or the anode chamber can be placed around the cathode chamber [53]. Tubular reactors can be operated vertically with additional up-flow anolyte circulation, i.e. up-flow reactors or down-flow circulation as Lu et al. operated [51,54]. Horizontally arranged tubular reactors are easy to connect one after another [15,52] (Figure 4B). The advantages and disadvantages of the example laboratory-scale MFC designs are summarized in Table 1.

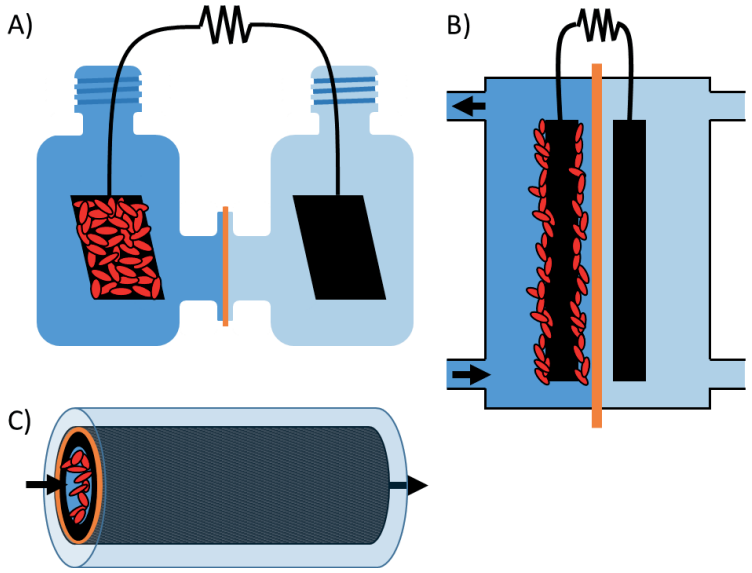


**Figure 3.** Schematic diagrams of widely used simple MFC designs: A) membrane separated H-type MFC, B) cubic MFC enabling continuous anolyte flow, and C) continuous flow tubular MFC where a membrane is pressed between the inner anode electrode and outer cathode electrode. Electrodes are shown in black or grey, membranes in orange, and bacteria in red.

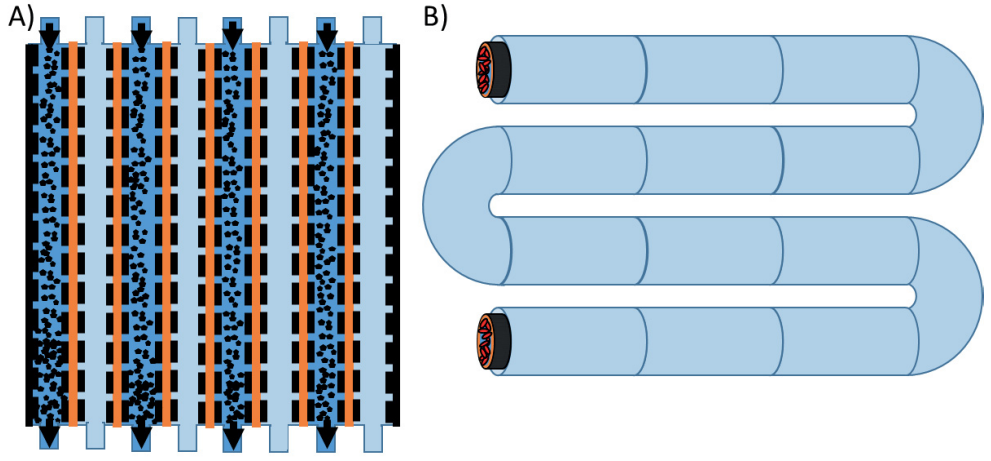


**Figure 4.** Examples of two complex reactor designs: A) stacked flat-plate MFCs with granular anode and metal nets as current collectors (both on anode and cathode), and B) tubular cascade (numerous MFCs placed one after another) where a membrane is pressed between the inner anode electrode and outer cathode electrode. In A) microbes (not shown) grow on granular anode material.

**Table 1.** Examples of MFC designs for laboratory-scale studies and their advantages and disadvantages.

| MFC types | | Advantages | Disadvantages | Reference |
|---|---|---|---|---|
| **H-type** | Simple | Autoclavable | Not for continuous operation, high resistance due to small membrane area and long distances between electrodes, only for laboratory scale studies | [47] |
| **Cubic** | Simple: long, high, flat[a] | Good mass transfer, gas accumulation prevented in up-flow mode, high surface area per volume in flat design | High construction costs | [49,55] |
| | Complex: stacked | Up-scalable, increased voltage or current with series or parallel connection | High construction costs, polarity reversal | [56] |
| **Tubular** | Simple: horizontal or vertical[b] | Suitable for continuous operation, simple to construct and operate, enable small internal resistance | | [57,58] |
| | Complex: cascade | Easy to connect many reactors, minimal pumping is needed, increased voltage or current with series or parallel connection | High construction costs, polarity reversal | [52,59] |

[a]Long, high and flat represent MFC shapes, from which long reactors are operated horizontally, high vertically and flat MFCs have the largest membrane area compared reactor volume; [b]Anolyte flow through the tubular MFC horizontally or vertically

To avoid the need for catholyte (e.g. in the previously mentioned MFC types), the cathode electrode can be superimposed over the membrane with other side of the electrode facing to air to construct an air-cathode MFC. Air-cathodes can be connected to many reactor configurations (including H-type, cubic and tubular MFCs) [13,52,60]. Single-chambered air-cathode MFCs are simple, but CE and power production may suffer from the oxygen penetration to the anode [55]. Also the reaction rates at air-cathode are limiting the power density without catalysts (such as platinum) on the cathode electrode [61].

MFCs compete with aerobic wastewater treatment processes and methane generating anaerobic treatment systems. Feasibility of the MFC technology for wastewater treatment requires efforts to minimize material costs and improving the power production coupled to high COD removal. From reactor materials, the membranes have the highest costs [15]. For this reason, Hiegemann et al. [14] studied membraneless MFC designs. However, in addition to increased oxygen diffusion to

anode electrode in air-cathode systems, also very short distance between the electrodes in membraneless designs may cause electrode contact and short circuiting [62]. Most wastewaters have low conductivity, which decreases the power density especially when anode and cathode electrodes cannot be placed very close to each other (e.g. in membraneless design due to the oxygen diffusion to anode) [62,63]. Reactor design can make use of thin, moldable electrode designs to place the electrodes close to each other, numerous electrodes to decrease the internal resistance compared to large electrode with lower anode electrode conductivity, or capacitive granular electrode material, which can be fluidized to provide short distance for ion transfer to cathode [64,65].

### 2.3.1 Anode materials

Anode electrodes provide a solid support for the growth of electrochemically active bacteria. For this reason, biocompatibility is one of the most important selection criteria for the anode electrode material. Carbon based electrode materials listed in Table 2 are all considered as biocompatible [66]. Also most of the metals studied as anode electrode materials have acceptable biocompatibility, whilst e.g. copper oxidizes easily and forms toxic oxides and therefore has to be coated to prevent the oxidation [67]. High specific surface area supports microbial growth and electron accumulation (double layer capacitance) [66,68]. However, to provide more area for microbial growth, the electrode surface needs to be accessible for bacteria with a diameter range of micrometers (e.g. *G. sulfurreducens* ~ 0.5 μm wide and ~2 μm long [69]) [70]. For example, in an activated carbon granule, 80% of the total pore volume are micropores (< 2nm width), which are too small for microbial growth, but support electron accumulation [68]. Due to the electron accumulation, activated carbon granules are capacitive enabling their utilization in MFC applications where granules occasionally collide with a separate current collector e.g. graphite plate [64,68]. These separate highly conductive current collectors may be needed to decrease internal resistances in the applications where the selected electrode material is not highly conductive (e.g. stainless steel frame with multiple cathode sheets), or if the granular anode material is fluidized [64,65]. Also conductivity and the shape of the electrode are important electrode material selection criteria to enable efficient electron transfer

especially in large anode electrodes and to enable short distances between anode and cathode electrodes in various reactor designs [66].

**Table 2.** Typical anode electrode materials and their surface areas and conductivities. Surface areas are given as appropriate to material (per projected area, volume or mass).

| Two dimensional electrodes | Surface area ($m^2cm^{-2}$) | ($m^2g^{-1}$) | Conductivity ($Sm^{-1}$) | Reference |
|---|---|---|---|---|
| Graphite plate | 0.6 | | | [71] |
| | | | $2\text{-}3\times10^5$ | [72] |
| Carbon paper | | 0.9 | 19000 | [73] |
| Carbon cloth | | 0.11 | 333 | [74] |
| | | 2.39 | | [75] |
| | | 13.89 | | [76] |
| Titanium | | | $2.38\times10^6$ | [72] |
| **Three dimensional electrodes** | **Surface area ($m^2cm^{-3}$)** | **($m^2g^{-1}$)** | **Conductivity ($Sm^{-1}$)** | **Reference** |
| Graphite felt | | 0.33 | | [77] |
| | | 1.565 | | [78] |
| | | 2.73 ± 0.05 | | [79] |
| | 0.022–0.023 | 1.1 | 370 | [80] |
| Reticulated vitreous carbon | 0.0038 | | | [70] |
| | | | 400–1200 | [81] |
| Carbon brush | 0.018[a] | | | [82] |
| | | 7.11[b] | | [83] |
| Graphite brush | 0.0054[a] | | | [84] |
| | 0.0072-0.018[a] | | | [48] |
| Activated carbon granules | | 843 | 750 | [74] |
| | 940 | 885 | | [68] |
| Graphite granules | 0.934 | 0.438 | NA | [68] |

[a]Carbon or graphite surface area per brush volume; [b]Carbon fiber specific area; NA not available

From the listed electrode materials (Table 2), titanium as metal has the highest conductivity, but low surface area without special treatments. Graphite based materials have higher conductivity than carbon materials and both materials are often used as anode electrodes [21,66]. Brush electrodes have coiled metal core and carbon or graphite threads provide a solid support for microbial growth [48]. The conductivity of carbon and graphite brush anodes depend on the length (metal as current collector) and the diameter (carbon or graphite fibers as current collector) of the brush.

Comparison of the specific surface areas of the listed anode materials is challenging due to their different structure (two- or three-dimensional). Metals and glassy carbon have small surface areas compared to geometrical surface area. However, the specific surface area can be increased by roughening [49]. From flat electrode materials, carbon cloth has higher surface area than carbon paper according to Zhou et al. and Sakai et al., but Karra et al. measured smaller surface area for carbon cloth [73–75]. To further increase the surface area of an anode electrode, different three-dimensional electrodes, such as felts, foams and brushes have been designed. Reticulated vitrous carbon is a carbon foam with open structure [81]. Due to the glassy carbon as material, the specific area is lower compared to other three-dimensional electrodes, but the open structure of the foam supports mass transport and biofilm formation [70]. Graphite felt has higher specific surface area ($m^2m^{-3}$) than brush electrodes (Table 2) due to more open space at the outer edge in the brush electrodes. Activated carbon has the highest specific surface area among the listed anode materials.

The shape of brush electrode is very suitable for applications, where small amounts of oxygen diffuses to anolyte, because the oxygen can be consumed in the outer edges of the cylindrical brush before entering to the center of the brush [62]. Foldable materials, such as graphite felt, are often used as folded to cylinder in tubular MFCs and plates in cubic MFCs [49,52]. In addition to the listed anode materials, also different nanomaterials have been studied in small scale reactors (for a review see [85]), but are not discussed here.

### 2.3.2 Cathode materials for oxygen reduction

In MFCs, the electrons and ions from substrate oxidation react with terminal electron acceptor on cathode electrode. As widely available compound, oxygen is considered as the most sustainable terminal electron acceptor in MFCs, but due to the high mass transfer efficiency, also soluble ferricyanide has been widely used as terminal electron acceptor in laboratory-scale MFCs [86,87]. Oxygen reduction rate at the cathode is often the limiting reaction in electricity generating MFCs [86]. To increase reaction rate, cathode electrodes can be coated with a catalyst, such as platinum [88]. However, due to the high costs and potential deactivation problems of platinum, more affordable solutions for increasing reaction rate have been studied for wastewater treatment [88]. Among carbonaceous catalysts, higher reaction rates were measured with activated carbon compared to carbon black possibly due to the

higher surface area [89]. Platinum group free catalysts, such as Mn, Fe, Co and Ni with aminoantipyrine precursor have shown higher reaction rates compared to activated carbon [90].

Most anode electrode materials listed in Table 2 can be used as cathode electrode as well. Different types of cathode electrodes can be constructed from e.g. carbon cloth, stainless steel, carbon felt, Ni-based paint and graphite [52,54,89,91]. For example in tubular air-cathode MFCs, catalyst containing Ni-based paint can be painted on a waterproof separator as cathode-separator assembly [52]. Also carbon cloth is suitable for air-cathodes and in laboratory scale two chamber systems, graphite plates can be used as cathode [14,54]. To increase the conductivity, stainless steel mesh can be added as current collector [65].

### 2.3.3 Separators

To increase electricity generation, oxygen diffusion to anode can be suppressed with a selective membrane between anode and cathode [92]. These selective membranes have the highest permittivity to ions ($H^+$ with proton and other cation exchange membranes, or anions such as $OH^-$ with anion exchange membrane) [93,94]. However, even the selective membranes cannot totally prevent oxygen penetration through membrane [55,95]. Another problem with the ion selective membranes is transportation of other ions than $H^+$ or $OH^-$ causing anolyte acidification and catholyte alkalinity and the increased Ohmic resistance caused by hindered ion transport especially when treating wastewaters with low conductivity [93,94]. For ion transportation through membrane, the ions with the highest concentration are favored. Although the permittivity of proton exchange membrane to $H^+$ is higher compared to other ions, the ions with significantly higher concentrations compete with $H^+$ transport [93]. E.g. in buffered solutions, the concentration of the added salt are usually higher than 1 mM, being several orders higher than the concentration of $H^+$ ($10^{-7}$ M at pH 7) [93].

Proton exchange membranes have been used in laboratory scale studies, but they are too expensive for wastewater treatment [55,92,96]. Another selective membrane for proton and other positive ion transportation is a cation exchange membrane (CEM), which is also extensively used in laboratory scale studies [35,91,97]. With CEM, the electricity generation may be decreased due to the anolyte acidification resulting from cation accumulation ($H^+$, $Na^+$, $K^+$, $Ca^{2+}$, $Mg^{2+}$ and $NH_4^+$) on anolyte

[95,98]. Anion exchange membranes (AEM) selectively pass anions from cathode side to anolyte decreasing anolyte acidification caused by cation accumulation (for a review, see Leong et al. [95]). However, all of these membranes are costly for wastewater treatment and need frequent cleaning or replacement to maintain the ion flow rate.

Membrane costs can be over 60% of the MFC total material costs [15]. For this reason, more economical options have been studied for wastewater treatment. In membraneless designs, oxygen (which is the terminal electron acceptor) can penetrate to anode decreasing CE and power density. Another option is to use low-cost materials as separator, such as Gore-Tex (polytetrafluoroethylene), Rhinohide, or polyvinylidene fluoride, although some oxygen can also diffuse through these materials. [52,91,99]. Also nanofiltration membrane has been studied by Ly et al., who reported higher proton permeability and lower oxygen penetration with nanofiltration membrane compared to a PEM (Nafion 117) [51].

To increase the cathodic reaction rates, membranes and cathodes can be coupled as membrane-cathode assemblies (or cloth-cathode assemblies) by e.g. hot-pressing with a conductive paint containing a catalyst [91]. Depending on the reactor configuration, the membrane-cathode assembly can be flat or e.g. tubular [13,52].

## 2.4 Energy yields and treatment performances

### 2.4.1 Brewery wastewater treatment in MFCs

The efficiency of wastewater treatment in MFCs is evaluated by electricity generation (power density and CE) and COD removal efficiency. For efficient electricity generation, the presence of electrochemically active microorganisms is crucial.

The highest power density reported with a brewery wastewater has been 24 $Wm^{-3}$ (Table 3). This was obtained at the highest OLR (17 $g_{COD}L^{-1}d^{-1}$) used among the reported brewery wastewater MFC studies [100]. The obtained power density was encouraging for bioelectrochemical treatment of brewery wastewater, but due to the low COD removal of 21%, further optimization is required for MFCs to be used as a part of wastewater treatment process [100].

Low OLR allows more time for efficient COD removal [51]. However, lower substrate concentrations are present at low OLR resulting in lower power densities.

For example, among the continuously operated MFCs in Table 3, Lu et al. reported the highest COD removal of 94.5% at the lowest OLR of 0.31 $g_{COD}L^{-1}d^{-1}$ with a low power density of 0.44 $Wm^{-3}$ [51].

Even though, the highest power density in Table 3 was reported at the highest OLR, high OLR may lead to low CE. At very low OLR, the growth of methanogenes is suppressed, which can be used as microbial selection pressure to increase the share of influent electrons used for electricity generation (i.e. CE) [35]. With brewery wastewater, the CEs have varied between 5.5 and 28% with OLRs < 1 $g_{COD}L^{-1}d^{-1}$ (Table 3). High max. power densities can be obtained also at lower OLRs in fed-batch operated MFCs due to the high variation in COD concentrations in time. For this reason, the studies in Table 3 have been divided in continuous and fed-batch operated experiments.

Also other operational parameters than OLR affect the electricity generation and COD removal, such as operation temperatures and wastewater buffering. The operation temperatures of MFC studies focusing on brewery wastewater treatment have varied between 20 and 30 °C. According to Feng et al. [63], higher power densities can be obtained at 30 °C compared to 20 °C due to increased cathodic performance. Also microbial growth rates and enzyme activity generally increase with temperature [101]. Most of the MFCs were fed with untreated or diluted brewery wastewater in Table 3. However, according to Wen et al. [100], PBS buffering increases COD removal and electricity generation by 14% and 48%, respectively (results of Wen et al. [100] in Table 3 shown for non-buffered wastewater). The PBS buffering stabilized pH and decreased Ohmic resistance 26% by increasing the wastewater conductivity [100].

**Table 3.** Brewery wastewater treatment in microbial fuel cells. The studies have been organized according to obtained max. power density in continuous and fed-batch experiments. The bars visualize the differences in max. power density (blue), COD removal (yellow), coulombic efficiency (red), and organic loading rate (green) between the studies.

| Continuous reactor types | Max power density ($Wm^{-3}$) | COD removal (%) | CE (%) | OLR ($g_{COD}L^{-1}d^{-1}$) | Energy yield ($Whkg_{COD}^{-1}$) | Conductivity ($mScm^{-1}$) | Ref. |
|---|---|---|---|---|---|---|---|
| Single-chamber | 24 | 21 | 2.6 | 17 | 160 | NA | [100] |
| Single-chamber | 9.5 | 43 | 10 | 7.1 | 75 | NA[a] | [102] |
| Serpentine-type | 4.1 | 87 | 6.3 | 1.1 | 110 | NA | [52] |
| Sequential anode-cathode two-chamber | 0.83 | 94 | NA | 4.3 | 5.0 | NA | [103] |
| Rectangular reactor with numerous electrodes | 0.60 | 88 | 8 | 0.55 | 30 | 0.6-2.3 | [16] |
| Stirred microbial electrochemical reactor | 0.44 | 75 | 1.5 | 7.4 | 2 | 3.2 | [104] |
| Tubular two-chamber | 0.44 | 95 | 5.5 | 0.31 | 36 | 2.4[a] | [51] |
| Tubular two-chamber | 0.42 | 76 | 7.5 | 0.39 | 34 | 2.4[a] | [51] |
| Two-chamber | 0.22 | 82 | 2.5 | 4.5 | 1.5 | NA | [105] |
| **Fed-batch reactor types** | **Max power density ($Wm^{-3}$)** | **COD removal (%)** | **CE (%)** | **OLR ($g_{COD}L^{-1}d^{-1}$)** | **Energy yield ($Whkg_{COD}^{-1}$)** | **Conductivity ($mScm^{-1}$)** | **Ref.** |
| Single-chamber up-flow | 18 | 70 | 27 | 1.5 | 400 | NA | [106] |
| Tubular single-chamber | 11 | 93 | 28 | 0.14-0.21 | NA | 6.0[a] | [91] |
| Single-chamber | 5.1 | 87 | 10 | NA | NA | 3.2 | [63] |
| Single-chamber | 4.3 | 85 | 8.9 | NA | NA | 3.2 | [63] |
| Two-chamber | 3.8 | 80 | NA | 1.0 | 110 | NA[a] | [107] |
| Single-chamber | 0.29 | 93 | 2.5 | NA | NA | 4.4 | [108] |

[a]Conductivity was increased e.g. with PBS, $NaHCO_3$ or NaCl; NA not available

### 2.4.2 Pulp and paper wastewater treatment

The reported COD removal rates of pulp and paper wastewater fed MFCs (≤0.52 $g_{COD}L^{-1}d^{-1}$ according to Table 4) have been significantly lower compared to brewery wastewater fed MFCs (0.29 – 5.6 $g_{COD}L^{-1}d^{-1}$ according to Table 3). Also electricity generation with 0.04-5.9 $Wm^{-3}$ power densities and COD removals of 26-78% were

lower compared to brewery wastewater treating MFCs with 0.22-24 $Wm^{-3}$ and 21-95%, respectively (Tables 3 and 4).

Pulp and paper wastewaters are characterized by low conductivity (~0.8 mS/cm Table 4), which decreases power production [84]. For this reason, the addition of PBS has been studied to increase electricity generation and COD removal [82,84]. According to Huang et al. [82], the PBS addition more than doubled the max power density. This is higher increase compared to the 48% reported with brewery wastewaters [100]. The results in Table 4 were reported at room temperature or at 22-26 °C.

**Table 4.** Pulp and paper wastewater treatment in microbial fuel cells. The studies have been organized according to obtained max. power density. The bars visualize the differences in max. power density (blue), COD removal (yellow), coulombic efficiency (red), and organic loading rate (green) between the studies

| Reactor type | Max. power density ($Wm^{-3}$) | COD removal (%) | CE (%) | OLR ($g_{COD}L^{-1}d^{-1}$) | Energy yield ($Whkg_{COD}^{-1}$) | Conductivity ($mScm^{-1}$) | Ref. |
|---|---|---|---|---|---|---|---|
| Single-chamber (continuous) | 5.9 | 26 | 21 | 2 | 270 | 0.8 | [82] |
| Single-chamber (continuous) | 2.8 | 41 | 39 | 0.5 | 330 | 0.8 | [82] |
| Single-chamber (fed-batch) | 2.67 | 78 | 26 | 0.24 | 340 | 1.39 | [109] |
| Single-chamber (fed-batch)[a] | 0.68 | 76 | 16 | 0.03 | 720 | 5.9 | [84] |
| Single-chamber (fed-batch) | 0.19 | 29 | NA | 0.03 | 540 | 0.8 | [84] |
| Single-chamber (fed-batch) | 0.04 | 59 | NA | 1.5 | 1 | NA | [110] |

[a]Conductivity was increased with 50 mM PBS; NA not available

As Tables 3 and 4 show, the optimal power density, COD removal and CE have not been obtained at the same time during the bioelectrochemical treatment of brewery or pulp and paper wastewater. Therefore, the operator needs to choose whether the aim is to obtain high power densities or high COD removal.

## 2.5 Scaling up of bioelectrochemical wastewater treatment

Most of the MFC studies with industrial wastewaters have been conducted in small MFCs (anodic liquid volume ≤ 90 L for brewery (Figure 5) and ≤0.5 L for pulp and paper wastewater [110]). However, according to Logan, also 1 $m^3$ pilot-scale study has been conducted in Queensland, Australia with brewery wastewater fed to 12

vertical MFC modules (each 3 m high) equipped with carbon brush anodes and graphite brush cathodes (results not available) [111].

In real wastewater treatment applications, the high volumes of the wastewater require the use of large-scale MFCs or numerous MFCs combined as a stack or a cascade. For example, Zhuang et al. and Hiegemann et al. connected several MFC units in cascade or parallel [14,52]. MFC stacks have also been successfully operated by Ieropoulos et al. for human urine treatment by connecting 432 MFCs to achieve 300 L total volume, but the high number of small reactors increases the material costs compared to MFCs with high reactor net volumes (liquid volume in the anode chamber) [112]. On the other hand, the wastewater treatment in MFCs with high reactor net volumes is challenging due to decreased volumetric power densities [13,111]. In air-cathode MFCs, this can be due to the smaller cathode area compared to anolyte volume [65]. Longer distances between electrodes, especially when wastewater conductivity is low, increase the internal resistance of the system. In addition, large electrodes have higher internal resistances, which significantly decrease power density if electrode material is not highly conductive [65,84]. Figure 5 clearly shows that the highest (24 $Wm^{-3}$) power densities with brewery wastewater fed MFCs have been obtained in small reactors (0.1 L anodic net volume), while the power densities in MFCs with volumes >1 L have been only 0.22-4.1 $Wm^{-3}$. The highest power density of 4.1 $Wm^{-3}$ among the MFCs with 1-100 L volume has been obtained in 10 L reactor net volume. This 10 L serpentine-type air-cathode MFC stack with 40 MFC units was operated in series enabling comparatively high electricity generation [52].

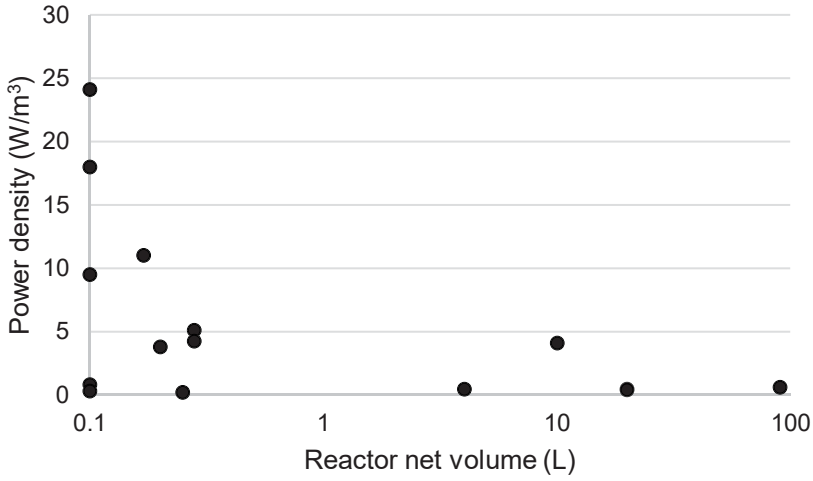


**Figure 5.** Volumetric power densities (W/m$^3$) as a function of reactor net volume (anode chamber liquid volume in litres) obtained from MFCs treating brewery wastewater. Referred MFC studies are listed in Table 3.

Various reactor designs have been studied to increase the electrode and membrane areas, or to decrease the distance between anode and cathode electrodes in MFCs with higher net volumes (Table 5). For example, Dong et al. increased the anode and cathode areas by placing numerous anode-cathode modules in one anode chamber with a volume of 90 L [16], while Rossi et al. studied multipaneled cathodes in 85 L MFC to increase the size of the cathode electrode without increasing the internal resistance caused by the long distances for electron transfer in a single electrode [65]. To decrease internal resistances caused by long distances between electrodes (especially with low conductive wastewaters) and small electrode area, Wang et al. and Deeke et al. studied fluidized systems with granular anode electrode material to bring anodic biofilm occasionally close to cathode electrode [64,113]. Moving capacitive anode particles transferred their charge for anodic current collectors at occasional collisions. Anode material fluidization also enables good contact between biofilm and available substrates in wastewater, but the need for recycle pump to keep granules fluidized increase the energy consumption [113]. This reactor design has been operated in 1-2 L volume, but the reactor design could be easily scalable with high COD removal efficiency [64,113]. All the example designs listed in Table 5 contained air-cathode, where efficient catalyst is needed to reach high power densities and diffusion layers, but avoid the need for catholyte solution.

**Table 5.** Examples of different continuously operated reactor designs (1-1000 L) for up-scaling.

| MFC type (and volume) | Anode electrode | Cathode electrode | Reference |
|---|---|---|---|
| Serpentine-type air-cathode stack (10 L) | Graphite felt | Cloth cathode assembly (conductive catalytic layer painted on PTFE[a]) | [52] |
| Baffled air-cathode MFC with anode-cathode modules (90L) | Carbon brush | Activated carbon and PTFE[a] | [16] |
| Membrane-free air-cathode containing 4 MFC units (45 L) | Graphite brush | Carbon cloth with diffusion layers and platinum catalyst | [14] |
| Stackable horizontal plug flow air-cathode MFC (1000 L) | Carbon brush | Carbon mesh (with platinum catalyst) | [13] |
| Rectangular tank multi-panel air-cathode MFC with multiple anodes (85 L) | Graphite brush | Activated carbon and PTFE[a] on stainless steel mesh | [65] |
| Membrane-free fluidized bed with air-cathode (1L) | Activated carbon granules with graphite rod current collector | Carbon cloth with diffusion layers and platinum catalyst | [113] |

[a]PTFE = polytetrafluoroethylene

## 2.6 Wastewater management and energy recovery with anaerobic bioprocesses

Brewery wastewater has been treated anaerobically in large-scale only by methanogenic wastewater treatment. Electricity production in MFCs and hydrogen production with dark fermentation are potential options for wastewater treatment, but so far most studies (except for one pilot with 1 $m^3$ volume [111]) have been conducted in laboratory scale (up to 90 L as shown in Figure 5 in section 2.5). To compare energy yields obtained as methane, hydrogen and electricity, obtained yields of these energy carriers have been converted to Wh per kg of removed COD using the lower heating values of 35.86 $MJm^{-3}$ and 10.78 $MJm^{-3}$ for methane and hydrogen, respectively.

The energy yield values from selected brewery wastewater treating methanogenic wastewater treatment processes were 2600 - 3100 $Whkg_{COD}^{-1}$ (Table 6). With dark fermentative hydrogen production, the energy yield from up-flow anaerobic contact filter reactor was approximately 20% of the methanogenic wastewater treatment energy yield, and with bioelectrochemical treatment, only 1-4%, being remarkably lower compared to both methanogenic wastewater treatment and dark fermentative hydrogen production. However, COD degradation in MFCs (85-95%) was at the same level with methanogenic wastewater treatment (80-98%), while with dark

fermentative hydrogen production the COD degradation was lower (69%). In dark fermentative hydrogen production, the carbohydrates are efficiently transformed to hydrogen and other compounds, but the VFAs left in the effluent decrease the COD removal [114]. For this reason, COD removal was lower compared to bioelectrochemical treatment and methanogenic wastewater treatment.

**Table 6.** Energy recovery and COD removal efficiency from brewery wastewater in various continuous anaerobic treatment systems including methanogenic wastewater treatment (often called anaerobic digestion AD), dark fermentative hydrogen production (DF) and electricity generating microbial fuel cells (MFC). The bars visualize the differences in energy yield (blue), COD removal (yellow) and organic loading rate (green) between the studies.

| Bioprocess and reactor type | Energy yield ($Whkg_{COD}^{-1}$)[a] | COD removal (%) | OLR ($kg_{COD}m^{-3}d^{-1}$) | Influent | Reference |
|---|---|---|---|---|---|
| **AD** Laboratory scale anaerobic membrane bioreactor | 3100 | 98 | 3.5-11.5 | brewery wastewater | [115] |
| **AD** Full scale (850 $m^3$) biogas-lift reactor | 2900 | 80 | 7.4 | brewery wastewater | [116] |
| **AD** Full scale (850 $m^3$) biogas-lift reactor | 2600 | 90 | 8.3 | brewery wastewater | [116] |
| **DF** Laboratory scale anaerobic contact filter | 490 | 69 | 2.5 | brewery wastewater | [11] |
| **MFC** Laboratory scale (10 L) tubular MFC | 110 | 87 | 1.1 | brewery wastewater | [52] |
| **MFC** Laboratory scale (20 L) tubular two-chamber | 36 | 95 | 0.31 | brewery wastewater diluted with 1g/L $NaHCO_3$ | [51] |
| **MFC** Laboratory scale (90 L) modular air-cathode MFC | 33 | 88 | 0.55 | brewery wastewater | [16] |

[a]Volumetric lower heating values of 35.86 $MJm^{-3}$ and 10.78 $MJm^{-3}$ were used for methane and hydrogen, respectively. These values were obtained from [117] using the density 0.717 $kg/m^3$ and 0.0899 $kg/m^3$ for hydrogen and methane, respectively.

The methane yields from various mechanical pulp mill wastewater treatment processes collected by Meyer and Edwards [118] were between 0.18 and 0.4 $m^3_{methane}$ per $kg_{removed\ COD}$ corresponding to energy yield of 2000-4000 Wh per $kg_{removed\ COD}$. The energy yields were at the same level with the energy yields obtained from brewery wastewater treatment (Table 6). There are only few studies on of dark

fermentation and MFC operation with pulp and paper wastewaters showing energy yields of 44-330 $Whkg_{COD}^{-1}$, which were ≤20% of the methanogenic wastewater treatment energy yields (Table 7).

COD removals with pulping wastewaters in MFCs and methanogenic wastewater treatment (26-41% and 45-83%, respectively) were lower compared to brewery wastewater studies due to the presence of slowly degrading lignins and cellulose [82,118,119]. However, methanogenic wastewater treatment is susceptible to toxic compounds, and the wood based antimicrobial compounds or process chemicals may disturb the process [9]. With dark fermentative hydrogen production, the COD removal from pulp and paper wastewater was higher (74-75%) compared to COD removal from brewery wastewater (69%), but due to the operation as batch process, the results are not comparable and in the study of Dessí et al. [12], the removal was potentially affected by COD adsorbance on granular activated carbon which was used as the solid support for microbial growth (Tables 6 and 7).

**Table 7.** Energy recovery and COD removal from pulp and paper in various anaerobic treatment systems including methanogenic wastewater treatment (often called anaerobic digestion AD), dark fermentative hydrogen production (DF) and electricity generating microbial fuel cells (MFC). The bars visualize the differences in energy yield (blue), COD removal (red) and organic loading rate (green) between the studies.

| Bioprocess and reactor type | Energy yield ($Whkg_{COD}^{-1}$)[a] | COD (%) | OLR ($kg_{COD}m^{-3}d^{-1}$) | Influent | Reference |
|---|---|---|---|---|---|
| **AD** Laboratory scale (6 L) submerged anaerobic membrane bioreactor | 1700 | 83 | 2 | TMP wastewater | [119] |
| **DF** Laboratory scale (17 mL) anaerobic tubes | 330 | 74 | batch operated | unamended TMP wastewater | [12] |
| **MFC** Laboratory scale air-cathode reactor | 330 | 41 | 0.5 | unamended paper recycling wastewater | [82] |
| **MFC** Laboratory scale air-cathode reactor | 270 | 26 | 2 | unamended paper recycling wastewater | [82] |
| **DF** Laboratory scale (1 L) stirred bioreactor | 44 | 75 | batch operated | enzymatically hydrolyzed raw pulp and paper wastewater | [120] |

[a]Volumetric lower heating values of 35.86 $MJm^{-3}$ and 10.78 $MJm^{-3}$ were used for methane and hydrogen, respectively. These values were obtained from [117] using the density 0.717 $kg/m^3$ and 0.0899 $kg/m^3$ for hydrogen and methane, respectively.

In addition to wastewater treatment, the excess biomass generated during the wastewater treatment needs treatment, such as drying. Streeck et al. calculated low

biomass growth of 0.05 $g_{biomass\ COD}$ per $g_{removed\ COD}$ (based on general equations for bacterial growth and decay) for an electrochemically active microbial community in a MFC [121]. Turkdogan reported significantly higher biomass growth of approximately 0.5 $g_{VSS}$ per $g_{removed\ COD}$ for pulp and paper wastewater fed methanogenic wastewater treatment processes, but their comparison with other studies revealed high variation in biomass yields (from 0.06 to 0.5 $g_{VSS}$ per $g_{removed\ COD}$) between different methanogenic wastewater treatment studies [122]. The variation in biomass growth yields between studies is caused by differences in operational parameters, feed and inoculum composition [122,123]. No measured biomass growth results were found for dark fermentative hydrogen production, but Oh et al. assumed 0.1 gVSS per g glucose at 55 °C [124].

If the availability of VFAs (the preferred substrate of electrochemically active organisms) is limiting electricity production, different pretreatment methods can be utilized for degrading organic wastewater compounds. According to Butti et al. [25] physical (heat treatment, ultrasonication, microwave treatment, sterilization, freezing/thawing and solid-liquid separation), chemical (base treatments) and biological treatments (fungal treatment and prefermentation) have been studied with different to wastewater type. Integration of various processes has also intrigued researchers. For example, Katuri et al. combined methanogenic wastewater treatment with a MFC in an up-flow reactor to break down the complex compounds in high strength wastewater by methanogenic treatment before the bioelectrochemical treatment [106]. Wang et al. studied brewery wastewater treatment by combining a MFC with anaerobic wastewater treatment to operate the combined system at high OLR of 7.4 $kg_{COD}m^{-3}d^{-1}$ [104], as for Sangeetha et al. and Tejedor-Sanz et al. combined MEC to methanogenic wastewater treatment and electrocoagulation, respectively [125,126], and Liu et al. combined a MFC with aerobic or anaerobic membrane bioreactors[127].

In summary, the large scale studies of methanogenic wastewater treatment have shown high energy yields with brewery and pulp and paper wastewaters. However, due to the lower biomass production, lower operation temperatures and lower susceptibility to inhibitory compounds in wastewater, electricity producing MFCs have several benefits compared to methanogenic wastewater treatment when treating industrial wastewater [13,14]. However, further research is required to optimize power density and COD removal for wastewater treatment in larger scale.

# 3 RESEARCH HYPOTHESES AND AIMS

The main focus of this work was to study the applicability of MFCs for treatment and resource recovery from industrial wastewaters. This was done by studying various start-up protocols and MFC designs, anodic electrode materials and operational conditions with synthetic and real industrial wastewaters.

Changes in industrial wastewater composition and flow rate may damage electrochemically active microbial community e.g. by inhibition, wash-out and starvation. To meet treatment requirements, prompt recovery of biological treatment process is of high importance. The fastest method for starting up a new MFC is to use an enrichment culture from similar operating conditions [36]. However, if such enrichment culture is not available, it was hypothesized that the start-up of MFC can be accelerated with e.g. electrochemical methods. Published results regarding the optimal adjusted anode potential or external resistances for electricity generation and start-up time are contradictory [18,33,37–40]. For this reason, the various adjusted anode potentials and external resistances were compared for start-up of identical brewery wastewater fed BESs (Paper I).

Another strategy for prompt start-up without existing enrichment culture is to store microbial community for further use. It has been demonstrated that anaerobic sludge survives well by drying [128] and aerobic granules as dewatered pellets [129], but little is known about the survival of electrochemically active microorganisms upon storage. Alam et al. studied the storing of biofilm on anode electrodes by refrigeration, freezing and dehydration, but the original current densities were not recovered [130]. They suggested that the decreased current densities were due to presence of dead cells in the biofilm preventing the contact between living cells and the electrode. Therefore it was hypothesized that MFCs can be effectively seeded with stored anolyte from working MFC to enrich an anodic biofilm in a new MFC. At e.g. pulp and paper wastewater treatment plant, storing of anolyte could be used as a preparation for process upsets. For this reason, the viability of stored electrochemically active anolyte cultures and start-up times of the xylose fed MFCs were studied by inoculating new MFCs with refrigerated or freezed anolyte samples from a xylose fed MFC (Paper II).

Thermomechanical pulping (TMP) wastewater is an example of industrial wastewater containing biodegradable organic compounds. TMP wastewaters are generated in large quantities, but there are no previous studies on bioelectrochemical TMP wastewater treatment. TMP is a mechanical pulping process and for this reason, TMP wastewater contains less toxic chemicals compared to wastewaters generated during chemical pulping. It was hypothesized that TMP wastewater is amenable to bioelectrochemical treatment because of its chemical composition, i.e. it contains easily anaerobically biodegradable organic compounds and lacks inhibitory compounds. The previous studies with other pulp and paper wastewaters have shown that power densities were restricted by low wastewater conductivity [82,84]. To increase buffering capacity and conductivity, $NaHCO_3$ was added to TMP wastewater. Bioelectrochemical TMP wastewater treatment was studied in a continuously operated up-flow MFC (Paper III).

Efficient bioelectrochemical wastewater treatment requires optimization of MFC design and operational conditions. It was hypothesized that anode electrode material selection significantly influence electricity generation and wastewater treatment efficiency. Therefore, the performance of a xylose-fed up-flow MFC was compared using various carbon-based (graphite plate and carbon cloth, with and without zeolite coating), metal-based (tin coated copper) and metal-carbon composed (granular activated carbon in stainless steel cage) anode electrode materials (paper III). OLR and HRT affect electricity generation in MFCs, because power densities increase with OLR, but at too low HRTs, diffusion and mass transfer limitations and the growth of other than electrochemically active organisms are increased [131,132]. Lay et al. [54] optimized recirculation rate of an xylose fed up-flow MFC for electricity generation. In this study, the electricity generation was further optimized by studying the ability of an up-flow MFC to convert xylose to electricity at HRTs of 0.17-3.5 d and OLRs of 0.15 to 3.2 $g_{COD}L^{-1}d^{-1}$ (paper IV).

It was hypothesized that anolyte storing methods and times (refrigeration and freezing) and different electrochemical start-up protocols affected anode electrode biofilm microbial communities. For this reason, polymerase chain reaction denaturation gradient gel electrophoresis (PCR-DGGE) analyses were conducted in the end of the MFC operation for comparing the DGGE profiles and identifying microorganisms enriched in the biofilm (papers I and II). PCR-DGGE analysis was also conducted after more than 200 d operation of xylose-fed up-flow MFC with decreasing HRTs to identify the enriched microorganisms on anode biofilm (paper IV).

Based on the hypotheses above, the general objective of this thesis was to enhance reliability of MFC operation with industrial wastewaters by optimizing anode electrode materials, operational parameters and start-up protocols. The specific objectives of this thesis were as follows:

- Compare different electrochemical start-up protocols (various adjusted anode potentials and external resistances) and anolyte storing at +4 °C and -20 °C for prompt BES recovery (papers I and II).

- Compare electricity generation with different anode electrodes and evaluate their potential for up-scaling (paper III).

- Study the effect of OLR on electricity generation and xylose degradation in an up-flow MFC (paper IV).

- Study the amenability of brewery and TMP wastewaters to bioelectrochemical treatment in an up-flow MFC and delineate the compositional changes occurring during the treatment (papers II and III).

- Study the viability of electrochemically active bacteria and the microbial community composition after stable operation following anolyte refrigeration or freezing and different start-up protocols (papers I and II).

# 4 MATERIALS AND METHODS

## 4.1 Experimental designs

The experimental designs used to study the effect of start-up protocols, anolyte storing, anode electrode material comparison and treatment of TMP wastewater, as well as HRT on MFC performance are visualized in Figures 6, 7, 8 and 9, respectively.

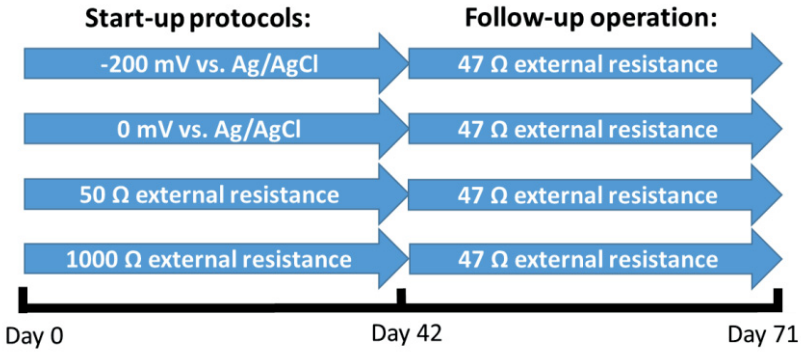


**Figure 6.** Schematic diagram of the experimental design related to start-up protocols (paper I). Different start-up protocols were used for enriching electrochemically active microbial community and after the start-up, the performance of the MFCs was compared in similar conditions (with 47 Ω external resistance).

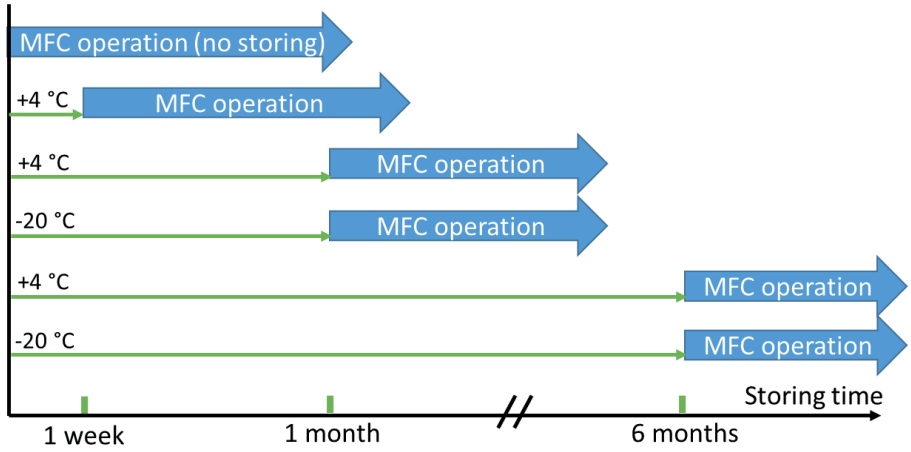


**Figure 7.** Schematic diagram of the experimental design related to MFC start-up with stored (refrigerated or freezed) anolyte (paper II). The effects of different inoculum storing methods on the start-up time, electricity generation and xylose oxidation were studied under similar conditions.

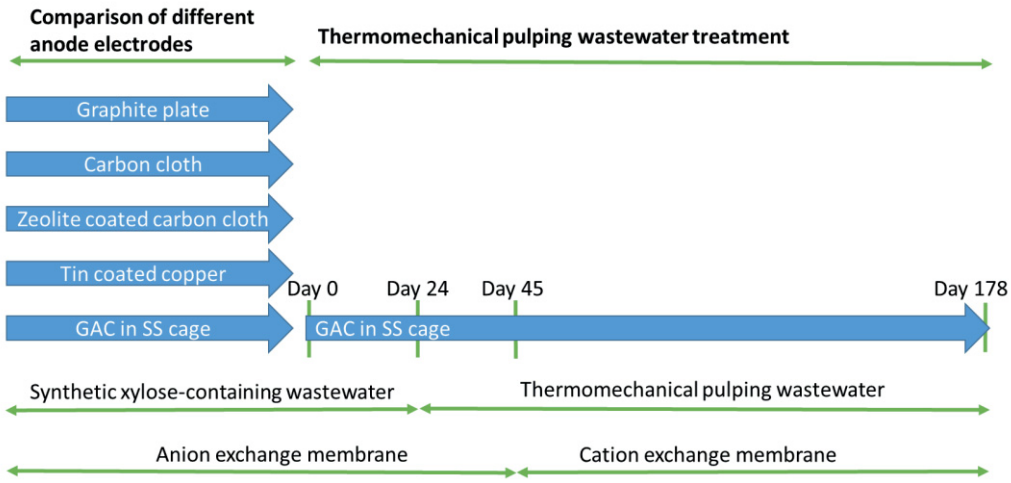


**Figure 8.** Schematic diagram of the experimental design on anode electrode comparison and TMP wastewater treatment (paper III). In the first part of the experiment, different anode electrode materials were compared. In the second part, thermomechanical pulping wastewater treatment was studied with the selected anode (GAC in SS cage). (Modified from paper III).

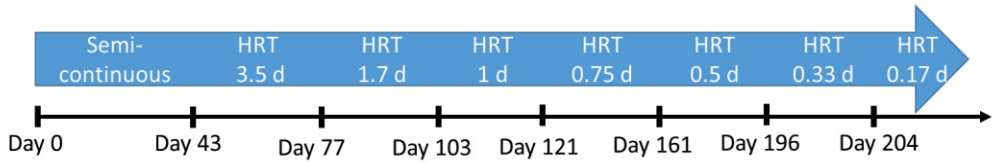


**Figure 9.** Schematic diagram of experiments focusing on the effect of HRT (paper IV). The effect of HRT on the performance was studied in continuously operated up-flow MFC after the semi-continuous start-up phase. HRT was decreased until the operation failed due to clogging of recirculation tube. Membranes were changed on days 78, 117, 132, and 160.

## 4.2 Sources of microorganisms

Mesophilic microbial communities originating either from anaerobic digesters or compost (Table 8) were pre-enriched in MFCs using xylose as substrate (papers II, III and IV), or they were enriched during the studied operation period (paper I). Enrichment was always started in semi-continuous operation mode. To transfer an enrichment culture into a new MFC, 10% (v/v) of anolyte from an operating MFC was mixed with the anolyte in the new MFC. Enrichment culture in experiments focusing on optimizing OLR of an xylose-fed MFC (paper IV) was pre-enriched by Mäkinen et al. [133] and Lay et al. [54] (Table 8).

**Table 8.** Sources of electrochemically active microbial communities.

| Source | Substrate at MFC studies | Paper(s) |
|---|---|---|
| Anaerobic digestate from municipal wastewater treatment plant (collected on January 2017) | Brewery wastewater | I |
| Anaerobic digestate from municipal wastewater treatment plant (collected on February 2015) | Xylose or TMP wastewater | II, III |
| Compost culture (received from C-H. Lay [54]) | Xylose | IV |

## 4.3 Synthetic and real wastewaters

MFCs were fed with synthetic (xylose containing) or real brewery or TMP wastewaters (Table 9). Due to the low buffering capacities, the real wastewaters were supplemented with $NaHCO_3$. Synthetic wastewater was buffered with 10.7 $gL^{-1}$ $NaH_2PO_4$, 3.2 $gL^{-1}$ $Na_2HPO4$ and 4 $gL^{-1}$ $NaHCO_3$.

**Table 9.** Real and synthetic wastewaters used as feed in the MFC experiments.

| Source | Main substrates for microorganisms | Supplementations | Paper(s) |
|---|---|---|---|
| Real wastewater from a Finnish brewery | Ethanol, sugars | 2.0 $gL^{-1}$ $NaHCO_3$ | I |
| Synthetic wastewater (prepared in laboratory) | Xylose | - | II, III, IV |
| Real wastewater from a Finnish TMP pulp mill | Cellulose and hemicellulose based (poly)saccharides | 0.8-2.0 $gL^{-1}$ $NaHCO_3$ | III |

## 4.4 Reactor designs

Electricity generation was studied in laboratory-scale air-cathode, three-chamber and up-flow MFCs (Table 10 and Figures 10 and 11).

**Table 10.** Continuous or semi-continuous microbial fuel cells used for electricity generation.

| Reactor design (anode chamber volume (L) | T (°C) | Specifications | Number of electrodes | Paper |
|---|---|---|---|---|
| Air-cathode (0.123) | ca. 29-30 | Anolyte circulated through a bottle in 37 °C water bath, (CEM 41 $cm^2$) with Pt catalyst, carbon cloth cathode | 2 anodes, 2 cathodes | I |
| Three-chamber (0.123) | ca. 29-30 | Anolyte circulated through a bottle in 37 °C water bath, CEM (41 $cm^2$) with PtNi catalyst, carbon cloth cathode, catholyte: aerated phosphate buffer solution | 2 anodes, 2 cathodes | II |
| Up-flow (0.5) | 37 | AEM (16 $cm^2$), graphite plate cathode $K_3Fe(CN)_6$ catholyte | 1 anode, 1 cathode | III |
| Up-flow (0.5) | 37 | CEM (16 $cm^2$), graphite plate cathode, $K_3Fe(CN)_6$ catholyte | 1 anode, 1 cathode | III |
| Up-flow (0.5) | 37 | AEM (16 $cm^2$), graphite plate cathode, $K_3Fe(CN)_6$ catholyte circulated | 1 anode, 1 cathode | IV |

CEM = cation exchange membrane; AEM = anion exchange membrane

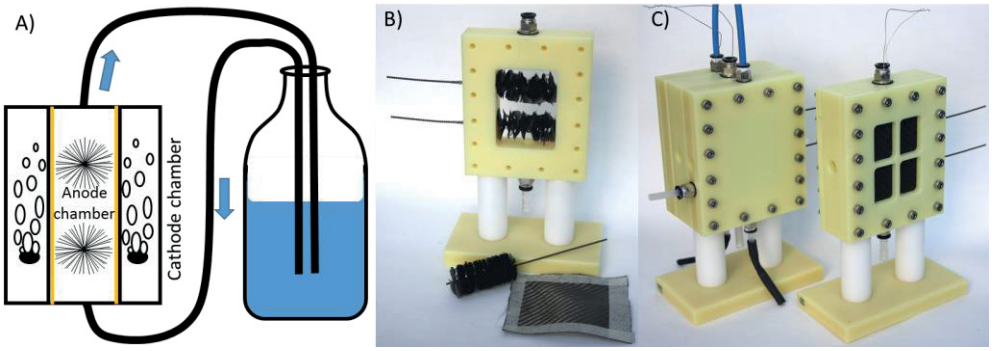


**Figure 10.** Air-cathode and three-chamber MFCs used in papers I and II. A) Schematic diagram of anolyte circulation and catholyte aeration in the three-chamber MFC (membranes highlighted with orange), B) photograph of electrode materials and anode compartment with anode electrodes installed and C) photograph of the three-chamber MFC (on the left) and the air-cathode MFC (on the right). (Photos: J. Haavisto)

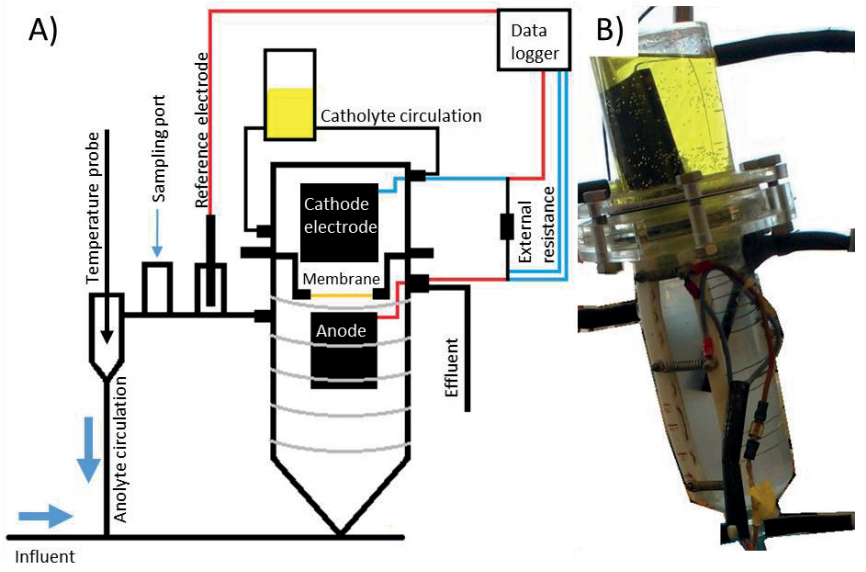


**Figure 11.** Up-flow MFC used in papers III and IV. A) Schematic diagram of the MFC and electrical connections (catholyte circulation was not used in paper III) and B) a photograph of the MFC. (Photo: J. Haavisto)

## 4.5 Electrodes

Anode electrodes used in this study were graphite plate, carbon cloth, tin coated copper, granular activated carbon in stainless steel cage and carbon brush (Figure 12). Carbon cloth and graphite plate were used also as cathode electrodes.

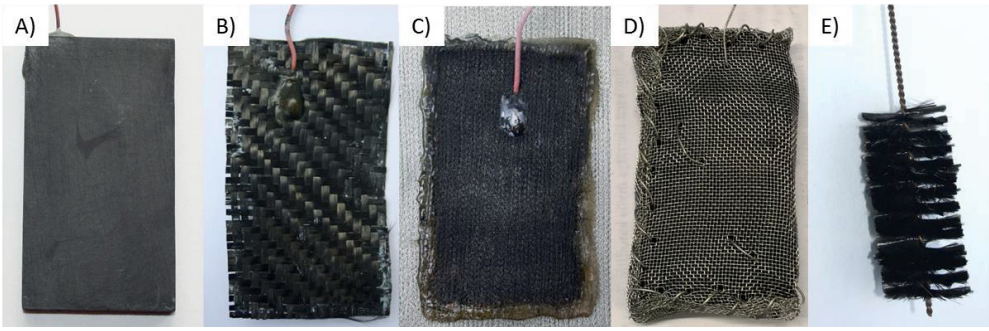


**Figure 12.** Photographs of anode electrodes used in papers I – IV. A) Graphite plate (papers III and IV), B) Carbon cloth (paper III), C) tin coated copper (paper III), D) Granular activated carbon in stainless steel cage (paper III), and carbon brush (papers I and II). (Photos: J. Haavisto)

## 4.6 Analytical methods

The electrochemical and chemical analyses conducted in this study are summarized in Table 11. In addition, microbial community was studied in papers I, II, and IV with PCR-DGGE. For the community analysis, microbial DNA was extracted from detached biofilm sample and amplified with PCR. Sequences from different organisms were separated with DGGE for DNA sequencing and further identification based on 16SrRNA (http://blast.ncbi.nlm.nih.gov/Blast.cgi).

**Table 11.** Summary of electrochemical and chemical analyses conducted in this study.

| Analysis | Instruments | Paper(s) |
|---|---|---|
| Conductivity | Multimeter | I, III |
| COD | Heater, titrator | I, III |
| CV/LSV | Potentiostat | I, II, III |
| Ethanol, butanol, acetate, propionate, isobutyrate, butyrate, valerate) | Gas chromatograph | I, II, III, IV |
| pH | pH electrode | I, II, III, IV |
| Sugars | Spectrophotometer | I, II, III, IV |
| Temperature | Thermometer, temperature electrode | I, III, IV |
| Voltage, electrode potential | Datalogger or multimeter | I, II, III, IV |
| Current | Potentiostat | I, II, III |
| Alkalinity | pH electrode, titrator | I, III |
| N | Heater, spectrophotometer | I, III |
| $PO_4$-P | Spectrophotometer | I, III |
| Anode potential compared to Ag/AgCl reference electrode | Datalogger or digital multimeter | I, II, III, IV |
| Biofilm protein mass | Freeze drier, balance, spectrophotometer | I |
| BOD | OxiTop measuring system | I |
| Microbial viability | Epifluorenscence microscope | II |
| Solids (VS, VSS, TS, TSS) | Oven, furnace, balance | III |
| CEM fouling and electrode surface morphology | Scanning electron microscope (SEM) equipped with an energy dispersive spectrometer (EDS) | III |
| Cations (sodium, potassium, magnesium, calcium) | Ion chromatography | III |
| Monosaccharides (glucose, xylose, arabinose, galactose and cellubiose | High performance liquid chromatography (HPLC) | III |

## 4.7 Calculations

Current (I) and power (P) were calculated according to Ohm's law (Equations 1 and 2) from the measured voltage (V) and the external resistance (R):

$$I = \frac{U}{R} \quad (1)$$

$$P = UI \quad (2)$$

Power density was calculated with relation to anode electrode projected area (both sides included) or to anode chamber volume. The measured carbohydrates and VFAs ($C_xH_yO_z$) were converted to theoretical COD by multiplying the mass of

organic molecules with a coefficient calculated according to van Haandel and Van der Lubbe [134].

$$COD_{tot} = \frac{8*(4x+y-2z)}{12x+y+16z}, \quad (3)$$

where x, y and z represent the number of carbon, hydrogen and oxygen atoms in an organic molecule. Coulombic efficiency (CE) was used to relate the produced electrical energy in coulombs divided by the electrical energy theoretically releasable from the substrate using Equation 4:

$$CE = \frac{\int I\, dt}{nFb}, \quad (4)$$

where n is molar amount of substrate, F is Faraday constant, and b is the amount of electrons releasable per mole of substrate. The theoretically releasable energy was calculated for the fed COD (in papers I and IV), removed xylose (in paper II), or removed (theoretical) COD (in paper III).

# 5 RESULTS AND DISCUSSION

The effects of different start-up methods (electrochemical protocols and anolyte storing) and means for process optimization (anode electrode materials and hydraulic retention time) on electricity generation were studied (Table 12). Bioelectrochemical treatment of industrial wastewaters was studied in semi-continuous air-cathode and three-chamber BES and continuously operated up-flow MFC (Table 12). The results with different substrates, reactor configurations and operation modes (semi-continuous vs. continuous) are not comparable, but give an indication of the effects of different parameters on electricity generation.

**Table 12.** The effects of compared operational conditions, electrode materials and substrates on volumetric power densities and Coulombic efficiencies (CEs). The colored bars visualize the effect of compared parameters and experimental designs (e.g. reactor design and substrate) on power density and CE.

| | Compared operational conditions, anode materials, or substrates | Power density ($Wm^{-3}$) | CE (%) |
|---|---|---|---|
| Electrochemical start-up protocols in semi-continuous air-cathode MFC (Paper I)[a] | -200 mV anode potential[c] | 0.65 | 12 |
| | 0 mV anode potential[c] | 0.42 | 12 |
| | 50 Ω external resistance[c] | 0.36 | 11 |
| | 1000 Ω external resistance[c] | 0.26 | 12 |
| Anolyte storing in semi-continuous three-chamber MFC (Paper II)[b] | 1 month at -20 °C | 1.8 | 14 |
| | 1 month at +4 °C | 1.2 | 12 |
| | 6 months at +4 °C | 0.07 | 2.8 |
| | 6 months at -20 °C | 0.004 | 0.7 |
| Anode electrode materials in continuous up-flow MFC (Paper III)[b] | Carbon cloth | 3.7 | 20.2 |
| | Graphite plate | 3.5 | 19.4 |
| | GAC in SS cage | 3.1 | 18.3 |
| | Zeolite coated carbon cloth | 3 | 18 |
| Hydraulic retention time in continuous up-flow MFC (Paper IV)[b] | 3.5 d HRT | 2.1 | 30.3 |
| | 1.7 d HRT | 3.05 | 18.2 |
| | 1 d HRT | 2.42 | 9.2 |
| | 0.75 d HRT | 0.77 | 3.9 |
| | 0.5 d HRT | 0.69 | 2.5 |
| | 0.33 d HRT | 0.53 | 1.5 |
| | 0.17 d HRT | 0.39 | 0.6 |
| Industrial wastewater treatment (Papers I and III) | Brewery wastewater (air-cathode MFC) | 0.51 | 11.8 |
| | TMP wastewater (up-flow MFC) | 0.24 | 1.5 |

[a]Fed with brewery wastewater; [b]Fed with xylose; [c]The results of electrochemical start-up protocols were obtained with 47 Ω external resistance after the different start-up protocols were utilized.

## 5.1 Storing and enrichment of electrochemically active cultures

As a preparation to operational upsets during MFC operation, electrochemical start-up protocols (paper I) and inoculum storing (paper II) were studied. To decrease lag time for electricity generation, especially when active enrichment culture is not available, electrochemical methods, such as optimization of adjusted anode potential or external resistance, can be utilized for enrichment of electrochemically active

microbial culture (paper I). Due to contradictory published results regarding the optimal anode potential or external resistances for enrichment of electrochemically active microbes [18,33,37–40], two adjusted anode potentials (-200 or 0 mV vs. Ag/AgCl) and external resistances (50 or 1000 Ω) were studied in brewery wastewater fed air-cathode BES reactors. The reactors were named based on the start-up protocols as follows; $BES_{-200mV}$, $BES_{0mV}$, $BES_{50\Omega}$ and $BES_{1000\Omega}$. Highest power densities after start-up were measured with $BES_{-200mV}$ (Table 12).

Even though the current densities during the start-up stabilized faster in $BES_{50\Omega}$ and $BES_{1000\Omega}$, ten-fold higher average current densities measured in $BES_{-200mV}$ and $BES_{0mV}$ during the start-up showed that adjusted anode potentials accelerated the current generation more than the use of external resistances (Table 12). The highest power density, average current density and current obtained in anodic LSV in $BES_{-200mV}$ together demonstrate that the adjusted anode potential of -200 mV was the most optimal start-up protocol for a brewery wastewater fed air-cathode BES. According to anodic LSV curves, current production was very low in $BES_{50\Omega}$ and $BES_{1000\Omega}$ at more positive anode potentials than -300 mV vs. Ag/AgCl. The results are in accordance with Hong et al. and Zhu et al. who reported that adaptation to higher current densities eliminated power overshoot and enabled higher current densities at broader anode potential range [135,136]. However, the optimal anode potential for obtaining the highest current density depend on the substrate, microbial community and the reactor configuration (e.g. oxygen penetration to anode biofilm) [33,37,137]. Thus, the optimal anode potential should be determined separately in each case. Also Aelterman et al. reported higher current densities with -200 mV vs. Ag/AgCl adjusted anode potential in two-chamber acetate-fed MFC compared to 0 and -400 mV. Zhang et al., on the other hand, reported inconsistent results for different wastewaters used as inoculum source [33,137].

To restart the bioelectrochemical treatment rapidly after a process upset, storing of anolyte (as a source of electrochemically active microbes) for up to six months at +4 °C or -20 °C was studied (paper II). After storing the anolyte at +4 °C or -20 °C for one month, the electricity generation was recovered, but not after six months (Table 12). The average power densities after one month storing were 76-111% of the power densities in MFCs started up with fresh anolyte, but after six months storage, power densities were <10% compared to the power densities of fresh anolyte.

Anolyte storing temperature (+4 or -20 °C) had only small effect on power density (Table 12). However, lag time for reaching 0.8 $Wm^{-3}$ was longer (7 ± 3 days) after the anolyte was stored for one month at -20 °C compared to storing at +4 °C

(5.0 ± 0.9 days). These measured lag times were 3-5 days longer compared to lag time of 1.9 ± 0.5 days with fresh anolyte. In addition, the lag time of 2.7 ± 0.3 days after one week storing at +4 °C showed that the lag time for refrigerated anolyte is affected by storing time. Shorter lag times for electricity generation after storing at +4 °C compared to -20 °C is in accordance with the results of Alam et al., who reported faster reactivation of electrochemical activity with biofilms stored at +4 °C compared to freezing with glycerol at -70 °C [130].

The effect of different start-up methods (electrochemical protocols or anolyte storing) on transformation of wastewater organic compounds was studied by influent and effluent VFA, alcohol, and sugar concentrations measurements. Electrochemical start-up protocols had only small effect on transformation of wastewater organic compounds (paper I). Sugars and alcohol from brewery wastewater were almost completely removed in all BESs and transformed to electricity or volatile fatty acids (mainly acetate and propionate). However, COD removal was negligible due to the high inoculum COD load (which was slowly dissolved to anolyte) and reactor design which was not optimized for COD removal. The anolyte storing methods, on the other hand, had an effect on the metabolic activity of the microbial community and the quantity of VFAs in anolyte (paper II). Over 99% of the synthetic wastewater xylose was removed after all storing methods, but lower acetate and propionate concentrations (16-18 mM acetate and 5-6 mM propionate) were measured after ≤ 1 month storing at +4 °C compared to 1-6 months storing at -20 °C and 6 months at +4 °C (22-27 mM acetate and 8-16 mM propionate). VFA accumulation after longer storing times indicated that fermenting organisms were viable also after six months storing, but VFA consuming organisms, such as electrochemically active bacteria, were not. This was confirmed by lower electricity generation (less than 10% power density compared to fresh anolyte) and microbial community analysis (discussed in more detail in Section 5.4). The viability of fermenting bacteria after the six months storing is in accordance with the results of Teather et al., who reported that fermentative bacteria from cow rumen stayed viable after at least two years of storing at -20 °C with glycerol, but at +4 °C the agar deep cultures lost viability after 0.5-2 years [138].

## 5.2 Optimization of bioelectrochemical wastewater treatment

### 5.2.1 Effects of anode electrode materials on MFC performance

Anode electrode material and surface area affect the biofilm growth and electricity generation in a MFC, because direct electron transfer is the most efficient electron transfer mechanism [29] and high conductivity is required for efficient electron transfer from the electrode to the electrical wires. Different anode materials were compared based on their performance (COD removal, power density and cyclic voltammetry peak current) and material characteristics (specific surface area and scalability) in a xylose-fed up-flow MFC (Table 12; paper III). Studied electrodes included granular activated carbon in stainless steel cage (GAC in SS cage), graphite plate, carbon cloth and zeolite coated carbon cloth. Only small differences were measured in power densities between the studied anode electrode materials (power densities between 3.0-3.7 $Wm^{-3}$ as shown in Table 12) and xylose was removed efficiently (>95% removal) with all the studied anode materials. Theoretical COD removal (calculated from added influent and measured effluent VFA and xylose concentrations) varied between 77 and 86%. Anodic cyclic voltammetry measured at turnover conditions showed that the highest current densities with GAC in SS cage and graphite plate (>5.2 $Am^{-2}$ for both anode materials) were significantly higher than the highest current densities with carbon cloth or zeolite coated carbon cloth (1.8 and 1.9 $Am^{-2}$, respectively).

The comparison of material characteristics was done based on literature and emphasized the potential of GAC as anode electrode material in up-scaled processes. The specific surface area of GAC is significantly higher compared to the other studied anode electrode materials (Table 2 in Section 2.3.1). However, the conductivity of graphite plate is >100 times higher compared to that of GAC (Table 2 in Section 2.3.1). In up-scaled systems, low conductivity of large electrodes decreases the power density, but capacitive anode material, such as GAC, can be utilized in fluidized systems with separate current collectors [139]. In this study, GAC was trapped in a highly conductive SS cage to decrease the losses due to the lower conductivity of GAC.

Chemical and mechanical strength and potential for using the electrode material in various reactor configurations also makes an anode material more attractive choice in up-scaled systems. Carbon cloth has low mechanical strength due to loose weaving, but it is corrosion resistant [66]. As a thin and flexible material, carbon cloth

has shown its potential as an electrode material in various MFC configurations [20,51,67]. Although graphite plate is brittle, it has relatively high mechanical strength and good resistance against corrosion [66,140]. As a hard material, graphite plate can be used as a flat plate e.g. in cubic MFCs [49]. GAC in SS cage has high mechanical strength due to the stainless steel cage and both materials (GAG and SS) are known to be corrosion resistant as MFC anode under anaerobic conditions [66,141]. GAC is adaptable to various electrode and MFC configurations [20,50,142]. By combining conductivity, chemical and mechanical strength and potential for using an electrode material in various reactor configurations as criteria for scalability, the studied electrodes were evaluated from + to +++ for overall rating in Table 13. For scalability +++ means that all scalability criteria used for the comparison were satisfactory, ++ that at least one aspect is challenging and + that at least one aspect is failing. According to overall rating, GAC in SS cage was considered as the most suitable option for further studies and was used as anode materials for TMP wastewater treatment (results described in Section 5.3).

**Table 13.** Anode electrode selection criteria for bioelectrochemical wastewater treatment. (Modified from paper III)

| | **Performance criteria[a]** | | | **Material characteristics** | | |
|---|---|---|---|---|---|---|
| **Anode electrode** | COD removal[b] | Power density[c] | Current[d] | Specific surface area[e] | Electrode scalability | **Overall rating** |
| GAC in SS cage | +++ | ++ | ++ | +++ | +++ | 1. |
| Carbon cloth | +++ | +++ | + | + | ++ | 2. |
| Graphite plate | ++ | +++ | ++ | + | ++ | 2. |
| Zeolite coated carbon cloth | ++ | ++ | + | + | ++ | 4. |

[a]Based on experimental data of this study; [b]Based on COD removal obtained during continuous feeding (>80% +++ , 60-80% ++, <60% +); [c]Based on the average, stable power densities under continuous feeding (>300 $mWm^{-2}$ +++, 250-300 $mWm^{-2}$ ++, <250 $mWm^{-2}$ +); [d]The highest current densities obtained during CV analysis at turnover conditions (>10 $Am^{-2}$ +++, 5-10 $Am^{-2}$ ++, <5 $Am^{-2}$ +); [e]Surface area of the electrodes calculated for the size of the electrodes used in this study (>1000 $m^2$ +++, 100-1000 $m^2$ ++, <100 $m^2$ +).

A rough cost estimate for tested electrodes according to material bulk prices on Alibaba (carbon cloth 10-20 US dollar per $m^2$, graphite plate 5-10 US dollar per kg, GAC 1 US dollar per kg, SS mesh 3-8 US dollars per $m^2$) shows the lowest price for GAC in SS cage electrode (0.04-0.1 US dollars). Carbon cloth electrode was 10-20% more expensive, and graphite plate electrode was the most expensive anode with over 300% higher costs per electrode. However, it is important to notice that the demand for the materials affect the prices.

### 5.2.2 Effect of organic loading rate on continuous flow MFC performance

OLR is an important operation parameter to optimize electricity generation and wastewater treatment. At high organic loading, same wastewater volume can be treated in a shorter time enabling the use of a smaller continuously operated reactor. However, too high organic loading rate can decrease COD removal and enrich fast growing microbes other than electrochemically active [131].

The effect of OLR on electricity generation was studied by decreasing the HRT stepwise from 3.5 d to 0.17 d, which increased the OLR from 0.15 to 3.2 $g_{COD}L^{-1}d^{-1}$ (paper IV). Before continuous operation, the MFC was started up under semi continuous feeding. The highest power densities of 2.42 and 3.05 $Wm^{-3}$ were measured at 1 and 1.7 d HRTs with OLRs 0.53 and 0.31 $g_{COD}L^{-1}d^{-1}$, respectively (Table 12).

CE decreased with the decreasing HRT from 30 to 0.6% (Table 12) due to the increased substrate loading and decreased current densities at HRTs lower than 1.7 d. On average, 99% of the xylose was removed at all HRTs, but the theoretical COD removal remained lower (57-96%) due to the presence of VFAs (mainly acetate and propionate) in the effluent. At HRTs of 1 d and 1.7 d, theoretical COD removals were 69 and 82%, respectively. The obtained COD removals are higher than Huang and Logan reported for xylose-fed MFC, but they used higher OLRs [143]. With OLRs of 2-20 $g_{COD}L^{-1}d^{-1}$ the COD removal in their MFC was 21-74%. However, CE in their system was higher (28-54%) compared to this study.

## 5.3 Treatment of brewery and thermomechanical pulping wastewaters in bioelectrochemical systems

Treatment of TMP and brewery wastewater was studied in continuous up-flow MFC (Paper IV) and semi-continuously fed air-cathode MFC (Paper I), respectively. As the used reactor configurations were different, the results obtained for the two wastewaters are not fully comparable.

The power density obtained from brewery wastewater fed air-cathode MFC was 2.1 times compared to the power density from TMP wastewater fed up-flow MFC (Table 12). The difference was even higher in CEs (11.8 vs. 1.5%) due to the higher OLR used in the TMP wastewater experiments (2 vs. 0.2 $g_{COD}L^{-1}d^{-1}$). Stable power density with brewery wastewater (0.51 $Wm^{-3}$) was lower than most of the reported max. power densities (varying between 0.29 and 18 $Wm^{-3}$) in fed-batch systems fed

with brewery wastewater (Table 3 in Section 2.4.1), but on the same level reported for three continuously fed MFCs (0.42-0.83 $Wm^{-3}$) [51,103,104]. This was the first study on TMP wastewater treatment in MFC. Huang et al. [82] reported 5.9 $Wm^{-3}$ max. power density for paper recycling wastewater, which is several orders higher than the stable power density of 0.24 $Wm^{-3}$ obtained in this study.

The power densities in up-flow MFC could be increased by decreasing the distance between the anode and cathode electrodes especially if wastewaters with low conductivity (e.g. 0.8 $mScm^{-1}$ with TMP wastewaters; Table 4 in Section 2.4.2) are treated [82]. Also small membrane area compared to anode electrode area (0.3 $m^2m^{-2}$) potentially affected the obtainable power densities in the up-flow MFC [144]. On the other hand, the electricity generation from brewery wastewater in the air-cathode MFC was potentially decreased by oxygen penetration to anolyte through air-cathodes with CEM membranes [17,47]. Also continuous feeding with brewery wastewater would stabilize the anolyte composition compared to semi-continuous feeding and enable further optimization of process parameters such as HRT and OLR [145]. COD removal was negligible from brewery wastewater due to semi-continuous feeding and high inoculum with slowly dissolving organic load, but 47 ± 13% of TMP wastewater COD was removed in up-flow MFC, which is 80% higher than Huang et al. reported for paper recycling wastewater [82].

The results show that the COD removals from the studied wastewaters were not sufficient for discharging to the environment, but if the bioelectrochemical treatment is used as pretreatment process, 47% COD removal from TMP wastewater could significantly reduce the energy needed for conventional aerobic wastewater treatment. However, further studies are needed to increase the power density of both air-cathode and up-flow MFCs. The easily degradable VFAs left in brewery effluent demonstrated that suitable substrates for electrochemically active bacteria were left and higher resource recovery can be obtained in form of electricity by optimizing the system and operational conditions. Lower VFA concentrations in TMP effluent (44% of the soluble COD) together with 47% COD removal indicated that wastewater pretreatment could increase electricity generation at more optimized conditions.

## 5.4 Anodic microbial community compositions

Anodic microbial community compositions were studied in papers I, II and IV. Although the microbial communities were enriched in different MFC types (air-

cathode, three-chamber, up-flow) from different origins (anaerobic digestate and compost) and using different substrates (brewery wastewater or xylose), fermentative and electrochemically active bacteria were detected in all reactor types (Table 14). These microbial groups have their specific roles in degradation of wastewaters with high sugar content: fermentative bacteria oxidize sugars to VFAs, which are further used by electrochemically active bacteria for electricity generation [28]. Also facultative anaerobes such as *Escherichia coli*, *Citrobacter freundii* and *Pluralibacter georgoviae*) [146–148] were detected from the biofilm samples. Due to their ability to consume the oxygen penetrating to anolyte, facultative anaerobes are especially important in air-cathode MFCs [28]. Electrochemically active *C. freundii* and *Geobacter* sp. were detected from all reactor types used in this study (Table 14 contains only species detected in biofilm samples, but *C. freundii* was detected from up-flow anolyte sample) [149,150]. It should also be noted that some of the detected bacteria belong to more than one of the mentioned groups (fermenting, facultative anaerobes, or electrochemically active bacteria).

**Table 14.** Bacterial species detected from the anodic biofilms of MFCs fed with brewery wastewater or xylose. Bacterial species indicated in bold were found from all reactor types. Known electrochemically active bacteria are marked in blue and fermenting bacteria in green.

| MFC-type / **substrate** / inoculum origin | **Detected bacterial species (Phylogenetic group)** | **Reference** |
|---|---|---|
| Air-cathode MFC / **brewery wastewater** / Anaerobic digestate from municipal wastewater treatment plant (Paper I) | uncultured *Azonexus* sp. (Betaproteobacteria) | [151] |
| | *Azospira* sp. (Betaproteobacteria) | |
| | ***Citrobacter* sp. (Gammaproteobacteria)** | [149] |
| | *Desulfovibrio marrakechensis* (Deltaproteobacteria) | |
| | *Escherichia coli* (Gammaproteobacteria) | [152] |
| | ***Geobacter* sp. (Deltaproteobacteria)** | [24] |
| | *Klebsiella* sp. (Gammaproteobacteria) | [41] |
| | *Schwartzia* sp. (Negativicutes) | |
| | *Selenomonas* sp. (Negativicutes) | [153] |
| Three-chamber MFC / **xylose** / Anaerobic digestate from municipal wastewater treatment plant (Paper II) | ***Citrobacter freundii* (Gammaproteobacteria)** | [149] |
| | ***Geobacter sulfurreducens* (Deltaproteobacteria)** | [24] |
| | *Escherichia coli* (Gammaproteobacteria) | [147] |
| | *Lentimicrobium saccharophilum* (Bacteroidia) | [154] |
| | *Phascolarctobacterium sp.* (Negativicutes) | |
| | *Pluralibacter gergoviae* (Gammaproteobacteria) | |
| | *Proteiniphilum acetatigenes* (Bacteroidia) | [155] |
| Up-flow MFC / **xylose** / Compost culture (Paper IV) | ***Geobacter* sp. (Deltaproteobacteria)** | [24] |
| | *Proteiniphilum acetatigenes* (Bacteroidia) | [155] |
| | Uncultured *spirochete* (Spirochaetia) | |
| | *Wolinella succinogenes* (Epsilonproteobacteria) | |

Microbial community samples were taken from the anode biofilms in the end of the experiments (papers I, II and IV). In paper I, BES operation was continued for 33 days with external resistance of 47 Ω after the different start-up protocols. In the end of the study, no clear difference in the microbial communities on anode electrode biofilms were observed, which indicates that under similar selection pressure after the start-up, same microbial species were enriched to the anode biofilms. This is in accordance with the power densities, which became similar (0.48-0.55 $Wm^{-3}$) towards the end of the operation.

The anolyte storing methods had a significant effect on the microbial communities of xylose fed MFCs (Paper II). Facultative anaerobes (*E. coli*, *C. freundii* or *P. georgoviae*) [146–148] and fermentative bacteria (*E. coli*, *Proteiniphilum acetatigenes*, *C. freundii* or *Lentimicrobium saccharophilum*) [147,154–156] were found from biofilm samples of all MFCs which were inoculated with anolyte stored at +4 or -20 °C for different duration. However, well known electrochemically active bacteria *C. freundii* and *G. sulfurreducens* [149,150] that were detected in biofilms inoculated with anolyte after ≤1 month storing time, were not detected from the anodic biofilms of MFCs inoculated with anolyte stored for six months. This clearly indicates that electrochemically active bacteria were not able to survive the storage of six months at +4 or -20 °C without chemical supplementations.

In addition to the biofilm microbial communities analyzed in the end of the experiments (Table 14), the effect of OLR on anolyte microbial communities was studied at different HRTs (paper IV). Although PCR-DGGE is a semi-quantitative method at best [157], the significantly higher intensity of *Christensenella minuta* bands on DGGE gel indicated that the share of a fermenting *C. minuta* increased at HRTs of ≤0.5 d indicating higher fermenting activity [158]. Other species detected from anolyte samples were *C. freundii*, *Clostridium indolis*, *Clostridium oroticum*, *Enterobacter* sp., *Petrobacter* sp., *Proteiniphilum acetatigenes*, uncultured *spirochete*, and *Wolinella succinogenes*. At the highest OLRs, the strongest bands belonged to *C. minuta*, *C. freudii*, C. *indolis*, and *P. acetatigenes*.

# 6 CONCLUSIONS

In this study, process reliability and electricity generation of industrial wastewaters in MFCs was studied by comparing electrochemical start-up protocols, effect of storing of inoculum, comparing anode electrode materials and optimizing OLR in bioelectrochemical systems. Also brewery and TMP wastewaters were treated in air-cathode and up-flow MFCs.

It was demonstrated that electrochemical start-up methods efficiently accelerate BES start-up. In brewery wastewater fed air-cathode BES, -200 mV (vs. Ag/AgCl) adjusted anode potential accelerated the start-up more than 0 mV adjusted anode potential or 50 and 1000 Ω external resistances. The start-up current densities were from 1.7 to 30 times, and the power densities after the start-up from 1.5 to 2.5 times the power and current densities obtained with 0 mV, 50 Ω and 1000 Ω start-up strategies (paper I).

Without active enrichment culture, the MFC start-up can be accelerated by using stored anolyte as inoculum. Similar power densities (1.2–1.8 $Wm^{-3}$) compared to the MFC inoculated with fresh anolyte (1.4 $Wm^{-3}$) were obtained in the MFCs inoculated with anolyte stored at +4 °C or –20 °C for one month. However, the storing increased lag time for power production from 1.9 ± 0.5 d with fresh anolyte to 2.7 ± 0.3 d and 5.0 ± 0.9 d after one or four week(s) storing at +4 °C. Six months storing time was too long for recovering electricity generation suggesting that electrochemically active bacteria could not survive the long storing. However, 99-100% xylose removal together with high VFA concentrations demonstrated the viability of fermenting organisms after ≤6 months storing at +4 or -20 °C (paper II).

Anode electrode materials and surface structure affect electrochemically active biofilm evolution and electron transfer efficiency in MFCs. In the xylose-fed up-flow MFC, the differences in stable power densities (3.0-3.7 $Wm^{-3}$) between graphite plate, carbon cloth and granular activated carbon in stainless steel cage were small. The highest currents with anodic cyclic voltammetry, on the other hand, were measured with granular activated carbon and graphite plate. According to overall evaluation, the most suitable anode material for bioelectrochemical treatment was capacitive granular activated carbon due to the high current density in a large potential range, scalability and very high surface area (paper III).

In xylose fed up-flow MFC, the highest power densities of 3.05 and 2.42 $Wm^{-3}$ were measured at 0.31 and 0.53 $g_{COD}L^{-1}d^{-1}$ OLR (with 1 and 1.7 days hydraulic retention times). By increasing OLR from 0.15 to 3.2 $g_{COD}L^{-1}d^{-1}$ $g_{COD}L^{-1}d^{-1}$, CE decreased from 30 to 0.6% and COD removal varied between 57 and 95% (paper IV).

Stable power density of 0.51 $Wm^{-3}$ was obtained in the air-cathode MFC fed with brewery wastewater. In the up-flow MFC fed with TMP wastewater, power density of only 0.24 $Wm^{-3}$ was generated due to high internal resistances caused by low wastewater conductivity, long distance between electrodes and membrane fouling. On the other hand, the COD removal was 47% in up-flow MFC fed with TMP wastewater, but negligible in air-cathode MFC fed with brewery wastewater.

Electrochemically active and fermentative bacteria were detected in all MFC types. MFCs were operated at mesophilic temperatures (29-37 °C) and they all contained known electrochemically active bacteria *C. freundii* and *Geobacter* sp. Share of fermentative organisms in anolyte increased at high loading rates and in biofilms after six months storing. Electrochemically active microbes were viable after one month storing at +4 °C or -20 °C, but not after six months. No differences in anode biofilm microbial communities were associated with electrochemical start-up protocols after 33 d operation in same conditions with 47 Ω external resistances.

In summary, the results of this study show that the reliability of MFC operation can be increased by storing anolyte as a preparation for the possible process upset, or if healthy enrichment culture is not available, the lag time for electricity generation can be decreased by adjusting the anode potential during the start-up. To further optimize the MFC performance, granular activated carbon can be utilized with a current collector at the OLR which is optimized for the studied process.

# 7 RECOMMENDATIONS TO FUTURE STUDIES

Comparison of different adjusted anode potentials and external resistances did not show significant differences in long-term electricity production between studied start-up strategies. To validate the result at larger range of anode potentials and external resistances, higher number of different potentials and resistances should be studied.

The results of this study demonstrated that electrochemically active microbial community can be stored for one month, but not for six months without significantly affecting the power density obtained after storing. Due to the long gap in storing time between one and six months, further experiments are needed to determine whether storage times longer than one month can be used. Also, the possibility of utilizing electrochemically active sporulative bacteria (such as *Bacillus subtilis*) should be studied, because the storing of endospores could significantly increase the possible storing times [159,160]. Microbial communities were studied with PCR-DGGE to profile microbial communities in biofilm or anolyte samples. For quantitative results of bacteria and their activity in samples, more sophisticated techniques are available and should be used, such as high-throughput sequencing of DNA or cDNA [161].

It was demonstrated in this study, that TMP wastewater can be treated in a MFC. However, the electricity production was low and future studies are required to optimize the reactor design and process operation in order to increase CE and power density. Especially the losses due to the low conductivity of the wastewater should be considered when designing new experiments to avoid the need for wastewater amendments to increase the conductivity. Also wastewater pretreatment prior to bioelectrochemical treatment could increase electricity production by increasing VFA content of TMP wastewater and this should be further studied.

Operation temperature of a MFC should reflect the temperature of the real wastewater streams to minimize the need for heating or cooling of the wastewater. For example, the TMP wastewaters have higher temperatures (50-80 °C) than brewery wastewaters (usually 25-38 °C) and for this reason TMP wastewater treatment should be studied at elevated temperatures [5,162]. The preliminary experiments in an H-type MFCs with xylose demonstrated electricity generation at

55 °C, but more research is needed at different temperatures and with real wastewaters to study the feasibility of TMP wastewater bioelectrochemical treatment at higher temperatures [161].

The experiments conducted in different MFCs demonstrated that higher COD removals were obtained in the up-flow MFC compared to the air-cathode and three-chamber MFCs. In the up-flow MFCs, the anolyte flow increases the availability of substrates for the biofilm growing on the solid anode increasing the rate of wastewater treatment and improving mass transfer and diffusion [54,113]. Up-flow MFCs with granular anode materials could also be suitable for bioelectrochemical treatment [113]. However, the studied up-flow MFC still requires further optimization to increase power density due to the small membrane area between anode and cathode electrodes and the long distance between the electrodes [144]. Also potassium ferricyanide is suitable only in laboratory-scale experiments, but not in real applications [86]. The terminal electron acceptor should be replaced with more sustainable oxidant, such as oxygen in an air-cathode.

# 8 REFERENCES


[1] I. Punda, Agribusiness Handbook, FAO, 2009. www.eastagri.org.

[2] European Commission, Best Available Techniques (BAT) Reference Document for the Production of Pulp, Paper and Board, 2015. doi:10.2791/370629.

[3] Food and Agriculture Organization of the United Nations, FAOSTAT, (2018). http://www.fao.org/faostat/en/#data/QD/visualize (accessed January 16, 2019).

[4] R. Toczyłowska-Mamińska, Limits and perspectives of pulp and paper industry wastewater treatment – A review, Renew. Sustain. Energy Rev. 78 (2017) 764–772. doi:10.1016/j.rser.2017.05.021.

[5] G.S. Simate, J. Cluett, S.E. Iyuke, E.T. Musapatika, S. Ndlovu, L.F. Walubita, A.E. Alvarez, The treatment of brewery wastewater for reuse: State of the art, Desalination. 273 (2011) 235–247. doi:10.1016/j.desal.2011.02.035.

[6] G. Mininni, G. Laera, G. Bertanza, M. Canato, A. Sbrilli, Mass and energy balances of sludge processing in reference and upgraded wastewater treatment plants, Environ. Sci. Pollut. Res. 22 (2015) 7203–7215. doi:10.1007/s11356-014-4013-2.

[7] A.E. Cioabla, I. Ionel, G.-A. Dumitrel, F. Popescu, Comparative study on factors affecting anaerobic digestion of agricultural vegetal residues, Biotechnol. Biofuels. 5 (2012) 1–9. doi:10.1186/1754-6834-5-39.

[8] A. Doubla, S. Laminsi, S. Nzali, E. Njoyim, J. Kamsu-Kom, J.L. Brisset, Organic pollutants abatement and biodecontamination of brewery effluents by a non-thermal quenched plasma at atmospheric pressure, Chemosphere. 69 (2007) 332–337. doi:10.1016/j.chemosphere.2007.04.007.

[9] K.J. Chae, M.J. Choi, K.Y. Kim, F.F. Ajayi, W. Park, C.W. Kim, I.S. Kim, Methanogenesis control by employing various environmental stress conditions in two-chambered microbial fuel cells, Bioresour. Technol. 101 (2010) 5350–5357. doi:10.1016/j.biortech.2010.02.035.

[10] R. Sierra-Alvarez, G. Lettinga, The methanogenic toxicity of wastewater lignins and lignin related compounds, J. Chem. Technol. Biotechnol. 50 (1991) 443–455.

[11] Vijayaraghavan, Biohydrogen Generation from Beer Brewery Wastewater Using an Anaerobic Contact Filter, J. Am. Soc. Brew. Chem. 65 (2007) 110–115. doi:10.1094/ASBCJ-2007-0208-01.

[12] P. Dessì, E. Porca, A.M. Lakaniemi, G. Collins, P.N.L. Lens, Temperature control as key factor for optimal biohydrogen production from thermomechanical pulping wastewater, Biochem. Eng. J. 137 (2018) 214–221. doi:10.1016/j.bej.2018.05.027.

[13] Y. Feng, W. He, J. Liu, X. Wang, Y. Qu, N. Ren, A horizontal plug flow and stackable pilot microbial fuel cell for municipal wastewater treatment, Bioresour. Technol. 156 (2014) 132–138. doi:10.1016/j.biortech.2013.12.104.

[14] H. Hiegemann, D. Herzer, E. Nettmann, M. Lübken, P. Schulte, K.G. Schmelz, S. Gredigk-Hoffmann, M. Wichern, An integrated 45 L pilot microbial fuel cell system at a full-scale wastewater treatment plant, Bioresour. Technol. 218 (2016) 115–122. doi:10.1016/j.biortech.2016.06.052.

[15] Z. Ge, Z. He, Long-term performance of a 200 liter modularized microbial fuel cell system treating municipal wastewater: Treatment, energy, and cost, Environ. Sci. Water Res. Technol. 2 (2016) 274–281. doi:10.1039/c6ew00020g.

[16] Y. Dong, Y. Qu, W. He, Y. Du, J. Liu, X. Han, Y. Feng, A 90-liter stackable baffled microbial fuel cell for brewery wastewater treatment based on energy self-sufficient mode, Bioresour. Technol. 195 (2015) 66–72. doi:10.1016/j.biortech.2015.06.026.

[17] R.K. Jung, S. Cheng, S.E. Oh, B.E. Logan, Power generation using different cation, anion, and ultrafiltration membranes in microbial fuel

cells, Environ. Sci. Technol. 41 (2007) 1004–1009. doi:10.1021/es062202m.

[18] M.E. Kokko, A.E. Mäkinen, M.L.K. Sulonen, J.A. Puhakka, Effects of anode potentials on bioelectrogenic conversion of xylose and microbial community compositions, Biochem. Eng. J. 101 (2015) 248–252. doi:10.1016/j.bej.2015.06.007.

[19] J. Hou, Z. Liu, Y. Li, S. Yang, Y. Zhou, A comparative study of graphene-coated stainless steel fiber felt and carbon cloth as anodes in MFCs, Bioprocess Biosyst. Eng. 38 (2015) 881–888. doi:10.1007/s00449-014-1332-0.

[20] H. Liu, S. Cheng, L. Huang, B.E. Logan, Scale-up of membrane-free single-chamber microbial fuel cells, J. Power Sources. 179 (2008) 274–279. doi:10.1016/j.jpowsour.2007.12.120.

[21] A. Janicek, Y. Fan, H. Liu, Design of microbial fuel cells for practical application: A review and analysis of scale-up studies, Biofuels. 5 (2014) 79–92. doi:10.4155/bfs.13.69.

[22] B.E. Logan, B. Hamelers, R. Rozendal, U. Schröder, J. Keller, S. Freguia, P. Aelterman, W. Verstraete, K. Rabaey, Microbial fuel cells: Methodology and technology, Environ. Sci. Technol. 40 (2006) 5181–5192. doi:10.1021/es0605016.

[23] D. Pant, A. Singh, G. Van Bogaert, S.I. Olsen, P.S. Nigam, L. Diels, K. Vanbroekhoven, Bioelectrochemical systems (BES) for sustainable energy production and product recovery from organic wastes and industrial wastewaters, RSC Adv. 2 (2012) 1248–1263. doi:10.1039/c1ra00839k.

[24] G. Reguera, K.P. Nevin, J.S. Nicoll, S.F. Covalla, T.L. Woodard, D.R. Lovley, Biofilm and nanowire production leads to increased current in Geobacter sulfurreducens fuel cells, Appl. Environ. Microbiol. 72 (2006) 7345–7348. doi:10.1128/AEM.01444-06.

[25] S.K. Butti, G. Velvizhi, M.L.K. Sulonen, J.M. Haavisto, E.O. Koroglu, A.Y. Cetinkaya, S. Singh, D. Arya, J. Annie Modestra, K. Vamsi Krishna, A. Verma, B. Ozkaya, A.-M. Lakaniemi, J.A. Puhakka, S. Venkata Mohan, Microbial electrochemical technologies with the perspective of harnessing bioenergy: Maneuvering towards upscaling, Renew. Sustain. Energy Rev.

53 (2016) 462–476. doi:10.1016/j.rser.2015.08.058.

[26] D.R. Bond, D.E. Holmes, L.M. Tender, D.R. Lovley, Electrode-Reducing Microorganisms That Harvest Energy from Marine Sediments, Science. 295 (2002) 483–485. doi:10.1126/science.1066771.

[27] W. Kong, Q. Guo, X. Wang, X. Yue, Electricity generation from wastewater using an anaerobic fluidized bed microbial fuel cell, Ind. Eng. Chem. Res. 50 (2011) 12225–12232. doi:10.1021/ie2007505.

[28] M. Kokko, S. Epple, J. Gescher, S. Kerzenmacher, Effects of wastewater constituents and operational conditions on the composition and dynamics of anodic microbial communities in bioelectrochemical systems, Bioresour. Technol. 258 (2018) 376–389. doi:10.1016/j.biortech.2018.01.090.

[29] K. Rabaey, J. Rodríguez, L.L. Blackall, J. Keller, P. Gross, D. Batstone, W. Verstraete, K.H. Nealson, Microbial ecology meets electrochemistry: Electricity-driven and driving communities, ISME J. 1 (2007) 9–18. doi:10.1038/ismej.2007.4.

[30] A.Y. Cetinkaya, O.K. Ozdemir, A. Demir, B. Ozkaya, Electricity Production and Characterization of High-Strength Industrial Wastewaters in Microbial Fuel Cell, Appl. Biochem. Biotechnol. 182 (2017) 468–481. doi:10.1007/s12010-016-2338-7.

[31] C. Gao, A. Wang, W.-M. Wu, Y. Yin, Y.-G. Zhao, Enrichment of anodic biofilm inoculated with anaerobic or aerobic sludge in single chambered air-cathode microbial fuel cells, Bioresour. Technol. 167 (2014) 124–132. doi:10.1016/j.biortech.2014.05.120.

[32] P.G. Dennis, B. Virdis, I. Vanwonterghem, A. Hassan, P. Hugenholtz, G.W. Tyson, K. Rabaey, Anode potential influences the structure and function of anodic electrode and electrolyte-associated microbiomes, Sci. Rep. 6 (2016) 1–11. doi:10.1038/srep39114.

[33] F. Zhang, X. Xia, Y. Luo, D. Sun, D.F. Call, B.E. Logan, Improving startup performance with carbon mesh anodes in separator electrode assembly microbial fuel cells, Bioresour. Technol. 133 (2013) 74–81. doi:10.1016/j.biortech.2013.01.036.

[34] G. Götz, S.U. Geißen, A. Ahrens, S. Reimann, Adjustment of the wastewater matrix for optimization of membrane systems applied for water reuse in breweries, J. Memb. Sci. 465 (2014) 68–77. doi:10.1016/j.memsci.2014.04.014.

[35] A. Kaur, H.C. Boghani, I. Michie, R.M. Dinsdale, A.J. Guwy, G.C. Premier, Inhibition of methane production in microbial fuel cells: Operating strategies which select electrogens over methanogens, Bioresour. Technol. 173 (2014) 75–81. doi:10.1016/j.biortech.2014.09.091.

[36] P. Chatterjee, P. Dessì, M. Kokko, A.M. Lakaniemi, P. Lens, Selective enrichment of biocatalysts for bioelectrochemical systems: A critical review, Renew. Sustain. Energy Rev. 109 (2019) 10–23. doi:10.1016/j.rser.2019.04.012.

[37] C.I. Torres, R. Krajmalnik-Brown, P. Parameswaran, A.K. Marcus, G. Wanger, Y.A. Gorby, B.E. Rittmann, Selecting Anode-Respiring Bacteria Based on Anode Potential : Phylogenetic , Electrochemical , and Microscopic Characterization, 43 (2009) 9519–9524. doi:10.1021/es902165y.

[38] X. Zhu, M.D. Yates, M.C. Hatzell, H.A. Rao, P.E. Saikaly, B.E. Logan, Microbial Community Composition Is Unaffected by Anode Potential, Environ. Sci. Technol. 48 (2014) 1352–1358. doi:10.1021/es404690q.

[39] Y. Ahn, B.E. Logan, Domestic wastewater treatment using multi-electrode continuous flow MFCs with a separator electrode assembly design, Appl. Microbiol. Biotechnol. 97 (2013) 409–416. doi:10.1007/s00253-012-4455-8.

[40] O. Lefebvre, Y. Shen, Z. Tan, A. Uzabiaga, I.S. Chang, H.Y. Ng, A comparison of membranes and enrichment strategies for microbial fuel cells, Bioresour. Technol. 102 (2011) 6291–6294. doi:10.1016/j.biortech.2011.02.003.

[41] X. Xia, X. Cao, P. Liang, X. Huang, S. Yang, G. Zhao, Electricity generation from glucose by a Klebsiella sp. in microbial fuel cells, Appl. Microbiol. Biotechnol. 87 (2010) 383–390. doi:10.1007/s00253-010-2604-5.

[42] Y. Qu, Y. Feng, X. Wang, B.E. Logan, Use of a Coculture To Enable Current Production by Geobacter sulfurreducens, Appl. Environ. Microbiol. 78 (2012) 3484–3487. doi:10.1128/aem.00073-12.

[43] L. Lu, D. Xing, N. Ren, B.E. Logan, Syntrophic interactions drive the hydrogen production from glucose at low temperature in microbial electrolysis cells, Bioresour. Technol. 124 (2012) 68–76. doi:10.1016/j.biortech.2012.08.040.

[44] D. Xing, S. Cheng, B.E. Logan, J.M. Regan, Isolation of the exoelectrogenic denitrifying bacterium Comamonas denitrificans based on dilution to extinction, Appl. Microbiol. Biotechnol. 85 (2010) 1575–1587. doi:10.1007/s00253-009-2240-0.

[45] P.T. Ha, T.K. Lee, B.E. Rittmann, J. Park, I.S. Chang, Treatment of alcohol distillery wastewater using a bacteroidetes-dominant thermophilic microbial fuel cell, Environ. Sci. Technol. 46 (2012) 3022–3030. doi:10.1021/es203861v.

[46] P. Parameswaran, C.I. Torres, H.S. Lee, B.E. Rittmann, R. Krajmalnik-Brown, Hydrogen consumption in microbial electrochemical systems (MXCs): The role of homo-acetogenic bacteria, Bioresour. Technol. 102 (2011) 263–271. doi:10.1016/j.biortech.2010.03.133.

[47] B. Min, S. Cheng, B.E. Logan, Electricity generation using membrane and salt bridge microbial fuel cells, Water Res. 39 (2005) 1675–1686. doi:10.1016/j.watres.2005.02.002.

[48] B. Logan, S. Cheng, V. Watson, G. Estadt, Graphite fiber brush anodes for increased power production in air-cathode microbial fuel cells, Environ. Sci. Technol. 41 (2007) 3341–3346. doi:10.1021/es062644y.

[49] A. ter Heijne, H.V.M. Hamelers, M. Saakes, C.J.N. Buisman, Performance of non-porous graphite and titanium-based anodes in microbial fuel cells, Electrochim. Acta. 53 (2008) 5697–5703. doi:10.1016/j.electacta.2008.03.032.

[50] S. Wu, H. Li, X. Zhou, P. Liang, X. Zhang, Y. Jiang, X. Huang, A novel pilot-scale stacked microbial fuel cell for efficient electricity generation and wastewater treatment, Water Res. 98 (2016) 396–403. doi:10.1016/j.watres.2016.04.043.

[51] M. Lu, S. Chen, S. Babanova, S. Phadke, M. Salvacion, A. Mirhosseini, S. Chan, K. Carpenter, R. Cortese, O. Bretschger, Long-term performance of a 20-L continuous flow microbial fuel cell for treatment of brewery wastewater, J. Power Sources. 356 (2017) 274–287. doi:10.1016/j.jpowsour.2017.03.132.

[52] L. Zhuang, Y. Yuan, Y. Wang, S. Zhou, Long-term evaluation of a 10-liter serpentine-type microbial fuel cell stack treating brewery wastewater, Bioresour. Technol. 123 (2012) 406–412. doi:10.1016/j.biortech.2012.07.038.

[53] A. Karluvali, E.O. Köroğlu, N. Manav, A.Y. Çetinkaya, B. Özkaya, Electricity generation from organic fraction of municipal solid wastes in tubular microbial fuel cell, Sep. Purif. Technol. 156 (2015) 502–511. doi:10.1016/j.seppur.2015.10.042.

[54] C.H. Lay, M.E. Kokko, J.A. Puhakka, Power generation in fed-batch and continuous up-flow microbial fuel cell from synthetic wastewater, Energy. 91 (2015) 235–241. doi:10.1016/j.energy.2015.08.029.

[55] B. Min, B.E. Logan, Continuous electricity generation from domestic wastewater and organic substrates in a flat plate microbial fuel cell, Environ. Sci. Technol. 38 (2004) 5809–5814. doi:10.1021/es0491026.

[56] P. Aelterman, K. Rabaey, H.T. Pham, N. Boon, W. Verstraete, Continuous electricity generation at high voltages and currents using stacked microbial fuel cells, Environ. Sci. Technol. 40 (2006) 3388–3394. doi:10.1021/es0525511.

[57] H. Liu, R. Ramnarayanan, B.E. Logan, Production of Electricity during Wastewater Treatment Using a Single Chamber Microbial Fuel Cell, Environ. Sci. Technol. 38 (2004) 2281–2285. doi:10.1021/es034923g.

[58] K. Rabaey, P. Clauwaert, P. Aelterman, W. Verstraete, Tubular microbial fuel cells for efficient electricity generation, Environ. Sci. Technol. 39 (2005) 8077–8082. doi:10.1021/es050986i.

[59] L. Zhuang, Y. Zheng, S. Zhou, Y. Yuan, H. Yuan, Y. Chen, Scalable microbial fuel cell (MFC) stack for continuous real wastewater treatment, Bioresour. Technol. 106 (2012) 82–88. doi:10.1016/j.biortech.2011.11.019.

[60] S. Ishii, S. Suzuki, T.M. Norden-Krichmar, K.H. Nealson, Y. Sekiguchi, Y.A. Gorby, O. Bretschger, Functionally stable and phylogenetically diverse microbial enrichments from microbial fuel cells during wastewater treatment, PLoS One. 7 (2012). doi:10.1371/journal.pone.0030495.

[61] C. Lv, B. Liang, M. Zhong, K. Li, Y. Qi, Activated carbon-supported multi-doped graphene as high-efficient catalyst to modify air cathode in microbial fuel cells, Electrochim. Acta. 304 (2019) 360–369. doi:10.1016/j.electacta.2019.02.094.

[62] Y. Ahn, M.C. Hatzell, F. Zhang, B.E. Logan, Different electrode configurations to optimize performance of multi-electrode microbial fuel cells for generating power or treating domestic wastewater, J. Power Sources. 249 (2014) 440–445. doi:10.1016/j.jpowsour.2013.10.081.

[63] Y. Feng, X. Wang, B.E. Logan, H. Lee, Brewery wastewater treatment using air-cathode microbial fuel cells, Appl. Microbiol. Biotechnol. 78 (2008) 873–880. doi:10.1007/s00253-008-1360-2.

[64] A. Deeke, T.H.J.A. Sleutels, T.F.W. Donkers, H.V.M. Hamelers, C.J.N. Buisman, A. Ter Heijne, Fluidized capacitive bioanode as a novel reactor concept for the microbial fuel cell, Environ. Sci. Technol. 49 (2015) 1929–1935. doi:10.1021/es503063n.

[65] R. Rossi, D. Jones, J. Myung, E. Zikmund, W. Yang, Y.A. Gallego, D. Pant, P.J. Evans, M.A. Page, D.M. Cropek, B.E. Logan, Evaluating a multi-panel air cathode through electrochemical and biotic tests, Water Res. 148 (2019) 51–59. doi:10.1016/j.watres.2018.10.022.

[66] C. Santoro, C. Arbizzani, B. Erable, I. Ieropoulos, Microbial fuel cells: From fundamentals to applications. A review, J. Power Sources. 356 (2017) 225–244. doi:10.1016/j.jpowsour.2017.03.109.

[67] X. Zhu, B.E. Logan, Copper anode corrosion affects power generation in microbial fuel cells, J. Chem. Technol. Biotechnol. 89 (2014) 471–474. doi:10.1002/jctb.4156.

[68] C. Borsje, D. Liu, T.H.J.A. Sleutels, C.J.N. Buisman, A. ter Heijne, Performance of single carbon granules as perspective for larger scale capacitive bioanodes, J. Power Sources. 325 (2016) 690–696. doi:10.1016/j.jpowsour.2016.06.092.

[69] D. Bond, D. Lovley, Electricity Production by Geobacter sulfurreducens Attached to Electrodes, Appl. Environ. Microbiol. 69 (2003) 1548–1555. doi:10.1128/AEM.69.3.1548–1555.2003.

[70] G. Lepage, F.O. Albernaz, G. Perrier, G. Merlin, Characterization of a microbial fuel cell with reticulated carbon foam electrodes, Bioresour. Technol. 124 (2012) 199–207. doi:10.1016/j.biortech.2012.07.067.

[71] Y. Liu, F. Harnisch, K. Fricke, U. Schröder, V. Climent, J.M. Feliu, The study of electrochemically active microbial biofilms on different carbon-based anode materials in microbial fuel cells, Biosens. Bioelectron. 25 (2010) 2167–2171. doi:10.1016/j.bios.2010.01.016.

[72] A.M. Helmenstine, Table of Electrical Resistivity and Conductivity, (n.d.). https://www.thoughtco.com/table-of-electrical-resistivity-conductivity-608499 (accessed May 30, 2019).

[73] K. Sakai, S. Iwamura, R. Sumida, I. Ogino, S.R. Mukai, Carbon paper with a high surface area prepared from carbon nanofibers obtained through the liquid pulse injection technique, ACS Omega. 3 (2018) 691–697. doi:10.1021/acsomega.7b01822.

[74] U. Karra, S.S. Manickam, J.R. McCutcheon, N. Patel, B. Li, Power generation and organics removal from wastewater using activated carbon nanofiber (ACNF) microbial fuel cells (MFCs), Int. J. Hydrogen Energy. 38 (2013) 1588–1597. doi:10.1016/j.ijhydene.2012.11.005.

[75] X.L. Zhou, T.S. Zhao, Y.K. Zeng, L. An, L. Wei, A highly permeable and enhanced surface area carbon-cloth electrode for vanadium redox flow batteries, J. Power Sources. 329 (2016) 247–254. doi:10.1016/j.jpowsour.2016.08.085.

[76] F. Yu, C. Wang, J. Ma, Capacitance-enhanced 3D graphene anode for microbial fuel cell with long-time electricity generation stability, Electrochim. Acta. 259 (2018) 1059–1067. doi:10.1016/j.electacta.2017.11.038.

[77] X. LI, K. HUANG, S. LIU, N. TAN, L. CHEN, Characteristics of graphite felt electrode electrochemically oxidized for vanadium redox battery application, Trans. Nonferrous Met. Soc. China (English Ed. 17 (2007) 195–199. doi:10.1016/S1003-6326(07)60071-5.

[78] F. Yu, M. Zhou, X. Yu, Cost-effective electro-Fenton using modified graphite felt that dramatically enhanced on H2O2 electro-generation without external aeration, Electrochim. Acta. 163 (2015) 182–189. doi:10.1016/j.electacta.2015.02.166.

[79] H.R. Jiang, W. Shyy, Y.X. Ren, R.H. Zhang, T.S. Zhao, A room-temperature activated graphite felt as the cost-effective, highly active and stable electrode for vanadium redox flow batteries, Appl. Energy. 233–234 (2019) 544–553. doi:10.1016/j.apenergy.2018.10.059.

[80] J. González-García, P. Bonete, E. Expósito, V. Montiel, A. Aldaz, R. Torregrosa-Maciá, Characterization of a carbon felt electrode: structural and physical properties, J. Mater. Chem. 9 (1999) 419–426. doi:10.1039/a805823g.

[81] O. Smorygo, A. Marukovich, V. Mikutski, V. Stathopoulos, S. Hryhoryeu, V. Sadykov, Tailoring properties of reticulated vitreous carbon foams with tunable density, Front. Mater. Sci. 10 (2016) 157–167. doi:10.1007/s11706-016-0338-8.

[82] L. Huang, S. Cheng, F. Rezaei, B.E. Logan, Reducing organic loads in wastewater effluents from paper recycling plants using microbial fuel cells, Environ. Technol. 30 (2009) 499–504. doi:10.1080/09593330902788244.

[83] Y. Feng, Q. Yang, X. Wang, B.E. Logan, Treatment of carbon fiber brush anodes for improving power generation in air-cathode microbial fuel cells, J. Power Sources. 195 (2010) 1841–1844. doi:10.1016/j.jpowsour.2009.10.030.

[84] L. Huang, B.E. Logan, Electricity generation and treatment of paper recycling wastewater using a microbial fuel cell, Appl. Microbiol. Biotechnol. 80 (2008) 349–355. doi:10.1007/s00253-008-1546-7.

[85] M. Zhou, M. Chi, J. Luo, H. He, T. Jin, An overview of electrode materials in microbial fuel cells, J. Power Sources. 196 (2011) 4427–4435. doi:10.1016/j.jpowsour.2011.01.012.

[86] H. Rismani-Yazdi, S.M. Carver, A.D. Christy, O.H. Tuovinen, Cathodic limitations in microbial fuel cells: An overview, J. Power Sources. 180 (2008) 683–694. doi:10.1016/j.jpowsour.2008.02.074.

[87] S. Oh, B. Min, B. Logan, Cathode Performance as a Factor in Electricity in Electricity Generation in Microbial Fuel Cells, Environ. Sci. Technol. 38 (2004) 4900–4904. doi:10.1021/es049422p.

[88] C. Santoro, A. Serov, L. Stariha, M. Kodali, J. Gordon, S. Babanova, O. Bretschger, K. Artyushkova, P. Atanassov, Iron based catalysts from novel low-cost organic precursors for enhanced oxygen reduction reaction in neutral media microbial fuel cells, Energy Environ. Sci. 9 (2016) 2346–2353. doi:10.1039/c6ee01145d.

[89] I. Merino-Jimenez, C. Santoro, S. Rojas-Carbonell, J. Greenman, I. Ieropoulos, P. Atanassov, Carbon-Based Air-Breathing Cathodes for Microbial Fuel Cells, Catalysts. 6 (2016) 1–13. doi:10.3390/catal6090127.

[90] M. Kodali, C. Santoro, A. Serov, S. Kabir, K. Artyushkova, I. Matanovic, P. Atanassov, Air Breathing Cathodes for Microbial Fuel Cell using Mn-, Fe-, Co- and Ni-containing Platinum Group Metal-free Catalysts, Electrochim. Acta. 231 (2017) 115–124. doi:10.1016/j.electacta.2017.02.033.

[91] L. Zhuang, C. Feng, S. Zhou, Y. Li, Y. Wang, Comparison of membrane- and cloth-cathode assembly for scalable microbial fuel cells: Construction, performance and cost, Process Biochem. 45 (2010) 929–934. doi:10.1016/j.procbio.2010.02.014.

[92] H. Liu, B. Logan, Electricity Generation Using an Air-Cathode Single Chamber Microbial Fuel Cell in the Presence and Absence of a Proton Exchange Membrane, Environ. Sci. Technol. 38 (2004) 4040–4046. doi:10.1021/es0499344.

[93] F. Harnisch, U. Schröder, F. Scholz, The suitability of monopolar and bipolar ion exchange membranes as separators for biological fuel cells, Environ. Sci. Technol. 42 (2008) 1740–1746. doi:10.1021/es702224a.

[94] T.H.J.A. Sleutels, H.V.M. Hamelers, R.A. Rozendal, C.J.N. Buisman, Ion transport resistance in Microbial Electrolysis Cells with anion and cation exchange membranes, Int. J. Hydrogen Energy. 34 (2009) 3612–3620. doi:10.1016/j.ijhydene.2009.03.004.

[95] J.X. Leong, W.R.W. Daud, M. Ghasemi, K. Ben Liew, M. Ismail, Ion exchange membranes as separators in microbial fuel cells for bioenergy

conversion: A comprehensive review, Renew. Sustain. Energy Rev. 28 (2013) 575–587. doi:10.1016/j.rser.2013.08.052.

[96] T.H. Pham, K. Rabaey, P. Aelterman, P. Clauwaert, L. De Schamphelaire, N. Boon, W. Verstraete, Microbial fuel cells in relation to conventional anaerobic digestion technology, Eng. Life Sci. 6 (2006) 285–292. doi:10.1002/elsc.200620121.

[97] E.O. Köroğlu, B. Özkaya, C. Denktaş, M. Çakmakci, Electricity generating capacity and performance deterioration of a microbial fuel cell fed with beer brewery wastewater, J. Biosci. Bioeng. 118 (2014) 672–678. doi:10.1016/j.jbiosc.2014.05.006.

[98] X. Zhang, S. Cheng, X. Huang, B.E. Logan, Improved performance of single-chamber microbial fuel cells through control of membrane deformation, Biosens. Bioelectron. 25 (2010) 1825–1828. doi:10.1016/j.bios.2009.11.018.

[99] B. Christgen, K. Scott, J. Dolfing, I.M. Head, T.P. Curtis, An evaluation of the performance and economics of membranes and separators in single chamber microbial fuel cells treating domestic wastewater, PLoS One. 10 (2015) 1–13. doi:10.1371/journal.pone.0136108.

[100] Q. Wen, Y. Wu, L. Zhao, Q. Sun, Production of electricity from the treatment of continuous brewery wastewater using a microbial fuel cell, Fuel. 89 (2010) 1381–1385. doi:10.1016/j.fuel.2009.11.004.

[101] D.A. Ratkowsky, J. Olley, T.A. McMeekin, A. Ball, Relationship between temperature and growth rate of bacterial cultures., J. Bacteriol. 149 (1982) 1–5. http://www.ncbi.nlm.nih.gov/pubmed/7054139%0Ahttp://www.pubmedcentral.nih.gov/articlerender.fcgi?artid=PMC216584.

[102] Q. Wen, Y. Wu, D. Cao, L. Zhao, Q. Sun, Electricity generation and modeling of microbial fuel cell from continuous beer brewery wastewater, Bioresour. Technol. 100 (2009) 4171–4175. doi:10.1016/j.biortech.2009.02.058.

[103] Q. Wen, Y. Wu, L. Zhao, Q. Sun, F. Kong, Electricity generation and brewery wastewater treatment from sequential anode-cathode microbial fuel cell, J. Zhejiang Univ. B (Biomedicine Biotechnol. 11 (2010) 87–93.

doi:10.1631/jzus.B0900272.

[104] H. Wang, Y. Qu, D. Li, J.J. Ambuchi, W. He, X. Zhou, J. Liu, Y. Feng, Cascade degradation of organic matters in brewery wastewater using a continuous stirred microbial electrochemical reactor and analysis of microbial communities, Sci. Rep. 6 (2016) 1–12. doi:10.1038/srep27023.

[105] A.Y. Çetinkaya, E.O. Köroğlu, N.M. Demir, D.Y. Baysoy, B. Özkaya, M. Çakmakçi, Electricity production by a microbial fuel cell fueled by brewery wastewater and the factors in its membrane deterioration, Chinese J. Catal. 36 (2015) 1068–1076. doi:10.1016/S1872-2067(15)60833-6.

[106] K.P. Katuri, K. Scott, Electricity generation from the treatment of wastewater with a hybrid up-flow microbial fuel cell, Biotechnol. Bioeng. 107 (2010) 52–58. doi:10.1002/bit.22778.

[107] W. Miran, M. Nawaz, A. Kadam, S. Shin, J. Heo, J. Jang, D.S. Lee, Microbial community structure in a dual chamber microbial fuel cell fed with brewery waste for azo dye degradation and electricity generation, Environ. Sci. Pollut. Res. 22 (2015) 13477–13485. doi:10.1007/s11356-015-4582-8.

[108] J.M. Angosto, J.A. Fernández-López, C. Godínez, Brewery and liquid manure wastewaters as potential feedstocks for microbial fuel cells: A performance study, Environ. Technol. (United Kingdom). 36 (2015) 68–78. doi:10.1080/09593330.2014.937769.

[109] S.B. Velasquez-Orta, I.M. Head, T.P. Curtis, K. Scott, Factors affecting current production in microbial fuel cells using different industrial wastewaters, Bioresour. Technol. 102 (2011) 5105–5112. doi:10.1016/j.biortech.2011.01.059.

[110] K.V. Krishna, O. Sarkar, S. Venkata Mohan, Bioelectrochemical treatment of paper and pulp wastewater in comparison with anaerobic process: Integrating chemical coagulation with simultaneous power production, Bioresour. Technol. 174 (2014) 142–151. doi:10.1016/j.biortech.2014.09.141.

[111] B.E. Logan, Scaling up microbial fuel cells and other bioelectrochemical systems, Appl. Microbiol. Biotechnol. 85 (2010) 1665–1671. doi:10.1007/s00253-009-2378-9.

[112] I.A. Ieropoulos, A. Stinchcombe, I. Gajda, S. Forbes, I. Merino-Jimenez, G. Pasternak, D. Sanchez-Herranz, J. Greenman, Pee power urinal-microbial fuel cell technology field trials in the context of sanitation, Environ. Sci. Water Res. Technol. 2 (2016) 336–343. doi:10.1039/c5ew00270b.

[113] X. Wang, X. Yue, Q. Guo, Production of electricity during wastewater treatment using fluidized-bed microbial fuel cells, Chem. Eng. Technol. 37 (2014) 703–708. doi:10.1002/ceat.201300241.

[114] L. Dong, Y. Zhenhong, S. Yongming, K. Xiaoying, Z. Yu, Hydrogen production characteristics of the organic fraction of municipal solid wastes by anaerobic mixed culture fermentation, Int. J. Hydrogen Energy. 34 (2009) 812–820. doi:10.1016/j.ijhydene.2008.11.031.

[115] H. Chen, S. Chang, Q. Guo, Y. Hong, P. Wu, Brewery wastewater treatment using an anaerobic membrane bioreactor, Biochem. Eng. J. 105 (2016) 321–331. doi:10.1016/j.bej.2015.10.006.

[116] F. Xu, Z. Huang, H. Miao, H. Ren, M. Zhao, W. Ruan, Identical full-scale biogas-lift reactors (BLRs) with anaerobic granular sludge and residual activated sludge for brewery wastewater treatment and kinetic modeling, J. Environ. Sci. (China). 25 (2013) 2031–2040. doi:10.1016/S1001-0742(12)60268-X.

[117] A.P. Simpson, A.E. Lutz, Exergy analysis of hydrogen production via steam methane reforming, Int. J. Hydrogen Energy. 32 (2007) 4811–4820. doi:10.1016/j.ijhydene.2007.08.025.

[118] T. Meyer, E.A. Edwards, Anaerobic digestion of pulp and paper mill wastewater and sludge, Water Res. 65 (2014) 321–349. doi:10.1016/j.watres.2014.07.022.

[119] W.J. Gao, M.N. Han, C. (Charles) Xu, B.Q. Liao, Y. Hong, J. Cumin, M. Dagnew, Performance of submerged anaerobic membrane bioreactor for thermomechanical pulping wastewater treatment, J. Water Process Eng. 13 (2016) 70–78. doi:10.1016/j.jwpe.2016.05.004.

[120] R. Lakshmidevi, K. Muthukumar, Enzymatic saccharification and fermentation of paper and pulp industry effluent for biohydrogen production, Int. J. Hydrogen Energy. 35 (2010) 3389–3400.

doi:10.1016/j.ijhydene.2009.12.165.

[121] J. Streeck, C. Hank, M. Neuner, L. Gil-Carrera, M. Kokko, S. Pauliuk, A. Schaadt, S. Kerzenmacher, R.J. White, Bio-electrochemical conversion of industrial wastewater-COD combined with downstream methanol synthesis-an economic and life cycle assessment, Green Chem. 20 (2018) 2742–2762. doi:10.1039/c8gc00543e.

[122] F.I. Turkdogan, J. Park, E.A. Evans, T.G. Ellis, Evaluation of pretreatment using UASB and SGBR reactors for pulp and paper plants wastewater treatment, Water. Air. Soil Pollut. 224 (2013). doi:10.1007/s11270-013-1512-6.

[123] K.P. Katuri, K. Scott, I.M. Head, C. Picioreanu, T.P. Curtis, Microbial fuel cells meet with external resistance, Bioresour. Technol. 102 (2011) 2758–2766. doi:10.1016/j.biortech.2010.10.147.

[124] Y.K. Oh, S.H. Kim, M.S. Kim, S. Park, Thermophilic biohydrogen production from glucose with trickling biofilter, Biotechnol. Bioeng. 88 (2004) 690–698. doi:10.1002/bit.20269.

[125] T. Sangeetha, Z. Guo, W. Liu, M. Cui, C. Yang, L. Wang, A. Wang, Cathode material as an influencing factor on beer wastewater treatment and methane production in a novel integrated upflow microbial electrolysis cell (Upflow-MEC), Int. J. Hydrogen Energy. 41 (2016) 2189–2196. doi:10.1016/j.ijhydene.2015.11.111.

[126] S. Tejedor-Sanz, J.M. Ortiz, A. Esteve-Núñez, Merging microbial electrochemical systems with electrocoagulation pretreatment for achieving a complete treatment of brewery wastewater, Chem. Eng. J. 330 (2017) 1068–1074. doi:10.1016/j.cej.2017.08.049.

[127] J. Liu, C. Tian, X. Jia, J. Xiong, S. Dong, L. Wang, L. Bo, The brewery wastewater treatment and membrane fouling mitigation strategies in anaerobic baffled anaerobic/aerobic membrane bioreactor, Biochem. Eng. J. 127 (2017) 53–59. doi:10.1016/j.bej.2017.07.009.

[128] J. Li, S.M. Zicari, Z. Cui, R. Zhang, Processing anaerobic sludge for extended storage as anaerobic digester inoculum, Bioresour. Technol. 166 (2014) 201–210. doi:10.1016/j.biortech.2014.05.006.

[129] H.-C. Xu, P.-J. He, G.-Z. Wang, G.-H. Yu, L.-M. Shao, Enhanced storage stability of aerobic granules seeded with pellets, Bioresour. Technol. 101 (2010) 8031–8037. doi:10.1016/j.biortech.2010.05.062.

[130] S. Saheb Alam, F. Persson, B.M. Wilén, M. Hermansson, O. Modin, Effects of storage on mixed-culture biological electrodes, Sci. Rep. 5 (2015) 1–10. doi:10.1038/srep18433.

[131] Y. Lee, S.W. Oa, High speed municipal sewage treatment in microbial fuel cell integrated with anaerobic membrane filtration system, Water Sci. Technol. 69 (2014) 2548–2553. doi:10.2166/wst.2014.179.

[132] I. Ieropoulos, J. Winfield, J. Greenman, Effects of flow-rate, inoculum and time on the internal resistance of microbial fuel cells, Bioresour. Technol. 101 (2010) 3520–3525. doi:10.1016/j.biortech.2009.12.108.

[133] A.E. Mäkinen, C.H. Lay, M.E. Nissilä, J.A. Puhakka, Bioelectricity production on xylose with a compost enrichment culture, Int. J. Hydrogen Energy. 38 (2013) 15606–15612. doi:10.1016/j.ijhydene.2013.04.137.

[134] A. Van Haandel, J. Van der Lubbe, Handbook biological waste water treatment : design and optimisation of activated sludge systems, Leidschendam: Quist Publishing, 2007.

[135] Y. Hong, D.F. Call, C.M. Werner, B.E. Logan, Adaptation to high current using low external resistances eliminates power overshoot in microbial fuel cells, Biosens. Bioelectron. 28 (2011) 71–76. doi:10.1016/j.bios.2011.06.045.

[136] X. Zhu, J.C. Tokash, Y. Hong, B.E. Logan, Controlling the occurrence of power overshoot by adapting microbial fuel cells to high anode potentials, Bioelectrochemistry. 90 (2013) 30–35. doi:10.1016/j.bioelechem.2012.10.004.

[137] P. Aelterman, S. Freguia, J. Keller, W. Verstraete, K. Rabaey, The anode potential regulates bacterial activity in microbial fuel cells, Appl. Microbiol. Biotechnol. 78 (2008) 409–418. doi:10.1007/s00253-007-1327-8.

[138] R. Teather, Maintenance of Laboratory Strains of Obligately Anaerobic Rumen Bacteria, Appl. Environ. Microbiol. 44 (1982) 499–501.

[139] J. Liu, F. Zhang, W. He, X. Zhang, Y. Feng, B.E. Logan, Intermittent contact of fluidized anode particles containing exoelectrogenic biofilms for continuous power generation in microbial fuel cells, J. Power Sources. 261 (2014) 278–284. doi:10.1016/j.jpowsour.2014.03.071.

[140] L.G.B. Manhani, L.C. Pardini, F. Levy Neto, Assessement of tensile strength of graphites by the Iosipescu coupon test, Mater. Res. 10 (2007) 233–239. doi:10.1590/s1516-14392007000300003.

[141] E. Guerrini, P. Cristiani, M. Grattieri, C. Santoro, B. Li, S. Trasatti, Electrochemical Behavior of Stainless Steel Anodes in Membraneless Microbial Fuel Cells, J. Electrochem. Soc. 161 (2014) H62–H67. doi:10.1149/2.096401jes.

[142] D. Jiang, M. Curtis, E. Troop, K. Scheible, J. McGrath, B. Hu, S. Suib, D. Raymond, B. Li, A pilot-scale study on utilizing multi-anode/cathode microbial fuel cells (MAC MFCs) to enhance the power production in wastewater treatment, Int. J. Hydrogen Energy. 36 (2011) 876–884. doi:10.1016/j.ijhydene.2010.08.074.

[143] L. Huang, B.E. Logan, Electricity production from xylose in fed-batch and continuous-flow microbial fuel cells, Appl. Microbiol. Biotechnol. 80 (2008) 655–664. doi:10.1007/s00253-008-1588-x.

[144] S.E. Oh, B.E. Logan, Proton exchange membrane and electrode surface areas as factors that affect power generation in microbial fuel cells, Appl. Microbiol. Biotechnol. 70 (2006) 162–169. doi:10.1007/s00253-005-0066-y.

[145] T.C. Pannell, R.K. Goud, D.J. Schell, A.P. Borole, Effect of fed-batch vs. continuous mode of operation on microbial fuel cell performance treating biorefinery wastewater, Biochem. Eng. J. 116 (2016) 85–94. doi:10.1016/j.bej.2016.04.029.

[146] L. Zhou, D. Deng, Y. Zhang, W. Zhou, Y. Jiang, Y. Liu, Isolation of a facultative anaerobic exoelectrogenic strain LZ-1 and probing electron transfer mechanism in situ by linking UV/Vis spectroscopy and electrochemistry, Biosens. Bioelectron. 90 (2017) 264–268. doi:10.1016/j.bios.2016.11.059.

[147] A. Hasona, Y. Kim, F.G. Healy, L.O. Ingram, K.T. Shanmugam, Pyruvate

formate lyase and acetate kinase are essential for anaerobic growth of Escherichia coli on xylose, J. Bacteriol. 186 (2004) 7593–7600. doi:10.1128/JB.186.22.7593-7600.2004.

[148] K.-G. Chan, K.K. Tee, W.-F. Yin, J.-Y. Tan, Complete Genome Sequence of Pluralibacter gergoviae FB2, an N-Acyl Homoserine Lactone-Degrading Strain Isolated from Packed Fish Paste, Genome Announc. 2 (2014). doi:10.1128/genomea.01276-14.

[149] S. Xu, H. Liu, New exoelectrogen Citrobacter sp. SX-1 isolated from a microbial fuel cell, J. Appl. Microbiol. 111 (2011) 1108–1115. doi:10.1111/j.1365-2672.2011.05129.x.

[150] E. Kipf, J. Erben, R. Zengerle, J. Gescher, S. Kerzenmacher, Systematic investigation of anode materials for microbial fuel cells with the model organism G . sulfurreducens, Bioresour. Technol. Reports. 2 (2018) 29–37. doi:10.1016/j.biteb.2018.03.005.

[151] Y. Jangir, S. French, L.M. Momper, D.P. Moser, J.P. Amend, M.Y. El-Naggar, Isolation and Characterization of Electrochemically Active Subsurface Delftia and Azonexus Species, Front. Microbiol. 7 (2016). doi:10.3389/fmicb.2016.00756.

[152] V.B. Wang, K. Sivakumar, L. Yang, Q. Zhang, S. Kjelleberg, S.C.J. Loo, B. Cao, Metabolite-enabled mutualistic interaction between Shewanella oneidensis and Escherichia coli in a co-culture using an electrode as electron acceptor, Sci. Rep. 5 (2015) 1–11. doi:10.1038/srep11222.

[153] R.A. Prins, Isolation, culture, and fermentation characteristics of Selenomonas ruminantium var. bryanti var. n. from the rumen of sheep., J. Bacteriol. 105 (1971) 820–825.

[154] L. Sun, M. Toyonaga, A. Ohashi, D.M. Tourlousse, N. Matsuura, X.Y. Meng, H. Tamaki, S. Hanada, R. Cruz, T. Yamaguchi, Y. Sekiguchi, Lentimicrobium saccharophilum gen. nov., sp. nov., a strictly anaerobic bacterium representing a new family in the phylum bacteroidetes, and proposal of lentimicrobiaceae fam. nov., Int. J. Syst. Evol. Microbiol. 66 (2016) 2635–2642. doi:10.1099/ijsem.0.001103.

[155] M. Zeppilli, M. Villano, F. Aulenta, S. Lampis, G. Vallini, M. Majone, Effect of the anode feeding composition on the performance of a

continuous-flow methane-producing microbial electrolysis cell, Environ. Sci. Pollut. Res. 22 (2015) 7349–7360. doi:10.1007/s11356-014-3158-3.

[156] F. Barbirato, J.P. Grivet, P. Soucaille, A. Bories, 3-Hydroxypropionaldehyde, an inhibitory metabolite of glycerol fermentation to 1,3-propanediol by enterobacterial species, Appl. Environ. Microbiol. 62 (1996) 1448–1451.

[157] D.G. Petersen, I. Dahllöf, Improvements for comparative analysis of changes in diversity of microbial communities using internal standards in PCR-DGGE, FEMS Microbiol. Ecol. 53 (2005) 339–348. doi:10.1016/j.femsec.2005.01.001.

[158] M. Morotomi, F. Nagai, Y. Watanabe, Description of Christensenella minuta gen. nov., sp. nov., isolated from human faeces, which forms a distinct branch in the order Clostridiales, and proposal of Christensenellaceae fam. nov, Int. J. Syst. Evol. Microbiol. 62 (2012) 144–149. doi:10.1099/ijs.0.026989-0.

[159] V.R. Nimje, C.Y. Chen, C.C. Chen, J.S. Jean, A.S. Reddy, C.W. Fan, K.Y. Pan, H.T. Liu, J.L. Chen, Stable and high energy generation by a strain of Bacillus subtilis in a microbial fuel cell, J. Power Sources. 190 (2009) 258–263. doi:10.1016/j.jpowsour.2009.01.019.

[160] P.T. Mckenney, A. Driks, P. Eichenberger, The Bacillus subtilis endospore: Assembly and functions of the multilayered coat, Nat. Rev. Microbiol. 11 (2013) 33–44. doi:10.1038/nrmicro2921.

[161] P. Dessì, E. Porca, J. Haavisto, A.-M. Lakaniemi, G. Collins, P.N.L. Lens, Composition and role of the attached and planktonic microbial communities in mesophilic and thermophilic xylose-fed microbial fuel cells, RSC Adv. 8 (2018) 3069–3080. doi:10.1039/c7ra12316g.

[162] J. Rintala, S. Lepistö, Anaerobic treatment of thermomechanical pulping whitewater at 35–70°C, Water Res. 26 (1992) 1297–1305.

# PUBLICATIONS

# PUBLICATION I

**The effect of start-up on energy recovery and compositional changes in brewery wastewater in bioelectrochemical systems**

Haavisto, J.M., Kokko, M.E., Lakaniemi A-M., Sulonen, M.L.K. & Puhakka, J.A.

Submitted for publication

# PUBLICATION II

**Storing of exoelectrogenic anolyte for efficient microbial fuel cell recovery**

Haavisto, J.M., Lakaniemi, A-M. & Puhakka

This is an original preprint of an article published by Taylor & Francis in Environmental Technology on 17 Jan 2018, available online: http://www.tandfonline.com/10.1080/09593330.2017.1423395.

# Storing of exoelectrogenic anolyte for efficient microbial fuel cell recovery

Johanna M. Haavisto[1,*], Aino-Maija Lakaniemi[1], Jaakko A. Puhakka[1]

[1] Tampere University of Technology, Laboratory of Chemistry and Bioengineering, Tampere, Finland

* Corresponding author: P.O. Box 541, FI-33101 Tampere, Finland; E-mail: johanna.haavisto@tut.fi; Telephone: +358400486070

## Acknowledgement

This work was supported by the Academy of Finland (New Indigo ERA-Net Energy 2014; Project no. 283013)

# Storing of exoelectrogenic anolyte for efficient microbial fuel cell recovery


## Abstract

Starting up a microbial fuel cell (MFC) requires often a long-term culture enrichment period, which is a challenge after process upsets. The purpose of this study was to develop low cost storage for microbial fuel cell enrichment culture to enable prompt process recovery after upsets. Anolyte of an operating xylose-fed MFC was stored at different temperatures and for different time periods. Storing the anolyte for one week or one month at +4 °C did not significantly affect power production, but lag time for power production was increased from 2 days to 3 or 5 days, respectively. One month storing at -20 °C increased the lag time to 7 days. The average power density in these MFCs varied between 1.2 and 1.7 $W/m^3$. The share of dead cells (measured by live/dead staining) increased with storing time. After six-month storage the power production was insignificant. However, xylose removal remained similar in all cultures (99-100%) whilst volatile fatty acids production varied. The results indicate that fermentative organisms tolerated the long storage better than the exoelectrogens. As storing at +4 °C is less energy intensive compared to freezing, anolyte storage at +4 °C for maximum of one month is recommended as start-up seed for MFC after process failure to enable efficient process recovery.



## Keywords

Exoelectrogenic culture; mixed culture storage; freezing; refridgerating; process recovery

# 1. Introduction

Microbial fuel cells (MFC) can be used for treating industrial wastewaters and producing electricity simultaneously [1]. Previous research with MFCs has shown promising results for treating wastewaters from very different industrial operations such as brewery [2], vegetable oil industry [3], dairy production [4], chocolate factory [5], cassava mill [6], corn stover biorefinery [7], pharmaceutical production [8], textile colour industry [9] and paper recycling [10]. Industrial wastewaters are often characterized by variations in water flow and compositions. For example in brewery wastewater, high substrate concentrations are typically present at the end of a brewing batch, and brewing is usually directly followed by the use of tank-washing chemicals [11]. Pulp and paper mills exploit continuous processes, but the chemical compositions of wastewaters from debarking, wood chipping, pulp manufacturing, bleaching, paper making and recycling processes are very different [12] and some wood extractives cause antimicrobial effects [13]. Also, interruptions in industrial processes can make the wastewater treatment process challenging. For example, shutdowns caused by maintenance work can disturb the microbial community of a MFC [14].

After disturbances, prompt wastewater treatment process recovery and start-up are required for interminable environmental protection. Depending on the wastewater, starting up a MFC can require very long time [15]. In our previous experiment with a xylose-fed up-flow MFC, the start-up time for stable electricity production was 44 days with anaerobic municipal wastewater sludge as a seed (data not shown). The start-up time can be shortened by using seed culture from an operating MFC maintained at similar conditions [16]. This can also increase the power

density of the MFC [17,18]. However, continuous MFC operation just for maintaining enrichment cultures is not practical. For these reasons, means for enabling fast and low-cost process start-up and recovery of enriched exoelectrogenic cultures are needed.

Pure cultures of microroganisms are often stored by freezing with 10% glycerol as cryoprotective agent at -80 °C or colder [19]. Also pure culture of exoelectrogenic *Geobacter sulfurreducens* has been successfully stored by freezing [20] whereas the recovering electricity production from frozen mixed cultures has been difficult [21]. Other storage methods include freezing with other or without any cryoprotective agents, refrigerating (+4 °C), encapsulation [22] and drying e.g. with acetone [23] or by freeze-drying [22].

Wastewater treatment is always based on open microbial cultures, because they are able to degrade complex mixtures of organic substrates [24] and aceptic techniques are not needed as would be the case with pure culture operations. Storing of mixed microbial cultures has been studied at different temperatures, in different solutions and with different pretreatments such as drying or seeding with pellets. For example, Yükselen [25] studied preservation of UASB sludge at -18 °C, +4 °C, room temperature, and +37 °C for one year achieving highest methanogenic activity after storing at +37 °C. Li et al. [26] stored anaerobic sludge by drying for 4 months with insignificant loss in methane yield. Adav et al. [27] and Xu et al. [28] stored aerobic granules successfully for 3 months in different solutions and for 3 weeks as seeded with pellets (dewatered aerobic granules), respectively. However, different bacterial species have different survival rates during the storing and sometimes the most effective storage as measured by cell

viability test does not result in the most active culture [29]. The survival of mixed cultures enriched for anodic electricity production can differ significantly from other anaerobic cultures. Only one previous study [21] reports on electrochemically active enrichment culture storage. Alam et al. [21] stored an exoelectrogenic biofilm on anode electrode by refrigerating, freezing, or dehydrating, but original current production was not reached after storing. They suggested that dead cells in the biofilm prevented contact between exoelectrogens and the electrode. Storing exoelectrogenic enrichment culture suspension instead of biofilm would overcome this problem.

In this work, the effect of simple and low cost MFC anolyte storage for recovering stable power density and lag time required for current production were studied. Anolyte from an operating xylose-fed MFC was freezed (-20 °C) or refrigerated (+4 °C) with different storing times (from 1 week to 6 months) and compared with fresh anolyte for MFC start-up. To our knowledge, this is the first study on the survival of exoelectrogenic cultures and their ability to regain current production by storing enriched MFC anolyte. Xylose was used as substrate, because forest industry wastewaters contain xylose from glucuronoxylan containing wood material [30,31].

# 2. Materials and methods

## 2.1 MFC construction and operation

Experiments were conducted in 3-chamber MFCs (one anode chamber and two cathode chambers) (Figure 1). The anode chamber (123 mL) was separated from the cathode chambers (62 mL each) on both sides with a 41 $cm^2$ cation exchange membrane (CME7000) coated with

PtNi (1:1) as described by Cetinkaya et al. [32] with an exception that they used air cathodes in place of cathode chambers. The total volume of anolyte was 500 mL from which the extra volume was circulated at a rate of 100 mL/min over a recirculation bottle placed in a 37 °C water bath. Two carbon brush electrodes with titanium wires as current collectors were used as anode electrodes. Reference electrode (BASi RE-5B Ag/AgCl) was positioned between the two carbon brush electrodes for anode potential measurements. The two anode electrodes were connected through 100 Ω external resistance to the two cathode electrodes forming a single circuit. Cathode chambers were equipped with air spargers (ouput 50 L/h) that provided dissolved oxygen as the terminal electron acceptor. Carbon cloth (one for each cathode chamber) located against the membrane was used as cathode electrode (projected area of 41 $cm^2$).

Catholyte solution (pH 7) contained 15.6 mM $Na_2HPO_4$, 34.4 mM $NaH_2PO_4$, and 150 mM NaCl in distilled water. Anolyte solution was prepared as described by Mäkinen et al. [33] without addition of EDTA and resazurin. In addition, the concentration of yeast extract was reduced to 0.03 g/L in the beginning of the experiment and to 0.003 g/L after the first feeding cycle. Xylose (1.0 g/L) was used as substrate and pH of the feeding solution was adjusted to 7.0 with NaOH. MFCs were fed with interval of 6-8 days by replacing 50 mL of anolyte solution with fresh feed. If the volume of the anolyte decreased during the feeding cycle, the volume was adjusted back to 500 mL with the removed anolyte. During the operation 5 M NaOH was added into the anolytes if needed after the feeding to ensure that pH did not decrease below 6.0.

MFCs were inoculated with anolyte from an operating fed-batch MFC using xylose as a substrate after five months of enrichment at similar conditions. This culture was originally enriched from an anaerobic digester of a municipal wastewater treatment plant (Viinikanlahti, Tampere, Finland). The anolyte solution to be used as inoculum for new MFCs (25 mL for each) was stored for the experiments in 60 mL batches in freezer (-20 °C) or fridge (+4 °C) under nitrogen atmosphere. Culture reactivation was tested after storing the anolyte for one week (+4 °C), one month (+4 °C and -20 °C), and six months (+4 °C and -20 °C). In addition to this, reference cultures were started straight after anolyte collection without storing the inoculum. Frozen anolyte batches were defrosted at room temperature. MFCs were washed with 1 M NaOH and 70 % ethanol between the experiments. All the experiments were conducted as duplicates.

## 2.2 Analyses

### 2.2.1 Electrochemical measurements and calculations

Cell voltage and anode potential were recorded with 2 min intervals using Agilent 34970A data Acquisition/Switch Unit (Agilent, USA). Current and power densities were calculated against anode chamber volume using measured cell voltage data and external resistance according to Ohm's law. Cell voltage data was used also for measuring lag time (d), which was determined as the time needed for achieving 100 mV cell voltage with 100 Ω external resistance.

Linear sweep voltammetry (LSV) was conducted using a potentiostat (Palmsens3, Netherlands) with the scan rate of 1 mV/s in the end of the experiment, 1-3 days after the last feeding. Analysis was conducted starting from 0-50 mV higher cell voltage values compared to open

141 circuit voltage [34], which was measured after 30 min of stabilization. The measurement was
142 continued by lowering the cell voltage from the starting value (150-550 mV) to the final value of
143 0.005 mV. Internal resistance was calculated from the LSV data ($R_{internal}$ = U/I) by drawing a
144 power curve against voltage to find the place of the power curve peak on voltage axis and using
145 the data of this point for internal resistance calculations.

146

147 Coulombic efficiency (CE) was calculated from the xylose degradation and electrical current
148 data over the last full feeding cycle with the Equation 1 (modified from [34])

149 $$C_E = \frac{M_S \int_0^{t_1} I dt}{F b_{es} \Delta m_{xylose}}, \quad (1)$$

150 where Ms = molecular weight of xylose (g/mol), $t_1$ = length of feeding cycle (d), F = Faraday's
151 constant (96 485 C/mol*e), $b_{es}$ = number of electrons released per mol of xylose (20 e-), $\Delta m_{xylose}$
152 (g). The mass of degraded xylose was calculated by subtracting the measured xylose in the end
153 of the cycle from the concentration in the beginning of the same cycle.

154

155 ### 2.2.2 Chemical analyses

156 Concentrations of xylose and fatty acids (VFAs) were measured from the anolyte samples taken
157 before each feeding and in the end of the experiment. Also the anolyte pH was measured (WTW
158 pH 330 meter) from the same samples. After pH measurement the solid particles were removed
159 by centrifuging (10 min, 7500 x g) followed by filtering (0.2 µm polyester filter). Samples were
160 stored at -20 °C. Xylose concentration was measured using phenol-sulphuric acid method [35]
161 with the modifications described by Haavisto et al. [30]. VFA and alcohol (acetate, propionate,

butyrate, isobutyrate, valeric acid, ethanol, and butanol) concentrations were measured with gas chromatograph as described by Haavisto et al. [30].

### 2.2.3 Microbial analyses

Microbial community samples were taken from the anode biofilms in the end of each experiment. The biofilm samples were obtained by sonicating the carbon brushes for 5 min in 0.9% NaCl. Then microbes were collected in a pellet with a centrifuge (10 min, 5000 x g) and by discarding the supernatant. The samples were stored at -20 °C and microbial communities were analyzed from defrosted samples as described by Haavisto et al. [30]. DNA was extracted with PowerSoil DNA isolation kit (MO BIO Laboratories, Inc., Carlsbad, CA, USA) and partial 16SrRNA genes were amplified with PCR using GC-BacV3f [36] and 907r [37] primers as described by Koskinen et al. [38]. After separating DNA sequences with DGGE according to Lakaniemi et al. [39] the sequences were reamplified according to Koskinen et al. [38] and sequenced at Macrogen Inc. (Seoul, Korea). Sequence data was analyzed with BioEdit software and compared to known sequences by using BLAST (http://blast.ncbi.nlm.nih.gov/Blast.cgi). Two separate DGGE gels were prepared from which one contained biofilm samples from all the duplicate reactors while in the other gel the amount of samples was reduced by selecting only the communities with higher current density for easier comparison of different storing methods and times.

Microbial viability of the differently treated anolytes was estimated with LIVE/DEAD© BacLight™ Bacterial Viability Kit. Bacteria were stained with SYTO®9 and propidium iodide

(pretreatment methods modified from [40]). Samples (1 mL) were mixed with 50 mL sterile filtered 0.9% NaCl followed by 1 min sonication (Finnsonic m03, Finland). Diluted samples (50 or 100 µL) were further diluted to 1 mL volume with 0.01 M $Na_4P_2O_7$ and 5 µL of the mixture (1:1) of fluorescent stains was mixed to samples by vortexing for 10 s. After incubating mixtures for 15 min in dark the samples were filtered with polycarbonate membrane filter followed by the examination with an epifluorescence microscope to determine the viability based on cell wall integrity.

# 3. Results and discussion

## 3.1 Electricity production

The MFCs containing reference cultures without anolyte storing and cultures with different storing methods were compared. Reference cultures reached an average power density of 1.6 $W/m^3$ (141 mV as cell voltage, Table 1). After storing at +4 °C or at -20 °C for one week and one month, the average power densities of the last full feeding cycles were 1.2 – 1.7 $W/m^3$ whilst storing for six months in either temperature decreased power density to 0.004-0.06 $W/m^3$. The corresponding current densities were 10 - 12 $A/m^3$ and 0.6 - 2 $A/m^3$, respectively. Average anode potentials were also more than 200 mV less negative after six months storing compared to the shorter storage times (Table 1). Alam et al. [21] reported 75% of the original current density after 5 weeks storage of biofilm containing anode electrode at +4 °C, representing higher activity reduction than obtained after one month in this study (87% of the current density remaining after the storage). Also freezing with 10% glycerol at -70 °C for 5 weeks decreased current density about 75% in the study of Alam et al. [21]. Our MFCs did not show decrease in the average

current density (based on the last full feeding cycle, days 14-21) after one month storing at -20 °C. However, the standard deviation between the duplicate MFCs after one month storing at -20 °C in this study was 20% of the average current density. In our study, internal resistance was over 700 Ω after six months storing at +4 and -20 °C, but only 40-47 Ω in all the other reactors. Massive increase in internal resistance during 6 month storage was likely due to changes in microbial community [41].

## 3.2 Lag time and cell viability

Lag time for reaching 100 mV cell voltage (i.e. power density of 0.8 $W/m^3$) was 1.9 d without storing and storing increased it by at least 0.8 days. Lag time increased with increasing storing time and was longest with storing at -20 °C for one month (Table 1). In all MFCs the power density increased close to the highest stable values in 1 ± 1 d after reaching the set point value of 0.8 $W/m^3$ (example power density curves in shown Figure S1). Average power densities (see section 3.1) and anode potentials (Table 1) obtained during the stable MFC operation (last full feeding cycle) were similar in MFCs started up with anolytes stored for one week and one month. After storing the anolyte for six months (at +4 °C or -20 °C) electrochemical activity did not recover. The observed lag times are well in accordance with Alam et al. [21] reporting faster re-activation in electrochemical activity after storing the anode biofilm at +4 °C compared to freezing (at -70 °C) with glycerol. The lag times (2-7 days) observed in this study were also significantly shorter than the start-up time (44 days) of our xylose-fed up-flow reactor seeded with anaerobic sludge from municipal wastewater treatment plant.

227 Cell viability after anolyte storing was calculated as live/dead stained cells by fluorescence
228 microscopy. Without storing, approximately half of the cells stained as alive. After one-week
229 storage at +4 °C, share of dead cells was 60%, while the longer storing times decreased viability
230 more. After one month storing at -20 °C or +4 °C, the share of dead cells were 80% and 85-95%,
231 respectively. After six months at +4 °C and -20 °C, the shares of dead cells were 95% and >98%,
232 respectively. The cell viability measurements were disturbed by background noise. In addition,
233 some of the cells may stain red with propidium iodide although being viable, as the method
234 actually assays membrane integrity and not directly cell viability [42,43]. However, the results
235 show that the relative share of cells stained as dead increased with increasing storing time
236 (Figure 2). Interestingly the share of dead cells was lower at -20 °C compared to +4 °C at the
237 same storing time, whilst the lag time for power production was longer for the anolyte stored at -
238 20 °C. This shows that total number of microorganisms that survived storing (i.e. retained their
239 membrane integrity) does not directly correlate with activity of stored exoelectrogenic
240 microorganisms. This is in accordance with the observations of Balfour-Cunningham et al. [29],
241 who reported that the most effective storage based on cell viability measurement does not always
242 result in the most active culture.

243 ### 3.3 Metabolic activity

244 Xylose removal (99-100%) during the last full feeding cycle after all tested storing times
245 indicated high activity of xylose-utilizing microorganisms. However, the CEs were relatively
246 low with the highest calculated values being 14 ± 3% (Table 2). After six months storing the CEs
247 were only 0.7 - 2.8%, but a CE of 10% or higher was obtained in all the other MFCs. Measured
248 CEs were low compared to the other published results for xylose-fed MFCs [44-46]. However, in

249 this study, the CE values were calculated against fed xylose as compared to Huang et al. [44],
250 Sun et al. [45], and Huang & Angelidaki [46], reporting values against removed COD.

251

252 Residual VFA concentrations in the end of the last full feeding cycle increased with storing time
253 indicating efficient recovery of VFA-producing fermentative microorganisms. VFAs included
254 mainly acetate, propionate and butyrate as also other xylose-fed MFCs [47,48]. The highest
255 concentrations of total VFAs were obtained after six months storing (Table 2). Residual
256 propionate and butyrate increased with increasing storing time, whereas acetate concentrations
257 were similar after one month and six months storing at -20 °C (Table 2). Propionate
258 concentrations in MFCs with anolyte after one month storing were only 50% of the values
259 obtained after six months storage. These results show that xylose fermenting microorganisms
260 regained their activity after storage. Acetate and propionate are typically suitable substrates for
261 exoelectrogens [49], but they were not efficiently utilized and rather accumulated to the anolyte.
262 This indicates that long-term storage at +4 and -20 °C directly affected the exoelectrogens rather
263 than other microorganisms involved in the anaerobic degradation of xylose.

264

## 265 3.4 Microbial community

266 Microbial community analysis (Figure 3) revealed the presence of well-known exoelectrogen
267 *Geobacter sulfurreducens* [50] with 97.9-99.6% similarity in all the MFCs with considerable
268 power production (reactors with anolyte storing time of one month or less). Alam et al. [21] also
269 found *G. sulfurreducens* after 5 weeks storing at +4 °C and freezing at -70 °C with glycerol, but
270 reported that the share of *G. sulfurreducens* in microbial community decreased from 70% in the

271 original biofilm to 10-30%. Alam et al. [21] also reported that the storing of the anode biofilm
272 increased the diversity of the microbial community. Similarly in this study, some
273 microorganisms that were not detected in MFC inoculated with fresh cultures, became enriched
274 and thus, detectable from MFCs inoculated with the stored anolytes. These included species
275 having high similarity to *Lentimicrobium saccharophilum*, *Pluralibacter gergoviae* and
276 *Citrobacter freundii* (Figure 3, Table 3). DGGE-profiling of mixed cultures is, at best, a semi-
277 quantitative analysis. This method does not detect minor quantities of DNA and some of the
278 microorganisms present in samples remain undetected [51,52]. This may be the case for some
279 microorganisms in fresh, unstored samples. During storage, the microbial composition may
280 change and re-cultivation may thus, result in enrichment of microorganisms that remained
281 undetected in original samples.

282

283 After one month storage at -20 °C, the electricity production in the duplicate reactors was
284 different. Therefore the microbial communities from both MFCs' anodes were characterized.
285 The anode biofilm with lower power density did not contain *G. sulfurreducens*, but another
286 exoelectrogen, *Citrobacter freundii* [53]. *C. freundii* was present also in the biofilm of other
287 MFCs started with anolyte stored for one month either at +4 °C or -20 °C. The only bacterium
288 with known exoelectogenic activity found after six months storing at +4 °C was *Escherichia coli*
289 [54], but after six months storing at -20 °C no known exoelectrogenic bacteria were detected.
290 According to sequencing results (Table 3), band 4 identified as *E. coli* could be also
291 *Tumebacillus flagellatus*, but as an aerobe, it is unlikely that *T. flagellatus* would grow in anode
292 biofilm [55]. *E. coli* was found also from the other biofilm samples after storing anolyte at +4
293 °C.

All the MFC biofilms contained known fermentative bacteria (*E. coli*, *Proteiniphilum acetatigenes*, *C. freundii*, or *Lentimicrobium saccharophilum*) [56-59] and facultative anaerobes (*E. coli*, *C. freundii*, or *Pluralibacter gergoviae*) [53,56,60]. The presence of facultative anaerobes is important for the strict anaerobes, because facultative anaerobes are able to consume oxygen, which is potentially penetrating to the anode chamber from the cathode. Among the identified bacteria, *E. coli* is known to be able to degrade xylose [56] and it was found from most of the samples. The results of microbial community analysis are in line with metabolic activity results and give further evidence that long-term storage had direct influence on exoelectrogenic bacteria.

## 3.5. Implications

Based on the power production, xylose removal, and microbial community data, fermentative bacteria tolerated the storage better than exoelectrogenic bacteria both at -20 °C and +4 °C when the storing time was six months. Previous studies have shown that fermentative bacteria e.g. from cow rumen can be stored at least for two years at -20 °C with glycerol [61]. However, at +4 °C agar deep cultures of the same microbes lost viability already after 0.5-2 years [61]. Lower storing temperatures and use of cryoprotective chemicals such as glycerol generally result in higher stability and more successful preservation of microbial viability and activity [62]. In case of frozen cultures, the rate of temperature changes both during freezing and thawing is also important for the survival of the microorganisms [62, 63].Temperatures below -140 °C are typically recommended for most efficient culture storage, as such temperatures rule out the

316 possibility of presence of even traces of liquid water that can cause cryoinjury especially if
317 temperature fluctuates during the storage [62, 64]. However, temperatures below -140 °C would
318 require specialized equipment and liquid nitrogen, while the focus of this study was on more
319 commonly available simple and low-cost storing methods available in e.g. wastewater treatment
320 facilities.

321

322 It has also been shown that subjection of microbial culture to certain adverse conditions before
323 storing can increase the tolerance of the culture to temperature shocks caused by storing at low
324 temperature [65]. No spore forming bacteria were identified in the biofilm samples of this study,
325 but some exoelectrogens, such as *Bacillus subtilis* [66,67], can form endospores to survive harsh
326 conditions, which could also significantly help storing exoelectrogenic cultures. However,
327 although inducing of intentional stress on the culture could be possible under laboratory
328 conditions, it would not be a viable option for real wastewater treatment applications, because it
329 could cause unwanted deterioration in the quality of the treated wastewater.

330

331 Based on the results of this study, storing time clearly affected the survival of bacteria and the
332 lag time for electricity production, when the anolyte what stored at +4 or -20 °C without any
333 cryoprotective agents or induced stress condition before the sampling. Storing anolyte of an
334 operating mixed culture MFC for one month at +4 or -20 °C can help to speed up the process
335 recovery with minimal power density losses on clean anode electrode after process disturbances.
336 In actual MFC treatment of wastewater, storage of effluent at +4 °C would serve as means to be

prepared for process upsets and their recovery. The stored anolyte should be changed with fresh on monthly basis.

## 4. Conclusions

The results of this study demonstrated that storing anolyte from an operating MFC for one month or less at +4 °C or -20 °C resulted in similar power density (1.2-1.7 $W/m^3$) as was obtained in reference MFCs started with fresh anolyte. Further, both the lag time of process recovery to reach reasonable cell voltage and the percentage of dead cells in the stored anolyte (based on live/dead staining) increased with increased storing time. After six months storing of the anolyte solution at either temperature, the power production remained negligible. Xylose removal was not affected by the storing remaining at 99-100% in all MFCs. Similarly, VFA producing microorganisms remained active in all storage conditions and produced acetate and propionate for exoelectrogens. Decreased power production during long-term storage was directly associated with exoelectrogenic bacteria. Anolyte storage at +4 °C for maximum of one month is recommended as start-up seed for MFC after process failure to enable efficient process recovery. This suggests that effluent storing from continuous-flow MFCs would be a practical way of being prepared for process upsets.

## References

[1] Butti, S., Velvizhi, G., Sulonen, M., Haavisto, J., Koroglu, E., Cetinkaya, A., Singh, S., Arya, D., Modestra, J., Krishna, K., Verma, A., Ozkaya, B., Lakaniemi, A-M., Puhakka,

J., Mohan, S. Microbial electrochemical technologies with the perspective of harnessing bioenergy: Maneuvering towards upscaling. Renev Sust Energ Rev. 2016; 53: 462-476.

[2] Feng, Y., Wang, X. Logan, B. & Lee, H. Brewery wastewater treatment using air-cathode microbial fuel cells. Appl Microbiol Biot. 2008; 78(5): 873-880.

[3] Abbasi, U., Jin, W., Pervez, A., Bhatti, Z., Tariq, M., Shaheen, S., Iqbal, A. & Mahmood, Q. Anaerobic microbial fuel cell treating combined industrial wastewater: Correlation of electricity generation with pollutants. Bioresour Technol. 2016; 200: 1-7.

[4] Venkata Mohan, S., Velvizhi, M., Babu, L. & Sarma, P. Bio-catalyzed electrochemical treatment of real field dairy wastewater with simultaneous power generation. Biochem Eng J. 2010; 51(1-2): 32-39.

[5] Patil, S., Surakasi, V., Koul, S., Ijmulwar, S., Vivek, A., Shouche, Y. & Kapadnis, B. Electricity generation using chocolate industry wastewater and its treatment in activated sludge based microbial fuel cell and analysis of developed microbial community in the anode chamber. Bioresour Technol. 2009; 100(21): 5132-5139.

[6] Kaewkannetra, P., Chiwes, W. & Chiu, T. Treatment of cassava mill wastewater and production of electricity through microbial fuel cell technology. Fuel. 2011; 90(8): 2746-2750.

[7] Pannell, T., Goud, R., Schell, D. & Borole, A. Effect of fed-batch vs. continuous mode of operation on microbial fuel cell performance treating biorefinery wastewater. Biochem Eng J. 2016; 116: 85-94.

[8] Velvizhi, G. & Venkata Mohan, S. Electrogenic activity and electron losses under increasing organic load of recalcitrant pharmaceutical wastewater. Int J Hydrogen Energ. 2012; 37(7): 5969-5978.

[9] Fernando, E., Keshavarz, T., Kyazze, G. & Fonseka, K. Treatment of colour industry wastewaters with concomitant bioelectricity production in a sequential stacked mono-chamber microbial fuel cells-aerobic system. Environ Technol. 2016; 37(2): 255-264.

[10] Huang, L,. Chen, S., Rezaei, F. & Logan, B. Reducing organic loads in wastewater effluents from paper recycling plants using microbial fuel cells. Environ Technol. 2009; 30(5): 499-504.

[11] Simate, G., Cluett, J., Iyuke, S., Musapatika, E., Ndlovu, S., Walubita, L. & Alvarez, A. The treatment of brewery wastewater for reuse: State of the art. Desalination. 2011; 273(2-3): 235-247.

[12] Ashrafi, O., Yerushalmi, L. & Haghighat, F. Wastewater treatment in the pulp-and-paper industry: A review of treatment processes and the associated greenhouse gas emission. J Environ Manage. 2015; 158: 146-157.

[13] Lindberg, L., Willför, S. & Holmbom, B. Antibacterial effects of knotwood extractives on paper mill bacteria. J Ind Microbiol Biotechnol. 2004; 31(3): 137-147.

[14] Jadhav, G. & Ghangrekar, M. Performance of microbial fuel cell subjected to variation in pH, temperature, external load and substrate concentration. Bioresour Technol. 2009; 100(2): 717-723.

[15] Liu, G., Yates, M., Cheng, S., Call, D., Sun, D. & Logan, B. Examination of microbial fuel cell start-up times with domestic wastewater and additional amendments. Bioresour Technol. 2011; 102(15): 7301-7306.

[16] Vogl, A., Bischof, F. & Wichern, M. Surface-to-surface biofilm transfer: a quick and reliable startup strategy for mixed culture microbial fuel cells. Water Sci Technol. 2016; 73(8): 1769-1776.

[17] Kim, J., Min, B. & Logan, B. Evaluation of procedures to acclimate a microbial fuel cell for electricity generation. Appl Microbiol Biotechnol. 2005; 68(1): 23-30.

[18] Baudler, A., Riedl, S. & Schröder, U. Long-term performance of primary and secondary electroactive biofilms using layered corrugated carbon electrodes. Front Energy Res. 2014; 2, Article number 30.

[19] Prakash, O., Nimonkar, Y., Shouche, Y. Practice and prospects of microbial preservation. FEMS Microbiol Lett. 2013; 339(1): 1-9.

[20] Jiang, X., Hu, J., Petersen, E., Fitzgerald, L., Jackan, C., Lieber, A., Ringeisen, B., Lieber, C. & Biffinger, J. Probing single- to multi-cell level charge transport in *Geobacter sulfurreducens* DL-1. Nat commun. 2013; 4, Article number: 2751.

[21] Alam, S., Persson, F., Wilén, B-M., Hermansson, M. & Modin, O. Effects of storage on mixed-culture biological electrodes. Sci Rep. 2015; 5, Article number: 18433.

436

437 [22] Bjerketorp, J., Håkansson, S., Belkin, S. & Jansson, J. Advances in preservation methods:
438 keeping biosensor microorganisms alive and active. Curr Opin Biotechnol. 2006; 17(1):
439 43-49.

440

441 [23] Lv, Y., Wan, C., Liu, X., Zhang, Y., Lee, D-J. & Tay, J-H. Drying and re-cultivation of
442 aerobic granules. Bioresour Technol. 2013; 129: 700-703.

443

444 [24] Liu, H. Microbial Fuel Cell: Novel Anaerobic Generation from Wastewater. In: Khanal,
445 S. Anaerobic Biotechnology for Bioenergy Production: Principles and Applications. USA
446 2008; Blackwell Publishing.

447

448 [25] Yükselen, M. Preservation characteristics of UASB sludges. J Environ Sci Health. Part
449 A. 1997; 32: 2069-2076.

450

451 [26] Li, J., Zicari, S., Cui, Z. & Zhang, R. Processing anaerobic sludge for extended storage as
452 anaerobic digester inoculum. Bioresour Technol. 2014; 166: 201-210.

453

454 [27] Adav, S., Lee, D-J. & Tay, J. Activity and structure of stored aerobic granules. Environ
455 Technol. 2007; 28(11): 1227-1235.

[28] Xu, H-C., He, P-J., Wang, G-Z, Yu, G-H. & Shao, L-M. Enhanced storage stability of aerobic granules seeded with pellets. Bioresour Technol. 2010; 101(21): 8031-8037.

[29] Balfour-Cunningham, A., Boxall, N., Banning, N. & Morris, C. Preservation of salt-tolerant acidophiles used for chalcopyrite bioleaching: Assessment of cryopreservation, liquid-drying and cold storage. Miner Eng. 2017; 106: 91-96.

[30] Haavisto, J., Kokko, M., Lay, C-H. & Puhakka, J. Effect of hydraulic retention time on continuous electricity production from xylose in up-flow microbial fuel cell. Int J Hydrogen Energ (in press). 2017; https://doi.org/10.1016/j.ijhydene.2017.05.068.

[31] Willför, S. Sundberg, A., Pranovich, A. & Holmbom, B. Polysaccharides in some industrially important hardwood species. Wood Sci Technol. 2005; 39(8): 601-617.

[32] Cetinkaya, A., Ozdemir, O., Demir, A. & Ozkaya, B. Electricity production and Characterization of High-Strength Industrial Wastewaters in Microbial Fuel Cell. Appl Biochem Biotechnol. 2017; 182(2): 468-481.

475 [33] Mäkinen, A. E., Nissilä, M. E. & Puhakka, J. A. Dark fermentative hydrogen production
476 from xylose by a hot spring enrichment culture. Int J Hydrogen Energ. 2012; 37(17):
477 12234-12240.

478

479 [34] Logan, B., Hamelers, B., Rozendal, R., Schröder, U., Keller, J., Freguia, S., Aelterman,
480 P., Verstraete, W. & Rabaey, K. Microbial Fuel Cells: Methodology and Technology.
481 Environ Sci Technol. 2006; 40(17): 5181-5192.

482

483 [35] Dubois, M., Gilles, K. A., Hamilton, J. K., Rebers, P. A. & Smith, F. Colorimetric
484 Method for Determination of Sugars and Related Substances. Anal Chem. 1956; 28(3):
485 350-356.

486

487 [36] Muyzer, G., de Waal E.C. & Uitterlinden A.G. Profiling complex microbial populations
488 by denaturing gradient gel electrophoresis analysis of polymerase chain reaction-
489 amplified genes coding for 16 S rRNA. Appl Environ Microb. 1993: 59(3): 695-700.

490

491 [37] Muyzer, G., Hottenträger, S., Teske, A. & Waver C. Denaturing gradient gel
492 electrophoresis of PCR-amplified 16S rRNA – a new molecular approach to analyse the
493 genetic diversity of mixed microbial communities. In: Akkermans ADL, van Elsas JD, de
494 Bruijn F. (eds), Molecular microbial ecology manual. 1996; Kluwer, Dordrecht.

495

[38] Koskinen, P. E. P., Kaksonen, A. H. & Puhakka, J. A. The relationship Between the Instability of H2 Production and Compositions of Bacterial Communities Within a Dark Fermentation Fluidized-Bed Bioreactor. Biotechnol Bioeng. 2007; 97(4): 742-758.

[39] Lakaniemi, A-M., Hulatt, C. J., Thomas, D. N., Tuovinen, O. H. & Puhakka, J. A. Biogenic hydrogen and methane production from *Chlorella vulgaris* and *Dunaliella tertiolecta* biomass. Biotechnol Biofuels. 2011; 4(34).

[40] Palmroth, M.R.T., Langwaldt, J.H., Aunola, T.A., Goi, A., Münster, U., Puhakka, J.A. & Tuhkanen, T.A. Effect of modified Fenton's reaction on microbial activity and removal of PAHs in creosote oil contaminated soil. Biodegradation. 2006; 17(2): 29-39.

[41] Pinto, R., Srinivasan, B., Manuel, M. & Tartakovsky, B. A two-population bio-electrochemical model of a microbial fuel cell. Bioresour Technol. 2010; 101(14): 5256-5265.

[42] Shi, L., Günther, S., Hübschmann, T., Wick, L., Harms, H., Müller, S. Limits of propidium Iodide as a Cell Viability Indicator for Environmental Bacteria. Cytometry A. 2007; 71(8): 592-598.

[43] Logan, B. & Regan, J. Electricity-producing bacterial communities in microbial fuel cells. Trends Microbiol. 2006; 14(12): 512-518.

[44] Huang, L., Zeng, R. & Angelidaki, I. Electricity production from xylose using a mediator-less microbial fuel cell. Bioresour Technol. 2008; 99(10): 4178-4184.

[45] Sun, G., Thygesen, A. & Meyer, A. Acetate is a superior substrate for microbial fuel cell initiation preceding bioethanol effluent utilization. Appl Microbiol Biotechnol. 2015; 99(11): 4905-4915.

[46] Huang, L. & Angelidaki, I. Effect of Humic Acids on Electricity Generation Integrated With Xylose Degradation in Microbial Fuel Cells. Biotechnol Bioeng. 2008; 100(3): 413-422.

[47] Kokko, M., Mäkinen, A., Sulonen, M., Puhakka, J. Effects of anode potentials on bioelectrogenic conversion of xylose and microbial community compositions. Biochem Eng J. 2015; 101: 248-252.

[48] Huang, L., Logan, B. Electricity production from xylose in fed-batch and continuous-flow microbial fuel cells. Appl Microbiol Biotechnol. 2008; 80(4): 655-664.

[49] Boghani, H., Kim, J., Dinsdale, R., Guwy, A. & Premier, G. Reducing the burden of food processing washdown wastewaters using microbial fuel cells. Biochem Eng J. 2017; 117: 210-217.

[50] Bond, D. & Lovley, D. Electricity production by *Geobacter sulfurreducens* Attached to Electrodes. Appl Environ Microbiol. 2003; 69(3): 1548-1555.

[51] Muyzer, G. & Smalla, K. Application of denaturing gradient gel electrophoresis (DGGE) and temperature gradient gel electrophoresis (TGGE) in microbial ecology. Anto Leeuw. 1998; 73(1): 127-141.

[52] Muyzer, G. DGGE/TGGE a method for identifying genes from natural ecosystems. Curr Opin Microbiol. 1999; 2(3): 317-322.

[53] Zhou, L., Deng, D., Zhang, Y., Zhou, W., Jiang, Y. & Liu Y. Isolation of a facultative anaerobic exoelectrogenic strain LZ-1 and probing electron transfer mechanism *in situ* by linking UV/Vis spectroscopy and electrochemistry. Biosens Bioelectron. 2017; 90: 264-268.

[54] Zhang, T., Cui, C., Chen, S., Ai, X., Yang, H., Shen, P. & Peng, Z. A novel mediatorless microbial fuel cell based on direct catalysis of *Escherichia coli*. Chem commun. 2006; 21: 2257-2259.

[55] Wang, Q., Xie, N., Qin, Y., Shen, N., Zhu, J., Mi, H. & Huang, R. *Tumebacillus flagellatus* sp. nov., an a-amylase/pullulanase-producing bacterium isolated from cassava wastewater. Int J Syst Evol Micr. 2013; 63: 3138-3142.

[56] Hasona, A., Kim, Y., Healy, F., Ingram, L. & Shanmugam, K. Pyruvate Formate Lyase and Acetate Kinase Are Essential for Anaerobic Growth of *Escherichia coli* on Xylose. J Bacteriol. 2004; 186(22): 7593-7600.

[57] Zeppilli, M., Villano, M., Aulenta, F., Lampis, S., Vallini, G. & Majone, M. Effect of the anode feeding composition on the performance of a continuous-flow methane-producing microbial electrolysis cell. Environ Sci Pollut Res Int. 2015; 22(10): 7349-7360.

[58] Barbirato, F., Grivet, J., Soucaille, P. & Bories, A. 3-Hydroxypropionaldehyde, an Inhibitory Metabolite of Glycerol Fermentation to 1,3-Propanediol by Enterobacterial Species. Appl and Environ Microbiol. 1996; 62(4): 1448-1451.

[59] Sun, L., Toyonaga, M., Ohashi, A., Tourlousse, D., Matsuura, N., Meng, X-Y., Tamaki, H., Hanada, S., Cruz, R., Yamaguchi, T. & Sekiguchi, Y. *Lentimicrobium saccharophilum* gen. nov., sp. nov., a strictly anaerobic bacterium representing a new family in the phylum Bacteroidetes, and proposal of Lentimicrobiaceae fam. nov. Int J Syst Evol Microbiol. 2016; 66: 2635-2642.

[60] Chan, K-G., Tee. K., Yin, W-F. & Tan, J-Y. Complete Genome Sequence of *Pluralibacter gergoviae* FB2, an *N*-Acyl Homoserine Lactone-Degrading Strain Isolated from Packed Fish Paste. Genome Announc. 2014; 2(6): 1-2.

[61] Teather, R. Maintenance of Laboratory Strains of Obligately Anaerobic Rumen bacteria. Appl Environ Microbiol. 1982; 44(2) 499-501.

[62] Heylen, K., Hoefman, S., Vekeman, B., Peiren, J. & De Vos, P. Safeguarding bacterial resources promotes biotechnological innovation. Appl Microbiol Biotechnol. 2012; 94(3): 565-574.

[63] Mazur, P. Freezing of living cells: Mechanisms and implications. Am J Physiol. 1984; 247: C125-C142.

[64] Smith, D. & Ryan, M. The impact of OECD best practice on the validation of cryopreservation techniques for microorganisms. CryoLetters. 2008; 29(1): 63-72.

[65] Morgan, C., Herman, N., White P., Vesey, G. Preservation of micro-organisms by drying; A review. J Microbiol Methods. 2006; 66(2): 183-193.

[66] Nimje, V., Chen, C-Y., Chen, C-Y., Jean, J-S., Reddy, A., Fan, C-W., Pan, K-Y., Liu, H-T. & Chen, J-L. Stable and high energy generation by a strain of *Bacillus subtilis* in a microbial fuel cell. J Power Sources. 2009; 190(2): 258-263.

[67] McKenney, P., Driks, A. & Eichenberg, P. The *Bacillus subtilis* endospore: assembly and functions of the multilayered coat. Nat Rev Microbiol. 2013; 11(1): 33-44.

**Table 1. Lag time for the start-up of MFCs, cell voltage and anode potential with 100 Ω resistance and internal resistance calculated from LSV data at the point of highest power density values. The standard deviation values show the difference between duplicate reactors. No lag time is reported after six months storing, because the cell voltage remained negligible.**

| | Lag time[(a)] (d) | Average cell voltage[(b)] (mV) | Average anode potential[(b)] (mV) | Internal resistance (Ω) |
|---|---|---|---|---|
| **Without storing** | 1.9 ± 0.5 | 141 ± 14 | -454 ± 7 | 41 ± 11 |
| **1 week at +4 °C** | 2.7 ± 0.3 | 146 ± 5 | -456 ± 16 | 47 ± 4 |
| **1 month at +4 °C** | 5.0 ± 0.9 | 123 ± 11 | -461 ± 7 | 44 ± 6 |
| **1 month at -20 °C** | 7 ± 3 | 150 ± 30 | -451 ± 4 | 40 ± 20 |
| **6 months at +4 °C** | - | 27 ± 12 | -240 ± 20 | 764 ± 13 |
| **6 months at -20 °C** | - | 7 ± 3 | -170 ± 30 | 900 ± 300 |

[(a)]Before cell voltage reached 100 mV (0.1 mW); [(b)]Values from the last full feeding cycle

**Table 2. Coulombic efficiency (CE), xylose degradation efficiency and VFA concentrations in the end of the last full feeding cycle. The standard deviation values show the differences between duplicate reactors. VFA concentrations were measured in the end of the feeding cycle.**

| | CE (%) | Xylose removal (%) | Acetate (mM) | Propionate (mM) | Butyrate (mM) |
|---|---|---|---|---|---|
| **Without storing** | 11.2 ± 1.2 | 99.0 ± 0.2 | 10.6 ± 1.4 | 2.7 ± 0.5 | n.d.[a] |
| **1 week at +4 °C** | 11.6 ± 0.5 | 99.12 ± 0.04 | 18 ± 2 | 5.0 ± 0.8 | n.d. |
| **1 month at +4 °C** | 11.9 ± 1.1 | 99.5 ± 0.3 | 16 ± 4 | 6.3 ± 0.5 | < 0.5[b] |
| **1 month at -20 °C** | 14 ± 3 | 99.10 ± 0.09 | 24.4 ± 0.9 | 8.2 ± 1.0 | 0.8 ± 0.3 |
| **6 months at +4 °C** | 2.8 ± 1.2 | 99.5 ± 0.3 | 27 ± 3 | 16 ± 2 | 1.38 ± 0.03 |
| **6 months at -20 °C** | 0.7 ± 0.4 | 99.2 ± 0.5 | 22 ± 17 | 15 ± 10 | 1.5 ± 0.7 |

**[a] n.d. = not detected; [b] below detection limit, which was 0.5 mM**

**Table 3. Identified organisms from DGGE gel shown in Figure 3. Variation in sequence length and similarity is caused by identification of multiple bands with similar affiliation.**

| Band label | SL | Sim (%) | Affiliation (acc number) | Class / Family | Origin of the sample |
|---|---|---|---|---|---|
| 1 | 406 | 99.5 | *Proteiniphilum acetatigenes* (NZ_KB905705.1) | Bacteroidia / *Porphyromonadaceae* | UASB reactor treating brewery wastewater |
| 2 | 257 | 98.4 | *Lentimicrobium saccharophilum* (NZ_DF968182.1) | Bacteroidia / *Lentimicrobiaceae* | Methanogenic Wastewater Treatment System |
| 3 | 384-424 | 98.7-99.8 | *Pluralibacter gergoviae* (NZ_CP009450.1) | Gammaproteobacteria / *Enterobacteriaceae* | Isolated from Packed Fish Paste |
| 4 | 414-426 | 98.6-100 | *Tumebacillus flagellatus* (NZ_JMIR01000093.1) | Bacilli / *Alicyclobacillaceae* | Cassava wastewater |
| | 414-426 | 98.6-100 | *Escherichia coli* (NC_011751.1) | Gammaproteobacteria / *Enterobacteriaceae* | Human urine |
| 5 | 379-446 | 97.9-99.6 | *Geobacter sulfurreducens* (NC_002939.5) | Deltaproteobacteria / *Geobacteraceae* | |
| 6 | 432 | 96.7 | *Phascolarctobacterium sp.* (NZ_GL830850.1) | Negativicutes / *Acidaminococcaceae* | Human gut |
| 7 | 365 | 99.2 | *Citrobacter freundii* (NZ_CP007557.1) | Gammaproteobacteria / *Enterobacteriaceae* | Sink aerator |

SL = sequence length of the sample, Sim (%) = similarity (%), Affiliation (acc number) = closest species in database and its accession number, and Origin of the sample = Origin of the sample with the closest match. Band number 4 matched with two different organisms in a similar way.

# Figures

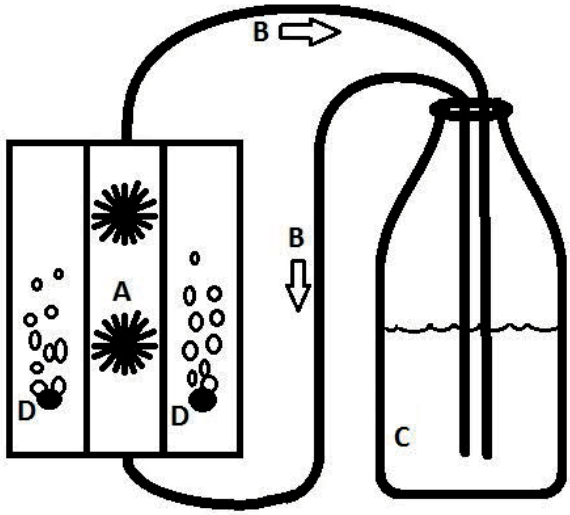


**Figure 1.** Schematic diagram of a MFC showing the anode and cathode chambers and anolyte circulation. A) Carbon brush electrodes in anode chamber, B) Anolyte circulation tubes (arrows show the liquid flow direction), C) Anolyte circulation bottle, D) Aeration stones used in the cathode chambers.

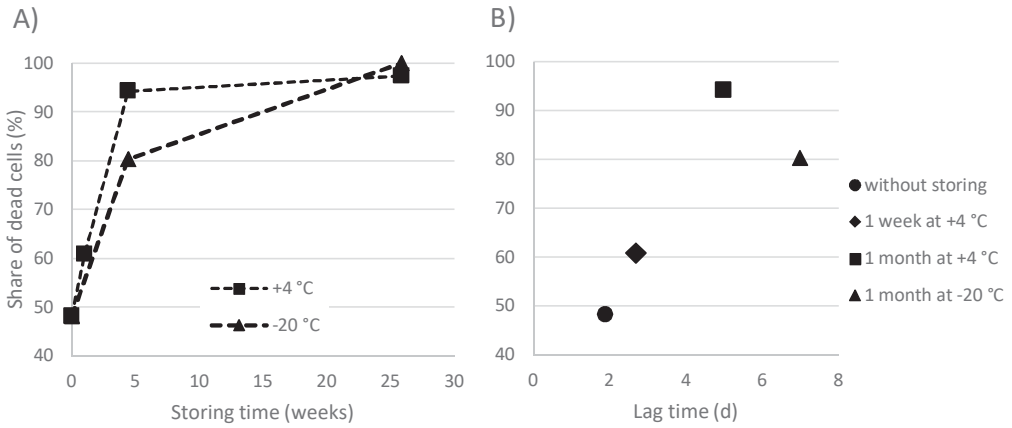


639

640 **Figure 2.** Share of cells stained as dead after different MFC anolyte storing times. Square shaped
641 markers stand for the storing at +4 °C, and the triangles the storing at -20 °C. (Here 1 month =
642 4.4 weeks, 6 months = 25.9 weeks)

643

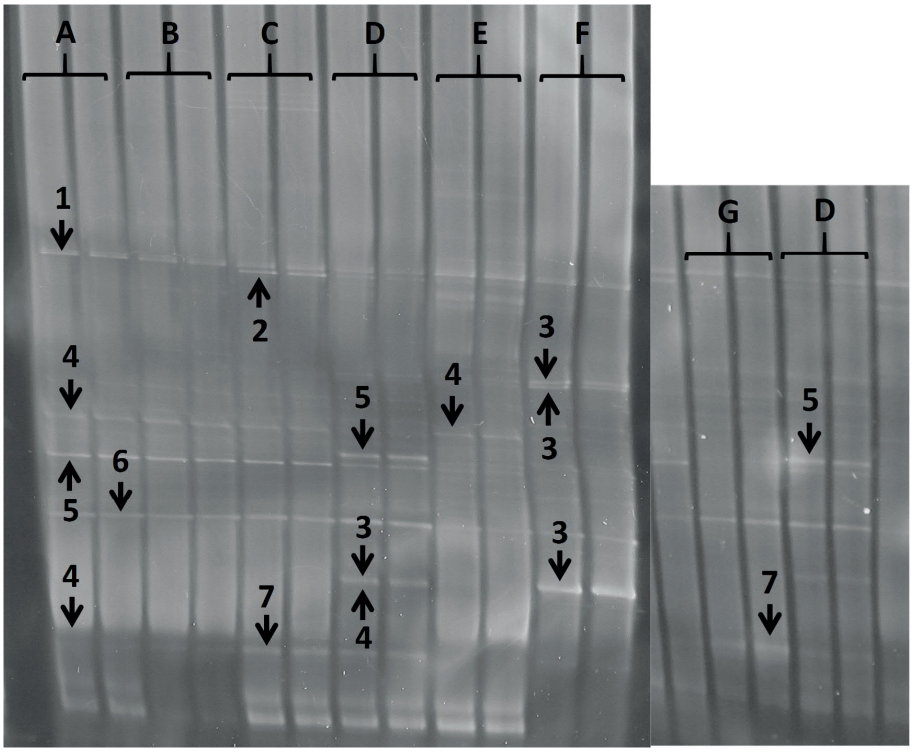


**Figure 3.** Microbial community samples from anode electrode biofilm. Samples A-F show the microbial community from the duplicate MFC that resulted in the higher power density of the two parallel reactors operated after similar inoculum treatment: A) without storing, B) 1 week at +4 °C, C) 1 month at +4 °C, D) 1 month at -20 °C, E) 6 months at +4 °C, and F) 6 months at -20 °C. Sample G represents the parallel reactor for D (1 month at -20 °C) another DGGE gel to elucidate the difference of the microbial communities of these duplicate MFCs that enabled quite different power densities.

# Supplementary material

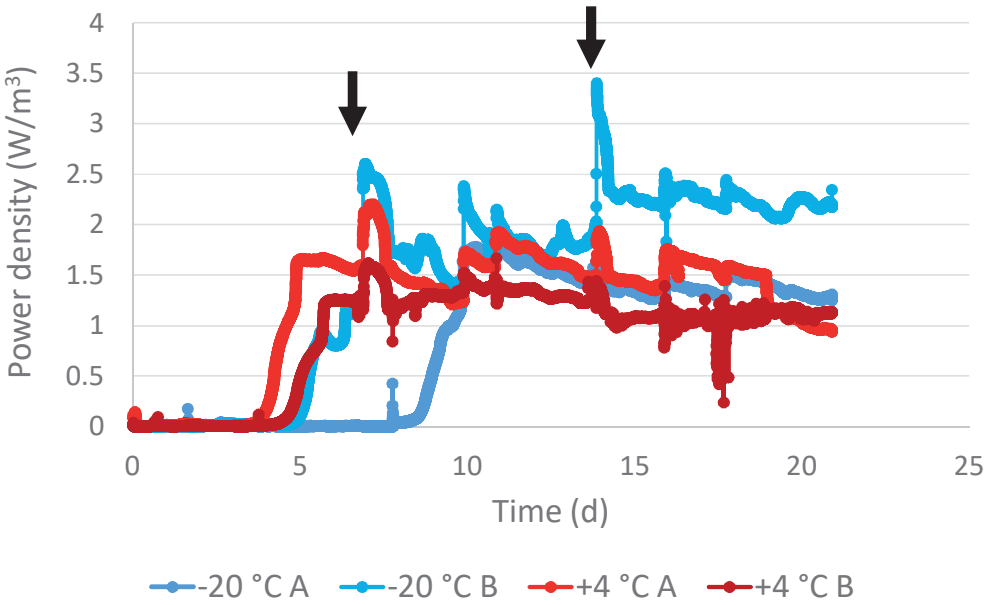


**Figure S1. Power density curves showing three feeding cycles after storing enrichment culture for one month at -20 °C (blue curves) or +4 °C (red curves). Black arrows show the feeding points. Average power densities (in section 3.1) of the last full feeding cycle were calculated between days 14 and 21 as an average of data from duplicate MFCs.**

# PUBLICATION III

**Effects of anode materials on electricity production from xylose and treatability of TMP wastewater in an up-flow microbial fuel cell**

Haavisto, J.M., Dessì, P., Chatterjee, P., Honkanen, M.H., Noori, M.T., Kokko, M.E., Lakaniemi A-M, Lens, P.N.L., Puhakka, J.A

Chemical Engineering Journal 372:141-150
https://doi.org/10.1016/j.cej.2019.04.090

Chemical Engineering Journal 372 (2019) 141–150

Contents lists available at ScienceDirect

Chemical Engineering Journal

journal homepage: www.elsevier.com/locate/cej

# Effects of anode materials on electricity production from xylose and treatability of TMP wastewater in an up-flow microbial fuel cell

Johanna Haavisto[a,1], Paolo Dessì[a,b,*,1], Pritha Chatterjee[a,c], Mari Honkanen[d], Md Tabish Noori[e], Marika Kokko[a], Aino-Maija Lakaniemi[a], Piet N.L. Lens[a,b], Jaakko A. Puhakka[a]

[a] Tampere University, Faculty of Engineering and Natural Sciences, PO Box 541, FI-33104 Tampere University, Finland
[b] National University of Ireland Galway, University Road, Galway H91 TK33, Ireland
[c] Indian Institute of Technology Hyderabad, Department of Civil Engineering, Hyderabad, India
[d] Tampere University, Tampere Microscopy Center, PO Box 692, FI-33104 Tampere University, Finland
[e] Kyung Hee University, Department of Environmental Science and Engineering, 446701 Seoul, South Korea

## HIGHLIGHTS

- Five electrodes were compared for electricity production from xylose in up-flow MFC.
- Activated carbon in steel cage electrode was chosen for treatment of TMP wastewater.
- Thermomechanical pulping (TMP) effluent was treated in MFC for the first time.
- COD removals of 77–86% and 47% obtained with synthetic and real wastewater.
- With TMP, membrane fouling decreased power output by > 90% after 30 operation days.

## GRAPHICAL ABSTRACT

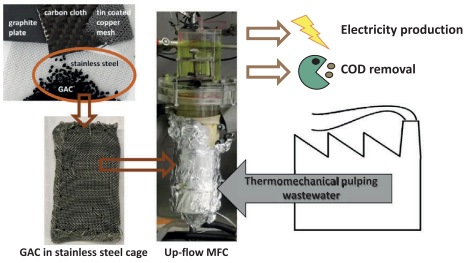


## ARTICLE INFO

*Keywords:*
Electricity production
Electrode material
Granular activated carbon
Membrane fouling
Microbial electrochemical technology
Thermomechanical pulping wastewater

## ABSTRACT

The aim of this study was to determine an optimal anode material for electricity production and COD removal from xylose containing synthetic wastewater in an up-flow microbial fuel cell (MFC), and assess its suitability for treatment of thermomechanical pulping (TMP) wastewater with an enrichment culture at 37 °C. The anode materials tested included carbon-based electrodes (graphite plate, carbon cloth and zeolite coated carbon cloth), metal-based electrodes (tin coated copper) and a metal-carbon assembly (granular activated carbon in stainless steel cage). During continuous operation with xylose, COD removal was 77–86% of which 25–28% was recovered as electricity. The highest power density of 333 ( ± 15) mW/m$^2$ was obtained with the carbon cloth electrode. However, based on an overall analysis including electrode performance, surface area and scalability, the granular activated carbon in stainless steel cage (GAC in SS cage) was chosen to be used as electrode for

*Abbreviations:* AEM, anion exchange membrane; APHA, animal and plant health association; CE (%), coulombic efficiency; CEM, cation exchange membrane; COD (g/L), chemical oxygen demand; CV, cyclic voltammetry; EDTA, ethylenediaminetetraacetic acid; EIS, electrochemical impedance spectroscopy; GAC, granular activated carbon; GC-FID, gas chromatograph-flame ionization detector; HPLC, high performance liquid chromatography; HRT (days), hydraulic retention time; LSV, linear sweep voltammetry; MFC, microbial fuel cell; OCV (V), open circuit voltage; $R_{ct}$, charge transfer resistance; RID, refractive index detector; $R_s$, ohmic resistance; SEM-EDS, scanning electron macroscope-energy dispersive x-ray spectroscopy; SS, stainless steel; TMP, thermomechanical pulping; TS (g/L), total solids; TSS (g/L), total suspended solids; VFA (g/L), volatile fatty acid; VS (g/L), volatile solids; VSS (g/L), volatile suspended solids

* Corresponding author at: National University of Ireland Galway, University Road, Galway H91 TK33, Ireland.
*E-mail address:* paolo.dessi@nuigalway.ie (P. Dessì).
[1] These two authors contributed equally to the manuscript.

https://doi.org/10.1016/j.cej.2019.04.090
Accepted 13 April 2019
Available online 15 April 2019
1385-8947/ 

bioelectrochemical treatment of TMP wastewater. The TMP fed MFC was operated in continuous mode with 1.8 days hydraulic retention time, resulting in 47 ( ± 13%) COD removal of which 1.5% was recovered as electricity with the average power production of 10–15 mW/m$^2$. During operation with TMP wastewater, membrane fouling increased the polarization resistance causing a 50% decrease in power production within 30 days. This study shows that MFC pretreatment removes half of the TMP wastewater COD load, reducing the energy required for aerobic treatment.

## 1. Introduction

Pulp and paper mills generate 10–100 m$^3$ of wastewater per ton of produced paper [1]. Such wastewaters may contain hundreds of organic and inorganic compounds, depending on the process where they are generated, and could therefore pollute the receiving water bodies if released untreated [2]. The cost associated with aerobic treatment of pulp and paper wastewaters, characterized by an organic load of 1–10 g/L chemical oxygen demand (COD) [1] is pushing towards implementation of an anaerobic treatment. This would result in energy recovery, e.g. in the form of biogas or bioelectricity, as well as decreasing the cost of the successive aerobic treatment step [3].

Thermomechanical pulping (TMP) wastewater is a potential substrate for anaerobic bioprocesses, as it is rich in carbohydrates (25–40% of the total COD) [3]. In addition, TMP wastewater contains only small concentrations of inhibitory compounds, such as fatty acids, resin acids, hydrogen peroxide, sulphite, and sulphate, which are more typical in chemical pulping wastewater [1]. Biological energy production from TMP wastewater has been demonstrated in the form of methane [4,5] and hydrogen [6].

Direct conversion of organic compounds into electricity in microbial fuel cells (MFCs) is a promising alternative for harnessing energy from wastewaters [7,8]. In MFCs, an anodic biological reaction is combined to a cathodic biotic or abiotic reaction to harness electrical energy from organic and inorganic substrates [9]. A variety of wastewaters has been used for electricity production in MFCs, including municipal [10,11], agricultural [12], and industrial wastewaters [13–15]. Despite its relatively high concentration of readily degradable carbohydrates and acetic acid [3], TMP wastewater has not yet been investigated for bioelectricity production and COD removal in MFCs.

The adoption of MFCs for wastewater treatment in large scale is currently hindered by the high cost of the materials, particularly the electrodes and membranes, and the low power densities [7]. In MFCs, an efficient anode electrode should be biocompatible, conductive, resistant to corrosion, and have a high surface area [16]. Carbon-based electrode materials are less conductive than metal-based materials, but are usually of lower-cost, more biocompatible and have a higher surface area [17]. Graphite plate and carbon cloth are widely studied carbon based anode materials, from which conductive carbon cloth with high surface area has shown its potential in many studies [17]. It has also been suggested that multi-material electrodes, e.g. combinations of carbon and metal materials, can significantly increase power production compared to plain carbon or metal electrodes [18,19]. Addition of functional groups to the anodic surface, for example pretreating the electrode with ammonium or acids, facilitates electron transfer and bacterial attachment [20,21]. Hydrophilic zeolite coating has been tested to increase bacterial attachment by enabling access of polar sugar molecules, which attract bacteria on the electrode surface [22]. In addition, the electrodes should have a large surface area and be easily scalable. An example of such material is granular activated carbon (GAC). Granular anode materials are exploited, e.g. in fluidized bed MFCs where moving particles collide with a current collector [23] or trapped in a conductive metal cage. In both cases, GAC offers a large surface area for microbial adhesion and charge accumulation. Furthermore, the capacitive nature of GAC enables charge transfer when fluidized or loosely packed granules are in contact with current collectors [24]. MFCs with capacitive anode materials can also be operated by repeating open and closed circuit cycles to increase the power density [25].

The purpose of this study was to compare carbon-based (graphite plate and carbon cloth, with and without zeolite coating), metal-based (tin coated copper) and metal-carbon composed (GAC in stainless steel cage) anode electrode materials for electricity production and COD removal in a continuous xylose-fed up-flow MFC with a mixed culture. The most promising anode material was then utilized to assess the bioelectrochemical treatment of TMP wastewater in MFCs in terms of electricity generation and COD removal.

## 2. Materials and methods

### 2.1. Inoculum and synthetic wastewater

The up-flow MFC used in this study was inoculated with effluent from another xylose fed up-flow MFC operated at 37 °C originally inoculated with anaerobic sludge (same seed as described by Haavisto et al. [26]) from a municipal wastewater treatment plant. The synthetic wastewater was prepared as described by Mäkinen et al. [27] without addition of EDTA and resazurin. The concentration of yeast extract was 0.02 g/L at start-up, and was omitted during continuous feeding. Xylose (1.0 g/L) was used as the substrate, and pH of the medium was adjusted to 7.0 with NaOH. The conductivity of the medium was 12–13 mS/cm.

### 2.2. Thermomechanical pulping wastewater

The wastewater used in this study, collected from a pulp and paper mill in Finland, was effluent of a thermomechanical pulping (TMP) process, in which wood was steamed at approximately 120 °C to obtain the pulp. The TMP wastewater had a pH of 5.1 and a composition as specified in Table 1. To minimize changes in the composition upon storage, which was demonstrated in a previous study [6], the TMP wastewater was kept at −20 °C in either 2 L or 5 L containers, and defrosted 24 h before use. To keep the pH close to 7.0 and increase the buffering capacity, $NaHCO_3$ (0.8 or 2 g/L, as specified in Section 2.5) was added to the TMP wastewater. The conductivity of the TMP wastewater was 1.4 mS/cm and increased to 2.0 and 2.9 mS/cm after

**Table 1**
Characteristics of the thermomechanical pulping (TMP) wastewater.

| Parameter | Concentration (mg/L) |
|---|---|
| TS | 4415 ± 30 |
| VS | 3350 ± 125 |
| TSS | 807 ± 148 |
| VSS | 755 ± 143 |
| Total COD | 3512 ± 77 |
| Soluble COD | 3170 ± 16 |
| Total nitrogen | 7.6 ± 0.2 |
| Phospate phosphorous ($PO_4^{3-}$-P) | 2.4 ± 0.1 |
| Total dissolved saccharides | 1112 ± 190 |
| Acetate | 279 ± 10 |
| Alkalinity[a] | 114 ± 1 |
| Sodium | 162.0 ± 0.0 |
| Potassium | 22.8 ± 0.2 |
| Magnesium | 4.2 ± 0.0 |
| Calcium | 43.9 ± 0.1 |

[a] Measured as mg $HCO_3^-$/L.

adding 0.8 and 2 g/L $NaHCO_3$, respectively. After defrosting and addition of $NaHCO_3$, the TMP wastewater was settled in a 2 L container for 12 h at 4 °C prior to utilization. The supernatant was then flushed with $N_2$ for 5 min prior to being fed to the up-flow MFC.

### 2.3. Anode electrodes

The anode electrodes used for comparison were: i) graphite plate, ii) carbon cloth, iii) carbon cloth with zeolite coating, iv) tin coated copper mesh, and v) granular activated carbon in stainless steel cage (GAC in SS cage) (Fig. S1 in the Supplementary information). All electrodes used for comparison had a projected surface area (including both sides of the electrode) of 0.0056 $m^2$, whereas the GAC in SS cage electrode used for TMP wastewater treatment was up-scaled to 0.0080 $m^2$. The graphite plate, carbon cloth (with and without zeolite) and tin coated copper electrodes were connected to a copper wire with conductive silver glue, which was covered with epoxy after hardening to prevent oxidation. The steel cage electrodes were sewed with Ti wire and the long end of the wire was used as electric wire (Fig. S1).

The graphite plate electrode was prepared by drilling holes on a graphite plate (McMaster-Carr, Aurora, OH) and reinforcing the electrical wire connection with a screw. The electrode was stored for two days in 1 M NaOH and rinsed with MilliQ® water prior to utilization. The graphite plate surface contained irregular surface structures with shapes < 10 µm in size according to scanning electron microscope (SEM) images (Fig. S2).

The carbon cloth electrodes had a fiber diameter of approximately 10 µm (Fig. S2) and the edges were reinforced with superglue to prevent fraying. Zeolite coating was done using sodium silicate and sodium aluminate solutions as described by Balkus and Ly [28]. Prior to coating, the electrode was pretreated in 10% $HNO_3$ solution at 90 °C for 3 h to increase the NaX zeolite attachment by introducing N-groups on carbon and making the carbon more hydrophilic [29]. Sodium silicate, sodium aluminate solutions and MilliQ® water were mixed after cooling down to room temperature until a homogenous mixture was formed and the electrode was immersed in the mixture immediately. The mixture was then treated at 90 °C for 3 h in a plastic container followed by rinsing with MilliQ® water. The presence of zeolite crystals on the electrode was confirmed by SEM-energy dispersive x-ray spectroscopy (EDS) analysis. Small crystals (< 1 µm in size, Fig. S2) contained Na, Si, O, and Al, which are the elements belonging to NaX zeolite [22].

The tin coated copper mesh anode electrode consisted of two overlapping mesh sheets (Canopy mesh fabric, Cat. #1208, Less EMF Inc.). The edges were treated with epoxy to prevent oxidation. The surface of the tin coated wire was smooth as shown by the SEM images (Fig. S2).

The GAC in SS cage anode electrode was prepared by pouring 9.2 g (for electrode comparison) or 15 g (for TMP wastewater treatment) of granular activated carbon (< 2 mm, Alfa Aesar) into a tightly folded stainless steel sheet (Tilox, 30 wires per inch, wire thickness 0.165 mm) sewed with Ti wire. The electrode was immersed in water overnight before use. Based on SEM, the granules had a very rough surface with irregularities varying from < 1 µm to > 1 mm (Fig. S2).

### 2.4. Up-flow MFC set-up

The up-flow MFC, described by Lay et al. [30] , consisted of a 500 mL anodic chamber and a 250 mL cathodic chamber separated by an anion exchange membrane (AEM) AMI-7001 or a cation exchange membrane (CEM) CMI-6001 (Membranes International Inc., USA), as specified in Section 2.5. Both membranes had a diameter of 4.5 cm. The catholyte was 250 mL of potassium ferricyanide (50 mM) in phosphate buffer (100 mM $Na_2HPO_4$, pH 7.0). Anode and cathode electrodes were connected through a 100 Ω resistor. A reference electrode (Ag/AgCl SENTEK QM710X in 3 M KCl) was connected to the recirculation tube through a glass capillary (QiS, the Netherlands). The temperature of the anode chamber was kept stable at 37 ( ± 1) °C using heating coils. The anolyte was recirculated at a flow rate of 60 mL/min using a peristaltic pump (Masterflex, USA). The cathode electrode was a graphite plate (0.00385 $m^2$, McMaster-Carr, Aurora, OH) pretreated for one hour with 1 M HCl, stored overnight in NaOH and rinsed with MilliQ® water prior to use. Sampling ports were located in the anode chamber inlet and outlet tubes.

### 2.5. Up-flow MFC operation

For electrode comparison, the up-flow MFC was started with 450 mL of xylose-containing synthetic wastewater and 50 mL of inoculum. The MFC was operated semi-continuously with each electrode until a similar power density (< 10% difference in maximum power densities) was obtained in three consecutive feeding cycles (5–7 days/cycle), and then switched to continuous mode (3.5 days HRT). To avoid depletion of the electron acceptor during continuous feeding, the catholyte was changed 2–3 times per week.

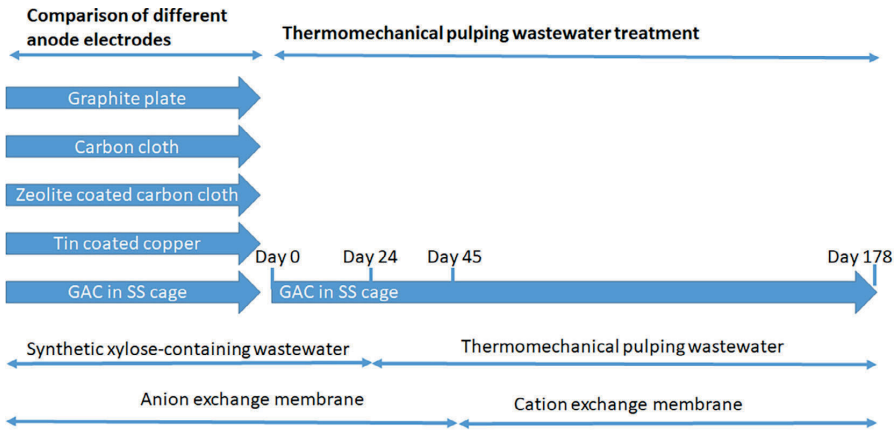


**Fig. 1.** Flow chart of the MFC studies presenting anode electrode comparison (26–42 days) and thermochemical wastewater treatment (178 days). Synthetic xylose-containing wastewater was used in the anode electrode comparison and for the start-up of thermomechanical pulping (TMP) wastewater treatment until the feeding solution was changed to TMP wastewater on day 24. An anion exchange membrane was used during the anode electrode comparison and changed to cation exchange membrane during TMP wastewater treatment (on day 45).

Prior to operation with TMP wastewater, the MFC was started up with the xylose-containing synthetic wastewater (450 mL), without inoculum, for 24 h, resulting in a voltage output of < 3 mV. Then, 50 mL of inoculum, previously stored at 4 °C for 7 days, was added and the MFC was operated in continuous mode for 23 days with 1 day HRT to reactivate the microbial community after storing. On day 24, the synthetic wastewater was replaced with thermomechanical pulping (TMP) wastewater, supplemented with 0.8 g/L $NaHCO_3$ (Fig. 1). The MFC was then operated in semi-continuous mode with TMP wastewater for two cycles of approximately 6 days each. On day 35, the MFC was switched to continuous mode. The HRT was set to 1.8 days due to the higher COD concentration (Table 1) and substrate recalcitrance of the TMP wastewater compared to the synthetic wastewater. On day 39, the $NaHCO_3$ concentration was increased to 2 g/L to keep the pH close to 7. On day 45, the AEM was replaced with a CEM and the MFC was operated with a CEM until day 178 (Fig. 1). Between days 1–108, the membrane was replaced periodically (approximately once per month) with a new one when the performance of the MFC was not restored after changing the catholyte. When changing the membrane, the catholyte solution was completely replaced (250 mL) with fresh ferricyanide solution. Between days 108–178, the CEM was not changed anymore in order to see how the prolonged operation with the same CEM affects the power production and effluent quality.

### 2.6. Analytical methods

During semi-continuous operation, anolyte samples were collected after every feeding, whereas during continuous feeding the anolyte inlet and outlet samples were collected every 2–3 days. The total and soluble COD was measured using the dichromate method according to the Finnish standard SFS 5504. Conductivity and pH were measured with a conductivity meter (Horiba LAQUAtwin, Japan) and a pH meter (WTW pH 330 m with Hamilton Slimtrode probe), respectively. Alkalinity, total solids, volatile solids, total suspended solids and volatile suspended solids were measured according to the APHA standards [31]. Cations were measured using DX-120 ion chromatograph (Dionex, USA) with AS40 autosampler, IonPac CS12A cation exchange column and CSRS 300 suppressor (4 mm). The eluent contained 2 mM methane sulphonic acid and the flow rate was 1 mL/min. Total nitrogen and phosphate phosphorous ($PO_4^{3-}$-P) were measured using the Hach (USA) Lange kits LCK 238 and LCK 349, respectively, following the supplier's instructions.

Total dissolved saccharides were measured as glucose equivalents by a colorimetric method modified from Dubois et al. [32]. The reactions contained 1 mL sample, 0.5 mL 5% phenol solution, and 2.5 mL sulfuric acid and absorbance was measured at 485 nm wavelength. Monosaccharides (glucose, xylose, arabinose, galactose and cellobiose) were measured by a high performance liquid chromatography (HPLC) system equipped with a Rezex RPM-Monosaccharide $Pb^+$ column (Phenomenex, USA) held at 85 °C and a refractive index detector (RID). MilliQ® water was used as the mobile phase at a 0.6 mL/min flow rate. Volatile fatty acids (VFAs) and alcohols were measured by a gas chromatograph (Shimadzu Ordior GC-2010 plus) with ZB-WAXplus column (Phenomenex, USA) and a flame ionization detector (GC-FID) as described by Haavisto et al. [33]. For the soluble COD and the VFA analysis, the samples were filtered with 0.45 μm syringe filters, whereas for the monosaccharides analysis with HPLC the samples were filtered with 0.2 μm syringe filters.

The surface of the CEM and the anode electrodes were studied by imaging and elemental analysis with a scanning electron microscope (SEM, ULTRAplus, Zeiss, Germany) equipped with an energy dispersive spectrometer (EDS, INCAx-act silicon-drift detector, Oxford Instruments, United Kingdom). The CEM was considered fouled when power production did not increase after changing the catholyte, approximately after 30 days of continuous up-flow MFC operation with TMP wastewater. Triplicate samples (approximately 1 × 1 cm) were cut from a fouled membrane by sterile scissors on day 101. A sample of unused CEM was also collected as a negative control. The samples were fixed in 4% paraformaldehyde and dehydrated with increasing ethanol concentration (25, 50, 75, 90 and 100%). Both electrode and membrane samples were attached on aluminium SEM stubs. Membrane samples were further coated with carbon to avoid sample charging during SEM-EDS analysis.

### 2.7. Electrochemical analyses

Voltage and anode potential (reported *vs.* Ag/AgCl reference electrode) were measured at a two minute interval using a data logger (Agilent 34970A, Agilent technologies, Canada). When comparing the anode electrodes, linear sweep voltammetry (LSV) and cyclic voltammetry (CV) were done with 0.001 V steps and 0.001 V/s scan rate, respectively, using a potentiostat (Palmsens3, Netherlands) after at least 10 days operation in continuous mode. For the GAC in SS cage electrode, CV analysis was repeated with another measurement device (BioLogic VMP3, France) as the current density (> 5.4 $A/m^2$) exceeded the upper detection limit of the Palmsens potentiostat. Both LSV and CV were performed after 30 min of stabilization in open circuit mode and the catholyte solution was changed before the measurements. The whole cell LSV limit was set to 0–50 mV above the open circuit voltage (OCV), whereas anodic CV and LSV were recorded between the anode potentials of −0.525 V and +0.2 V *vs.* Ag/AgCl.

During MFC operation with TMP wastewater, power and polarization curves were obtained on day 82 (with fresh CEM) and on day 94 (with fouled CEM) as previously described by Dessì et al. [34]. Whole cell electrochemical impedance spectroscopy (EIS) was performed on day 99 (with fouled CEM) and on day 105 (with fresh CEM) using a potentiostat (BioLogic VMP3, France) in a three-electrode set-up. The AC amplitude was set to 10 mV and the frequency was varied from 1 MHz to 0.1 Hz with 6 steps per decade. The EIS spectra were simulated in EC-Lab V11.21 software (BioLogic VMP3, France) using a best fit circuit to obtain different impedance values. The randomised simplex method with 5000 iteration was used for fitting and simulation.

### 2.8. Calculations

Current and power densities were calculated according to Ohm's law [9] and normalized to the projected anode surface area (0.0056 $m^2$ for electrode comparison or 0.0080 $m^2$ for TMP wastewater treatment) or anode chamber volume (500 mL). Average stable current and power densities for electrode comparison were calculated during three separate stable 24 h periods after catholyte replacements when current densities did not vary > 3% (later referred to as current and power densities). The internal resistance was estimated either from the LSV data, or from the slope of the polarization curve [9]. During anode material comparison, theoretical COD and electrons in the influent and effluent were calculated according to Van Haandel and Van der Lubbe [35] by converting xylose and VFA concentrations from the stable operation period to COD equivalents. Coulombic efficiency (CE) was calculated according to Logan et al. [9] based on theoretical COD removal (determined by calculating xylose and VFAs as COD equivalents) during electrode comparison, or on the total COD removal when the MFC was operated with TMP wastewater. An example of CE calculation based on the theoretical COD removal is given in the Supplementary information.

## 3. Results and discussion

### 3.1. Bioelectrochemical treatment of xylose-containing synthetic wastewater with different anode materials

#### 3.1.1. Power and current production

Power densities between 265 and 333 $mW/m^2$ were obtained from

xylose in a continuous MFC operation with the different carbon-based anode materials (Table 2). A slightly higher one-day average power density of 358 mW/m$^2$ was obtained with the tin coated copper mesh electrode on day 2 of semi-continuous operation. However, the power density declined on day 3 (Fig. S3) due to copper oxidation and solubilization. Copper has an excellent electrical conductivity and is widely used in electrical wires, but it is not stable in oxidative environments, such as the anodic chamber, and forms copper oxides toxic to microorganisms [36]. The results of Zhu and Logan [36] also indicated that copper corrosion can result in abiotic current production in MFCs. Despite the tin coating used in this study to prevent corrosion [37], the dark color of the electrode (Fig. S1) suggested its oxidation during MFC operation. Thus, MFC operation with this electrode was not continued.

A power density of 333 mW/m$^2$ was obtained with the carbon cloth electrode. Zeolite coating on carbon cloth, with pretreatment in 10% $HNO_3$ solution, decreased the power density by 20% in this study, which is in disagreement to Wu et al. [22], who reported a 152% increase in power density after applying a zeolite coating on a graphite felt. In this study, zeolite coated carbon cloth was also studied without the pretreatment in 10% $HNO_3$ solution, but due to the similar power densities (254 ± 10 mW/m$^2$) and CV curves (results not shown) to the zeolite coated carbon cloth with pretreatment, only the results with pretreatment are compared with the other electrodes. The power density with the graphite plate electrode (309 mW/m$^2$) was lower compared to non-coated carbon cloth, as was also reported by Pocaznoi et al. [38].The GAC in SS cage electrode resulted in a power density of 274 mW/m$^2$ (18% smaller than with the non-coated carbon cloth). The GAC was not fixed on the surface of the stainless steel mesh, and the loose contact of the irregularly shaped porous particles may have caused the relatively high internal resistance [39], which was the second highest (72 Ω) among the electrodes, after the zeolite coated carbon cloth (Table 2).

Although carbon cloth resulted in the highest current densities during continuous operation (0.77 A/m$^2$ at an anode potential of −433 mV), turnover CV curves show that at −400 mV anode potential, the highest current density (1.0 A/m$^2$) was measured with graphite plate, while the current densities with other materials were 0.24–0.40 A/m$^2$. Turnover CV curves also show that GAC in SS cage and graphite plate enabled considerably higher current densities than the other two electrode materials at more positive anode potentials (Fig. 2).

The maximum current densities of bare and zeolite coated carbon cloths were 1.8 and 1.9 A/m$^2$ at anode potentials of −270 and −300 mV, respectively, but the current densities were suppressed by power overshoot at more positive anode potentials (Fig. 2). Power overshoot is a complex phenomenon and has been suggested to occur due to, e.g., higher electron transfer rate from bacteria to the electrode compared to production rate [40], differences in microbial community composition and the amount of bacterial electron transfer components [41], or limited proton transfer out of the biofilm decreasing the biofilm pH [42]. Both the graphite plate and GAC in SS cage electrode showed higher current densities (> 5.2 A/m$^2$) in the CV analysis compared to carbon cloth at anode potentials higher than −0.19 V. One reason for the high current densities with GAC at a scan rate of 1 mV/s is the capacitance due to the very large surface area, which is a desired property for MFC anodes since it favours both bacterial attachment and charge accumulation [16,23].

#### 3.1.2. Treatment of synthetic wastewater

During continuous MFC operation with synthetic wastewater, the xylose removal efficiency was above 95% regardless of the electrode material and the anolyte pH ranged between 6.7 and 7.0. The effluent contained mainly acetate (4–5 mM) and propionate (ca. 1.5 mM). The theoretical COD removal efficiency (calculated from measured VFA and xylose concentrations) was the highest with the carbon cloth (86 ± 1%) and varied between 77 and 81% with the other electrodes (Table 3). CE varied between 25 and 28%. Electrons in the effluent and current production together accounted for 34–42% of the influent electrons, showing that the majority of the electrons was directed to other processes such as bacterial growth and methane generation [43].

#### 3.1.3. Electrode material selection

Electrode selection for bioelectrochemical treatment of TMP wastewater was based on performance criteria (COD removal, power density and obtainable current) and material characteristics (actual surface area and scalability) as summarized in Table 4 (more detailed material scalability comparison is given in Table S1). GAC in SS cage was rated as the best electrode material (Table 4) and selected for TMP wastewater treatment. GAC is an easily scalable electrode material that can be used in various reactor configurations due to its high specific surface area, capacitive behavior and 3D structure [23,24]. Graphite plate and carbon cloth were ranked equally to the second place due to higher COD removal with carbon cloth and higher current density in CV analysis with graphite plate. With zeolite coating on carbon cloth, both the average power density and COD removal efficiency decreased as compared to that of bare carbon cloth. Hence it was ranked fourth. With tin coated copper electrode, the MFCs never started to generate stable current density due to copper oxidation, hence it was ranked as the least favorable electrode material.

### 3.2. Bioelectrochemical treatment of TMP wastewater

#### 3.2.1. Power production

The up-flow MFC was started with synthetic wastewater containing xylose, at 1 day HRT, obtaining a power of about 150 mW/m$^2$ (2.4 W/m$^3$) within the first day of operation (Fig. S4a). However, the power production from xylose gradually decreased with time, being 65 mW/m$^2$ (1 W/m$^3$) on day 21, but then increased back to about 150 mW/m$^2$ after replacing the AEM with a fresh one (Fig. S4a). This suggests that the deterioration of the membrane was decreasing the MFC performance, as previously reported also by Miskan et al. [47].

On day 24, the change of substrate from xylose to TMP wastewater and the change of operation mode from continuous to semi-continuous caused a drop in the power production to as low as 1 mW/m$^2$ after two feeding cycles (Fig. S4b). The lower power production was likely caused by the lower conductivity of the TMP wastewater compared to the xylose-containing synthetic wastewater (2 mS/cm *vs.* 12–13 mS/cm), which increased the internal resistance and hampered ion transfer [48]. Furthermore, when the MFC was operated in semi-continuous mode, addition of 0.8 g/L $NaHCO_3$ to the TMP wastewater was not enough to prevent acidification of the anolyte. The anolyte pH decreased to below

**Table 2**
Effect of anode material on production of stable power and current densities, anode potential (mV *vs.* Ag/AgCl), and cell internal resistance according to linear sweep voltammetry obtained with the different electrode materials during continuous feeding.

| Anode electrode | Power density (mW/m$^2$) | Power density (W/m$^3$) | Current density (A/m$^2$) | Anode potential (mV) | Internal resistance (Ω) |
|---|---|---|---|---|---|
| Carbon cloth | 333 ± 15 | 3.7 ± 0.2 | 0.77 ± 0.02 | −433 ± 2 | 54 |
| Graphite plate | 309 ± 15 | 3.5 ± 0.2 | 0.74 ± 0.02 | −428 ± 6 | 61 |
| GAC in SS cage[a] | 274 ± 15 | 3.1 ± 0.2 | 0.70 ± 0.02 | −402 ± 4 | 72 |
| Zeolite coated carbon cloth | 265 ± 14 | 3.0 ± 0.2 | 0.69 ± 0.02 | −433 ± 2 | 88 |

[a] Granular activated carbon in stainless steel cage.

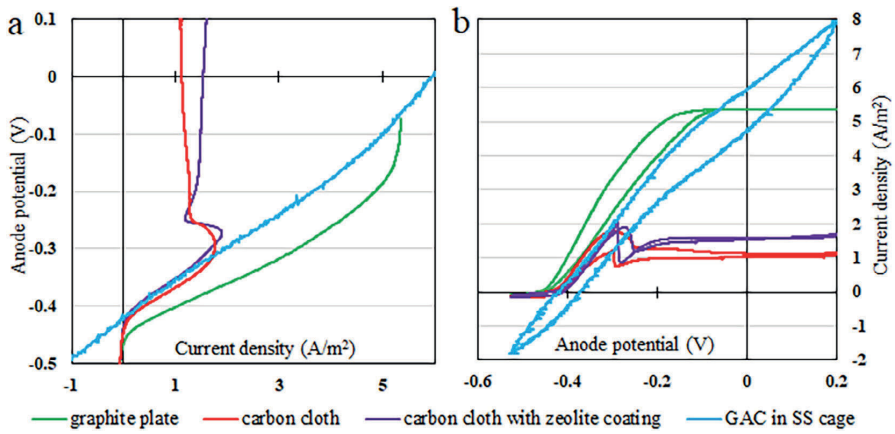


**Fig. 2.** Anodic linear sweep (a) and cyclic (b) voltammetry obtained with the different anode electrodes during continuous MFC operation with xylose. GAC in SS cage stands for granular activated carbon in stainless steel cage.

**Table 3**
Theoretical COD removal efficiency, share of the supplied electrons in the effluent in the form of acetate, propionate and xylose, and Coulombic efficiency during stable, continuous operation with synthetic wastewater.

| Anode electrode | Theoretical COD removal efficiency (%) | Electrons in effluent (%) | CE (%) |
|---|---|---|---|
| Graphite plate | 77 ± 4 | 23 ± 4 | 28 |
| Carbon cloth | 86 ± 1 | 14 ± 1 | 26 |
| Zeolite coated carbon cloth | 79 ± 9 | 21 ± 9 | 25 |
| GAC in SS cage[a] | 81 ± 3 | 19 ± 3 | 25 |

[a] Granular activated carbon in stainless steel cage.

6 in a few days, likely reducing the activity of anodic microorganisms [49].

Switching the operation mode from semi-continuous to continuous (HRT 1.8 days) on day 35, the power production only slightly increased to 2.5 mW/m$^2$ (Fig. S4c). After starting the continuous feeding, the pH remained low (< 6). On day 39, increasing the $NaHCO_3$ concentration to 2 g/L not only stabilized the pH to values close to 7 and conductivity to about 3 mS/cm, but also increased the power production to an average of 5 mW/m$^2$ (Table 5; Fig. S4c). However, it should be noted that the AEM was replaced with a fresh one on day 39 as well, which could have contributed to the increasing power production, especially in the first operating days with the fresh membrane.

On day 45, replacing the AEM with a CEM resulted in a 2 to 3-fold increase in the obtained power density (Table 5). The low power production with the AEM was likely due to the flow of phosphate anions from the cathodic to the anodic chamber [50], which may have caused precipitation of salts when in contact with the $Ca^{2+}$ ions present in the wastewater (Table 1). Such an issue was mitigated, although not solved, using a CEM (as discussed in Section 3.2.3).

During the operation in continuous mode (Fig. 3), power peaks of 75–100 mW/m$^2$ were obtained when the CEM was replaced with a fresh one (on days 45, 71, and 109). This can be attributed to the high surface area of the fresh CEM available for proton exchange, as compared to the used one, in which CEM fouling likely limited proton diffusion (see Section 3.2.3). Furthermore, the catholyte was entirely (250 mL) replaced with fresh 50 mM ferricyanide solution when the CEM was changed, increasing the availability of the electron acceptor at the cathode. Within a few days after replacing the CEM, the power decreased to 10–15 mW/m$^2$ and remained stable for 20–35 days (Fig. 3; Table 5). For longer operation periods, the power production decreased further to an average of 2.4 mW/m$^2$, and the performance of the MFC was not recovered after replacing the catholyte due to CEM fouling (Fig. 3; Table 5).

An average CE below 2% was obtained from TMP wastewater in the

**Table 4**
Selection criteria for anode electrodes for bioelectrochemical wastewater treatment.

| | Performance criteria[a] | | | Material characteristics | | |
|---|---|---|---|---|---|---|
| Anode electrode | COD removal[b] | Power density[c] | Current[d] | Actual surface area[e] | Electrode scalability[f] | Overall rating |
| GAC in SS cage | + + + | + + | + + | + + + | + + + | 1. |
| Carbon cloth | + + + | + + + | + | + | + + | 2. |
| Graphite plate | + + | + + + | + + | + | + + | 2. |
| Zeolite coated carbon cloth | + + | + + | + | + | + + | 4. |
| Tin coated copper | n.a. | n.a. | n.a. | + | + | 5. |

n.a. Not analysed (current production with tin coated copper deteriorated before continuous feeding was started).
[a] Based on experimental data of this study.
[b] Based on COD removal obtained during continuous feeding (> 80% + + +, 60–80% + +, < 60% +).
[c] Based on the average, stable power densities under continuous feeding (> 300 mW/m$^2$ + + +, 250–300 mW/m$^2$ + +, < 250 mW/m$^2$ +).
[d] The highest current densities obtained during CV analysis at turnover conditions (> 10 A/m$^2$ + + +, 5–10 A/m$^2$ + +, < 5 A/m$^2$ +).
[e] Surface area of the electrodes calculated for the size of the electrodes used in this study (> 1000 m$^2$ + + +, 100–1000 m$^2$ + +, < 100 m$^2$ +). The specific surface areas are based on literature: carbon cloth Brunauer-Emmett-Teller (BET) 2.39 m$^2$/g [44]; graphite plate BET 0.6 m$^2$/cm$^2$ [45]; GAC 500–2000 m$^2$/g [46]; tin coated copper mesh area was calculated from electrode weight (1.0 g), copper density (8.96 g/cm$^2$) and wire diameter (0.1 mm) assuming smooth surface.
[f] Scalability criteria are specified in more detail in Table S1.

**Table 5**
Average power and current densities, influent and effluent COD, and Coulombic efficiency (CE) obtained in the up-flow MFC continuously fed with thermomechanical pulping wastewater with either an anion or a cation exchange membrane.

| Operation days | Membrane[a] | Power density (mW/m$^2$) | Power density (W/m$^3$) | Current density (mA/m$^2$) | Influent $COD_{tot}$[b] (g/L) | Effluent $COD_{tot}$[b] (g/L) | CE (%) |
|---|---|---|---|---|---|---|---|
| 39–45 | AEM | 5.0 | 0.08 | 0.08 | 4.23 | 3.30 | 1.7 |
| 45–55 | CEM | 11.0 | 0.18 | 0.12 | 4.94 | 2.77 | 1.1 |
| 71–91 | CEM | 15.0 | 0.24 | 0.14 | 4.29 | 2.38 | 1.5 |
| 108–142 | CEM | 14.0 | 0.22 | 0.13 | 4.36 | 1.98 | 1.1 |
| 60–71, 92–101, 147–178 | Fouled CEM | 2.4 | 0.04 | 0.04 | 4.10 | 2.00 | 0.5 |

[a] AEM, anion exchange membrane; CEM, cation exchange membrane.
[b] Total chemical oxygen demand.

upflow MFC. The CE was calculated based on the total COD removal (i.e. the difference between influent and effluent COD). Although the TMP wastewater was settled before feeding to the MFC, some suspended solids were present in the influent, and accumulated in the MFC. The presence of VFAs in the effluent, as shown in Section 3.2.2, suggests that the HRT of 1.8 days was likely not enough for achieve a full conversion of VFAs to electricity, requiring optimization. Electrons may also have been consumed via reduction of sulphate, found in TMP wastewater with concentrations of 140–300 mg/L [5], whereas methane or hydrogen were not detected in the gas bag. Furthermore, a small share of electrons was directed to microbial growth.

As shown by the polarization data (Fig. 4) collected 10 days after CEM replacement on day 81, a maximum power of 28 mW/m$^2$ was obtained at a current density of 83 mA/m$^2$ (500 Ω external resistance). In the following days, the power production decreased, and a maximum power of only 15 mW/m$^2$ was obtained when the polarization analysis was repeated on day 94 (Fig. 3). This was attributed to the CEM fouling (see Section 3.2.3), which caused an increase of the whole cell internal resistance from 470 Ω on day 81 to 786 Ω on day 94, as estimated from the slope of the linear part of the polarization curves (Fig. 4).

A power density up to 71 mW/m$^2$ (during polarization) was obtained from wastewater produced by hydrothermal treatment of raw wood (3.3 g/L total COD) in an air-cathode MFC [14] as compared to 28 mW/m$^2$ obtained in this study. The characteristics of such wastewater were similar to those of the TMP wastewater used in this study, suggesting that the difference in power output can be attributed to the different MFC configuration. In particular, the distance between the anode and cathode electrode, in combination with the low conductivity of the TMP wastewater, likely resulted in high ohmic losses in this study.

### 3.2.2. COD removal from thermomechanical pulping wastewater

For continuous mode operation with TMP wastewater as the substrate (days 39–178), the up-flow MFC was fed with 4.1 ( ± 1.3) g/L total COD, of which 3.1 ( ± 0.5) g/L was soluble COD (Fig. 5). The total COD concentration in the influent varied during the operation and increased occasionally up to 8–9 g/L (Fig. 5a) due to variations in the quantity of suspended solids in the feed (not removed by settling) or due to the detachment of biomass that colonized the influent tubes after the first two weeks of MFC operation with TMP wastewater. Microorganisms attached in the influent tubing were likely partially fermenting the sugars present in the TMP wastewater, resulting in a concentration of 0.7 ( ± 0.2) g/L COD acetate and 0.2 ( ± 0.1) g/L COD butyrate in the MFC influent, higher than the concentrations detected when characterizing the TMP wastewater (Table 1).

An average COD removal efficiency (both total and soluble) of 47–48% was obtained between days 45–178. This resulted in an effluent containing 2.1 ( ± 0.4) g/L total COD and 1.6 ( ± 0.3) g/L

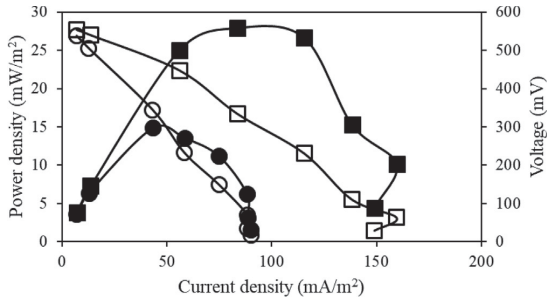


**Fig. 4.** Power (black) and polarization (white) curves obtained from the up-flow MFC continuously fed with thermomechanical pulping wastewater. The analysis was done with fresh (squares) and fouled (circles) cation exchange membrane on day 82 and 94, respectively.

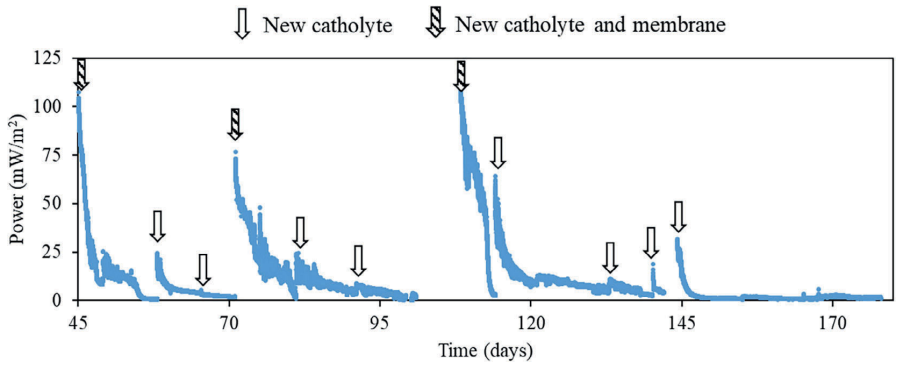


**Fig. 3.** Power generated from thermomechanical pulping wastewater in the up-flow MFC operated in continuous mode with a cation exchange membrane. The white arrow represents the replacement of catholyte with fresh ferricyanide solution, and the black-white arrow represents the replacement of both the membrane and catholyte.

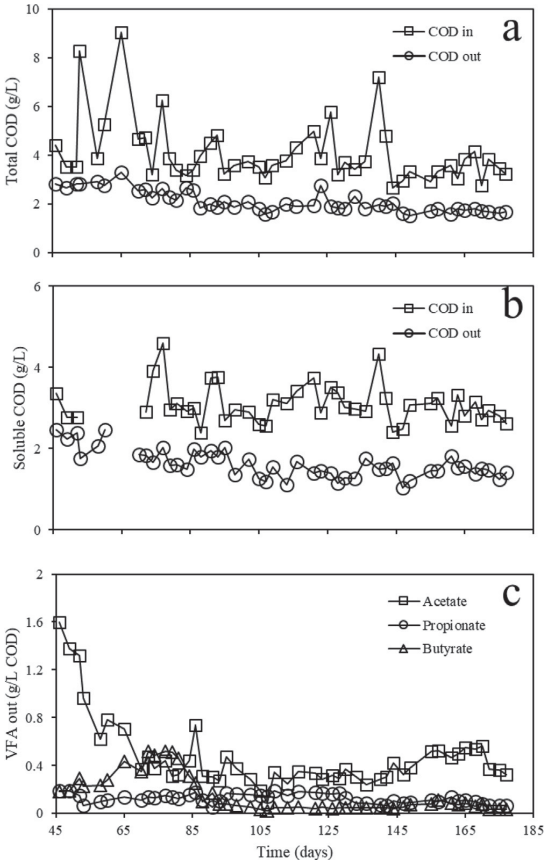


**Fig. 5.** Concentration of total (a) and soluble (b) COD in the influent and effluent of the up-flow MFC and volatile fatty acids detected in the effluent (c) during the operation in continuous mode with thermomechanical pulping wastewater as the substrate using a cation exchange membrane.

soluble COD (Fig. 5a and b), having a pH of 7.2 ( ± 0.3). This suggests that, despite the presence of recalcitrant compounds [3] and low concentration of nutrients (Table 1), TMP wastewater can be treated in an MFC to decrease its COD content. A lower total COD (29%) and a similar soluble COD removal (51%) efficiency was obtained by Huang and Logan [48] in a MFC treating paper recycling plant wastewater (1.4 and 0.2 g/L total and soluble COD). They were able to increase the total and soluble COD removal efficiencies to 70 and 75% upon addition of 50 mM phosphate buffer due to the increased conductivity and buffering capacity [48].

During continuous operation with TMP wastewater and AEM, the acetate concentration in the effluent increased up to 1.6 g/L COD on day 45, although the anolyte pH remained stable at 7.0 ( ± 0.2). When the AEM was replaced by a CEM, the acetate concentration in the effluent decreased to 0.4 g/L COD by day 70 (Fig. 5c), suggesting an increased activity of acetate utilizing microorganisms although acetate was not totally consumed. This was likely due to the higher availability of protons for the cathodic reactions, and the consequent lower resistance for the electricity producing pathway at the anode. Butyrate and propionate were generally detected at low concentrations in the effluent, although butyrate reached 0.5 g/L COD on days 65–81, before decreasing again to < 0.1 g/L COD (Fig. 5c). On days 45–178, when the up-flow MFC was operated with a CEM, VFAs accounted for 44 ( ± 14)

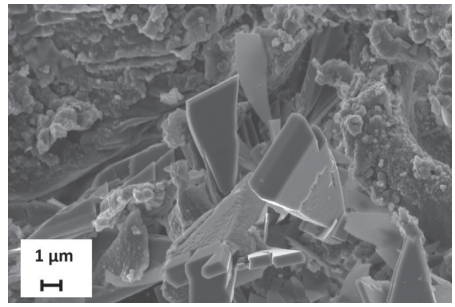


**Fig. 6.** SEM image of the crystalline structures found on the cation exchange membrane after 30 days of MFC operation with thermomechanical pulping wastewater containing 2 g/L $NaHCO_3$.

% of the soluble COD in the effluent, whereas monosaccharides were not detected. A share of the uncharacterized soluble COD was likely from derivates of lignin, which are recalcitrant to biological treatment and have been reported to account for 16–49% of COD in TMP wastewater [3].

### 3.2.3. Characterization of the membrane fouling

SEM-EDS analysis of the anodic side of the CEM after 30 days of operation showed a prevalence of inorganic fouling, which likely caused the power density drop from 70 mW/$m^2$ (on day 71) to 2 mW/$m^2$ (on day 101) (Fig. 3). Bacterial cells (Figs. 6 and S5) and nucleic acid (measured by Nanodrop) were not observed on the membrane surface in this study, confirming a minor role of biofouling. According to SEM-EDS, most of the surface of the membrane analysed was covered by crystals mainly consisting of calcium, phosphorous and oxygen (Figs. 6 and S5a–c). $Ca^{2+}$ ions, detected in the TMP wastewater with a concentration of 43.9 mg/L (Table 1), were likely occupying the active sites (sulphonate groups, Fig. S5d) of the CEM, as previously reported by Choi et al. [51]. The phosphorous concentration in the TMP wastewater was low (Table 1), but a cross-over of phosphate from the cathodic to the anodic chamber through the CEM cannot be excluded. However, such an issue is not relevant for possible full-scale application if the ferricyanide in phosphate buffer is replaced with a more sustainable catholyte such as air, or with a biocathode.

The EIS was performed to characterize the resistance of the CEMs used in the MFCs at different time points. As shown by the Nyquist plot of the EIS experimental data (Fig. 7a) and its simulation according to the equivalent circuit (Fig. 7b), the charge transfer resistance ($R_{ct}$) was the major kinetic limitation in the up-flow MFC. $R_{ct}$ increased from 81 to 466 Ω, as estimated from the diameter of the semi-circles [52], due to CEM fouling, which limited proton conductivity. In fact, the internal resistance caused by the separator is a key factor in MFC performance [12], especially if the membrane has been fouled. As expected, the ohmic resistance ($R_S$), represented by the intercept of the impedance curves with the x-axis, was about 95–100 Ω regardless of the fouling level of the CEM.

## 3.3. Practical implications

The results of this study suggest that bioelectrochemical pretreatment can be implemented to reduce the COD concentration of TMP wastewater by about 50%. This would reduce the energy required for aeration in the subsequent conventional activated sludge process, which is typically 900–1000 Wh/kg COD removed [53], as well as generate an average electrical power of 3.5–5 Wh/kg COD removed (10–15 mW/$m^2$) with a 1.8 days HRT. However, for further process development, ferricyanide should be replaced with an air cathode or biocathode to reduce costs and environmental impacts, and distance

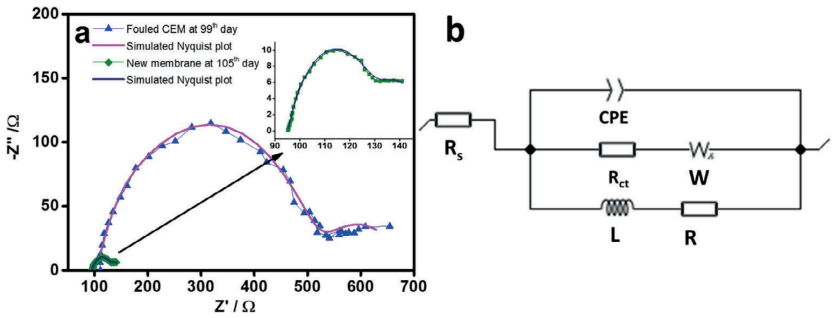


**Fig. 7.** Nyquist plot of the impedance spectrum obtained from the up-flow MFC continuously fed with thermomechanical pulping wastewater with fresh and fouled cation exchange membrane (a) and best fit circuit diagram for the up-flow MFC used in this study (b).

between anode and cathode electrodes should be reduced to improve the power production and CE by decreasing the internal resistance.

Sustainability of the electrode materials could be enhanced by replacing the GAC with e.g. conductive biochar granules obtained from high temperature pyrolysis of waste material. For example, the use of biochar from coconut shells as anode in sediment MFCs has been reported by Chen et al. [54]. Alternatively, the GAC granules could be fluidized to decrease mass transport limitations [23].

In case of fouling, mitigation strategies such as modification of membrane charge, hydrophobicity and roughness, use of cleaning agents, and electrical methods such as polarity reversal, pulse electric field or overlimiting current regime need to be evaluated [55]. Among them, a pulse electric field can be easily implemented to MFCs using a square electric wave generator connected to the two electrodes. The application of 8 mA/cm$^2$ (10 V) pulses for 2 h, with a sequence of 2.5 s pulse and 0.5 s pause were tested during this study, but they failed in remediating the fouled CEM (50 days MFC operation with TMP wastewater, results not shown). Higher voltages and optimized sequence time could possibly help in reducing membrane fouling, but installation of an auxiliary anode electrode is suggested for applying the pulses to avoid damaging the anodic microbial community [56].

## 4. Conclusions

Similar power output and theoretical COD removals are obtained from xylose during stable operation of an up-flow MFC with graphite plate, carbon cloth and granular activated carbon in stainless steel cage anode electrodes. Carbon cloth enables the highest power density (333 mW/m$^2$). However, granular activated carbon in stainless steel cage is considered the most suitable anode electrode for bioelectrochemical treatment based on its high current density in a wide potential range, high surface area and scalability.

Long-term continuous operation with TMP wastewater results in 47% total COD removal with an average power output of 10–15 mW/m$^2$ at an HRT of 1.8 d. To our knowledge, this is the first report on bioelectrochemical treatment of TMP wastewater. Bioelectrochemical pretreatment reduces the COD load of TMP wastewater, decreasing the energy required for aeration in the aerobic treatment whilst the Coulombic efficiency remains low.

## Conflict of interest

The authors declare no conflict of interest.

## Acknowledgements

This work was supported by the Academy of Finland (New Indigo ERA-Net Energy 2014; Project no. 283013) and the Marie Skłodowska-Curie European Joint Doctorate (EJD) in Advanced Biological Waste-To-Energy Technologies (ABWET) funded from Horizon 2020 under grant agreement no. 643071. This work utilized the Tampere Microscopy Center facilities at Tampere University (Finland). We thank the anonymous reviewers for insightful suggestions that were helpful in improving the manuscript.

## Appendix A. Supplementary data

Supplementary data to this article can be found online at https://doi.org/10.1016/j.cej.2019.04.089.

## References

[1] T. Meyer, E.A. Edwards, Anaerobic digestion of pulp and paper mill wastewater and sludge, Water Res. 65 (2014) 321–349.
[2] M. Kamali, Z. Khodaparast, Review on recent developments on pulp and paper mill wastewater treatment, Ecotoxicol. Environ. Saf. 114 (2015) 326–342.
[3] J.A. Rintala, J.A. Puhakka, Anaerobic treatment in pulp- and paper-mill waste management: a review, Bioresour. Technol. 47 (1994) 1–18.
[4] W.J. Gao, M.N. Han, C.C. Xu, B.Q. Liao, Y. Hong, J. Cumin, M. Dagnew, Performance of submerged anaerobic membrane bioreactor for thermomechanical pulping wastewater treatment, J. Water Process Eng. 13 (2016) 70–78.
[5] J.A. Rintala, S.S. Lepistö, Anaerobic treatment of thermomechanical pulping whitewater at 35–70 °C, Water Res. 26 (1992) 1297–1305.
[6] P. Dessì, E. Porca, A.M. Lakaniemi, G. Collins, P.N.L. Lens, Temperature control as key factor for optimal biohydrogen production from thermomechanical pulping wastewater, Biochem. Eng. J. 137 (2018) 214–221.
[7] S.K. Butti, G. Velvizhi, M.L.K. Sulonen, J.M. Haavisto, E. Oguz Koroglu, A. Yusuf Cetinkaya, S. Singh, D. Arya, J. Annie Modestra, K. Vamsi Krishna, A. Verma, B. Ozkaya, A.-M. Lakaniemi, J.A. Puhakka, S. Venkata Mohan, Microbial electrochemical technologies with the perspective of harnessing bioenergy: maneuvering towards upscaling, Renew. Sustain. Energy Rev. 53 (2016) 462–476.
[8] B.E. Logan, K. Rabaey, Conversion of wastes into bioelectricity and chemicals by using microbial electrochemical technologies, Science 337 (2012) 686–690.
[9] B.E. Logan, B. Hamelers, R. Rozendal, U. Schröder, J. Keller, S. Freguia, P. Aelterman, W. Verstraete, K. Rabaey, Microbial fuel cells: methodology and technology, Environ. Sci. Technol. 40 (2006) 5181–5192.
[10] P. Liang, R. Duan, Y. Jiang, X. Zhang, Y. Qiu, X. Huang, One-year operation of 1000-L modularized microbial fuel cell for municipal wastewater treatment, Water Res. 141 (2018) 1–8.
[11] J. Choi, Y. Ahn, Continuous electricity generation in stacked air cathode microbial fuel cell treating domestic wastewater, J. Environ. Manage. 130 (2013) 146–152.
[12] B. Min, J.R. Kim, S.E. Oh, J.M. Regan, B.E. Logan, Electricity generation from swine wastewater using microbial fuel cells, Water Res. 39 (2005) 4961–4968.
[13] A. Callegari, D. Cecconet, D. Molognoni, A.G. Capodaglio, Sustainable processing of dairy wastewater: long-term pilot application of a bio-electrochemical system, J. Clean. Prod. 189 (2018) 563–569.
[14] R. Toczyłowska-Mamińska, K. Szymona, M. Kloch, Bioelectricity production from wood hydrothermal-treatment wastewater: enhanced power generation in MFC-fed mixed wastewaters, Sci. Total Environ. 634 (2018) 586–594.
[15] U. Abbasi, W. Jin, A. Pervez, A.Z. Bhatti, M. Tariq, S. Shaheen, A. Iqbal, Q. Mahmood, Anaerobic microbial fuel cell treating combined industrial wastewater: correlation of electricity generation with pollutants, Bioresour. Technol. 200 (2016) 1–7.
[16] C. Feng, Z. Lv, X. Yang, C. Wei, Anode modification with capacitive materials for a microbial fuel cell: an increase in transient power or stationary power, Phys. Chem. Chem. Phys. 16 (2014) 10464–10472.
[17] C. Santoro, C. Arbizzani, B. Erable, I. Ieropoulos, Microbial fuel cells: from fundamentals to applications. A review, J. Power Sour. 356 (2017) 225–244.
[18] K. Guo, D. Hidalgo, T. Tommasi, K. Rabaey, Pyrolytic carbon-coated stainless steel

felt as a high-performance anode for bioelectrochemical systems, Bioresour. Technol. 211 (2016) 664–668.
[19] J. Hou, Z. Liu, Y. Li, S. Yang, Y. Zhou, A comparative study of graphene-coated stainless steel fiber felt and carbon cloth as anodes in MFCs, Bioprocess Biosyst. Eng. 38 (2015) 881–888.
[20] S. Cheng, B.E. Logan, Ammonia treatment of carbon cloth anodes to enhance power generation of microbial fuel cells, Electrochem. Commun. 9 (2007) 492–496.
[21] X. Wang, S. Cheng, Y. Feng, M.D. Merrill, T. Saito, B.E. Logan, Use of carbon mesh anodes and the effect of different pretreatment methods on power production in microbial fuel cells, Environ. Sci. Technol. 43 (2009) 6870–6874.
[22] X.-Y. Wu, F. Tong, T.-S. Song, X.-Y. Gao, J.-J. Xie, C.C. Zhou, L.-X. Zhang, P. Wei, Effect of zeolite-coated anode on the performance of microbial fuel cells, J. Chem. Technol. Biotechnol. 90 (2015) 87–92.
[23] J. Liu, F. Zhang, W. He, X. Zhang, Y. Feng, B.E. Logan, Intermittent contact of fluidized anode particles containing exoelectrogenic biofilms for continuous power generation in microbial fuel cells, J. Power Sour. 261 (2014) 278–284.
[24] A. Deeke, T.H.J.A. Sleutels, T.F.W. Donkers, H.V.M. Hamelers, C.J.N. Buisman, A. Ter Heijne, Fluidized capacitive bioanode as a novel reactor concept for the microbial fuel cell, Environ. Sci. Technol. 49 (2015) 1929–1935.
[25] K.R. Fradler, J.R. Kim, H.C. Boghani, R.M. Dinsdale, A.J. Guwy, G.C. Premier, The effect of internal capacitance on power quality and energy efficiency in a tubular microbial fuel cell, Process Biochem. 49 (2014) 973–980.
[26] J.M. Haavisto, A.M. Lakaniemi, J.A. Puhakka, Storing of exoelectrogenic anolyte for efficient microbial fuel cell recovery, Environ. Technol. 17 (2018) 1–9.
[27] A.E. Mäkinen, M.E. Nissilä, J.A. Puhakka, Dark fermentative hydrogen production from xylose by a hot spring enrichment culture, Int. J. Hydrogen Energy 37 (2012) 12234–12240.
[28] K.J. Balkus, K.T. Ly, The preparation and characterization of an X-type zeolite: an experiment in solid-state chemistry, J. Chem. Educ. 68 (1991) 875–877.
[29] X. Wu, F. Tong, X. Yong, J. Zhou, L. Zhang, H. Jia, Effect of NaX zeolite-modified graphite felts on hexavalent chromium removal in biocathode microbial fuel cells, J. Hazard. Mater. 308 (2016) 303–311.
[30] C.H. Lay, M.E. Kokko, J.A. Puhakka, Power generation in fed-batch and continuous up-flow microbial fuel cell from synthetic wastewater, Energy 91 (2015) 235–241.
[31] APHA, Standard Methods for the Examination of Water and Wastewater, 20th ed., American Public Health Association/American Water Works Association/Water Environment Federation, Washington DC, 1998.
[32] M. Dubois, K. Gilles, J.K. Hamilton, P. Rebers, F. Smith, Colorimetric method for determination of sugars and related substances, Anal. Chem. 28 (1956) 350–356.
[33] J.M. Haavisto, M.E. Kokko, C.-H. Lay, J.A. Puhakka, Effect of hydraulic retention time on continuous electricity production from xylose in up-flow microbial fuel cell, Int. J. Hydrogen Energy 42 (2017) 27494–27501.
[34] P. Dessì, E. Porca, J. Haavisto, A.-M. Lakaniemi, G. Collins, P.N.L. Lens, Composition and role of the attached and planktonic active microbial communities in mesophilic and thermophilic xylose-fed microbial fuel cells, RSC Adv. 8 (2018) 3069–3080.
[35] A. Van Haandel, J. Van der Lubbe, Handbook of Biological Wastewater Treatment: Design and Optimisation of Activated Sludge Systems, Quist Publishing, Leidschendam, The Netherlands, 2012.
[36] X. Zhu, B.E. Logan, Copper anode corrosion affects power generation in microbial fuel cells, J. Chem. Technol. Biotechnol. 89 (2014) 471–474.
[37] E. Taskan, H. Hasar, Comprehensive comparison of a new tin-coated copper mesh and a graphite plate electrode as an anode material in microbial fuel cell, Appl. Biochem. Biotechnol. 175 (2014) 2300–2308.
[38] D. Pocaznoi, A. Calmet, L. Etcheverry, B. Erable, A. Bergel, Stainless steel is a promising electrode material for anodes of microbial fuel cells, Energy Environ. Sci. 5 (2012) 9645–9652.
[39] J. Liu, F. Zhang, W. He, W. Yang, Y. Feng, B.E. Logan, A microbial fluidized electrode electrolysis cell (MFEEC) for enhanced hydrogen production, J. Power Sour. 271 (2014) 530–533.
[40] J.N. Roy, S. Babanova, K.E. Garcia, J. Cornejo, L.K. Ista, P. Atanassov, Catalytic biofilm formation by *Shewanella oneidensis* MR-1 and anode characterization by expanded uncertainty, Electrochim. Acta 126 (2014) 3–10.
[41] X. Zhu, J.C. Tokash, Y. Hong, B.E. Logan, Controlling the occurrence of power overshoot by adapting microbial fuel cells to high anode potentials, Bioelectrochemistry 90 (2013) 30–35.
[42] C.I. Torres, A.K. Marcus, B.E. Rittmann, Proton transport inside the biofilm limits electrical current generation by anode-respiring bacteria, Biotechnol. Bioeng. 100 (2008) 872–881.
[43] H.S. Lee, P. Parameswaran, A. Kato-Marcus, C.I. Torres, B.E. Rittmann, Evaluation of energy-conversion efficiencies in microbial fuel cells (MFCs) utilizing fermentable and non-fermentable substrates, Water Res. 42 (2008) 1501–1510.
[44] X.L. Zhou, T.S. Zhao, Y.K. Zeng, L. An, L. Wei, A highly permeable and enhanced surface area carbon-cloth electrode for vanadium redox flow batteries, J. Power Sour. 329 (2016) 247–254.
[45] A. ter Heijne, H.V.M. Hamelers, M. Saakes, C.J.N. Buisman, Performance of non-porous graphite and titanium-based anodes in microbial fuel cells, Electrochim. Acta 53 (2008) 5697–5703.
[46] D. Mohan, K. Singh, Granular activated carbon, Water encyclopedia (eds. J. H. Lehr and J. Keeley), 2005.
[47] M. Miskan, M. Ismail, M. Ghasemi, J. Md Jahim, D. Nordin, M.H. Abu Bakar, Characterization of membrane biofouling and its effect on the performance of microbial fuel cell, Int. J. Hydrogen Energy 41 (2016) 543–552.
[48] L. Huang, B.E. Logan, Electricity generation and treatment of paper recycling wastewater using a microbial fuel cell, Appl. Microbiol. Biotechnol. 80 (2008) 349–355.
[49] Y. Yuan, B. Zhao, S. Zhou, S. Zhong, L. Zhuang, Electrocatalytic activity of anodic biofilm responses to pH changes in microbial fuel cells, Bioresour. Technol. 102 (2011) 6887–6891.
[50] J.R. Kim, S. Cheng, S.-E. Oh, B.E. Logan, Power generation using different cation, anion, and ultrafiltration membranes in microbial fuel cells, Environ. Sci. Technol. 41 (2007) 1004–1009.
[51] M.-J. Choi, K.-J. Chae, F.F. Ajayi, K.-Y. Kim, H.-W. Yu, C. Kim, I.S. Kim, Effects of biofouling on ion transport through cation exchange membranes and microbial fuel cell performance, Bioresour. Technol. 102 (2011) 298–303.
[52] M.T. Noori, S.C. Jain, M.M. Ghangrekar, C.K. Mukherjee, Biofouling inhibition and enhancing performance of microbial fuel cell using silver nano-particles as fungicide and cathode catalyst, Bioresour. Technol. 220 (2016) 183–189.
[53] G. Mininni, G. Laera, G. Bertanza, M. Canato, A. Sbrilli, Mass and energy balances of sludge processing in reference and upgraded wastewater treatment plants, Environ. Sci. Pollut. Res. 22 (2015) 7203–7215.
[54] S. Chen, J. Tang, L. Fu, Y. Yuan, S. Zhou, Biochar improves sediment microbial fuel cell performance in low conductivity freshwater sediment, J. Soils Sediments 16 (2016) 2326–2334.
[55] S. Mikhaylin, L. Bazinet, Fouling on ion-exchange membranes: classification, characterization and strategies of prevention and control, Adv. Colloid Interface Sci. 229 (2016) 34–56.
[56] S.E. Oh, J.R. Kim, J.H. Joo, B.E. Logan, Effects of applied voltages and dissolved oxygen on sustained power generation by microbial fuel cells, Water Sci. Technol. 60 (2009) 1311–1317.

# Effects of anode materials on electricity production from xylose and treatability of TMP wastewater in an up-flow microbial fuel cell

*Johanna Haavisto [a,#], Paolo Dessì [a, b, #,*], Pritha Chatterjee [a,c], Mari Honkanen [d], Md Tabish Noori [e], Marika Kokko [a], Aino-Maija Lakaniemi [a], Piet N. L. Lens [a, b], Jaakko A. Puhakka [a]*

## SUPPORTING INFORMATION

[a]*Tampere University, Faculty of Engineering and Natural Sciences, PO Box 541, FI-33104 Tampere University, Finland*

[b]*National University of Ireland Galway, University Road, Galway, H91 TK33, Ireland*

[c]*Indian Institute of Technology Hyderabad, Department of Civil Engineering, Hyderabad, India*

[d]*Tampere University, Tampere Microscopy Center, PO Box 692, FI-33104 Tampere University, Finland*

[e]*Kyung Hee University, Department of Environmental Science and Engineering, 446701, Seoul, South Korea*

*****Corresponding author: Phone: +353 830678774, e-mail: paolo.dessi@nuigalway.ie, mail: National University of Ireland Galway, University Road, Galway, H91 TK33, Ireland

[#] These two authors contributed equally to the manuscript

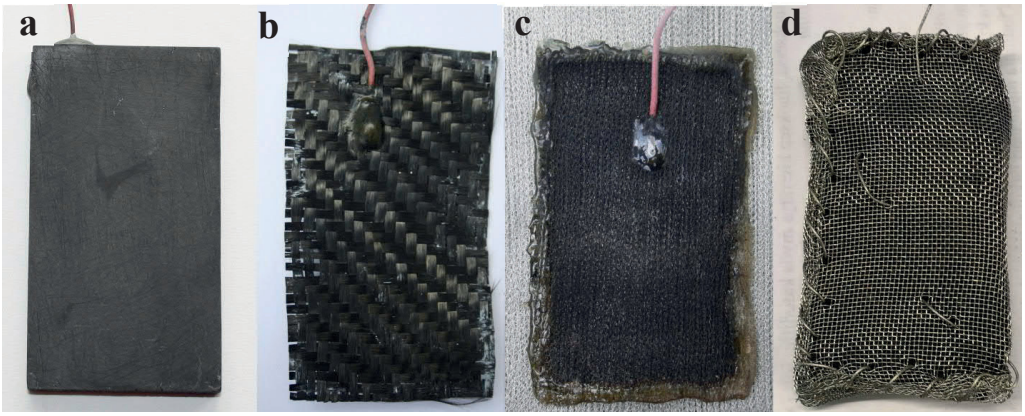


**Figure S1.** Photos of a) graphite plate, b) carbon cloth with zeolite coating and c) tin coated copper mesh after use, and d) granular activated carbon in stainless steel cage before use. The appearance of the graphite plate and carbon cloths (bare and zeolite coated) did not change during the MFC operation. The tin coated copper mesh electrode is placed over a similar unused mesh to show a clear color difference caused by copper oxidation. Copper wires were used as current collectors with all the other materials, but stainless steel cage was closed with titanium wire and the end of the wire was also used as current collector.

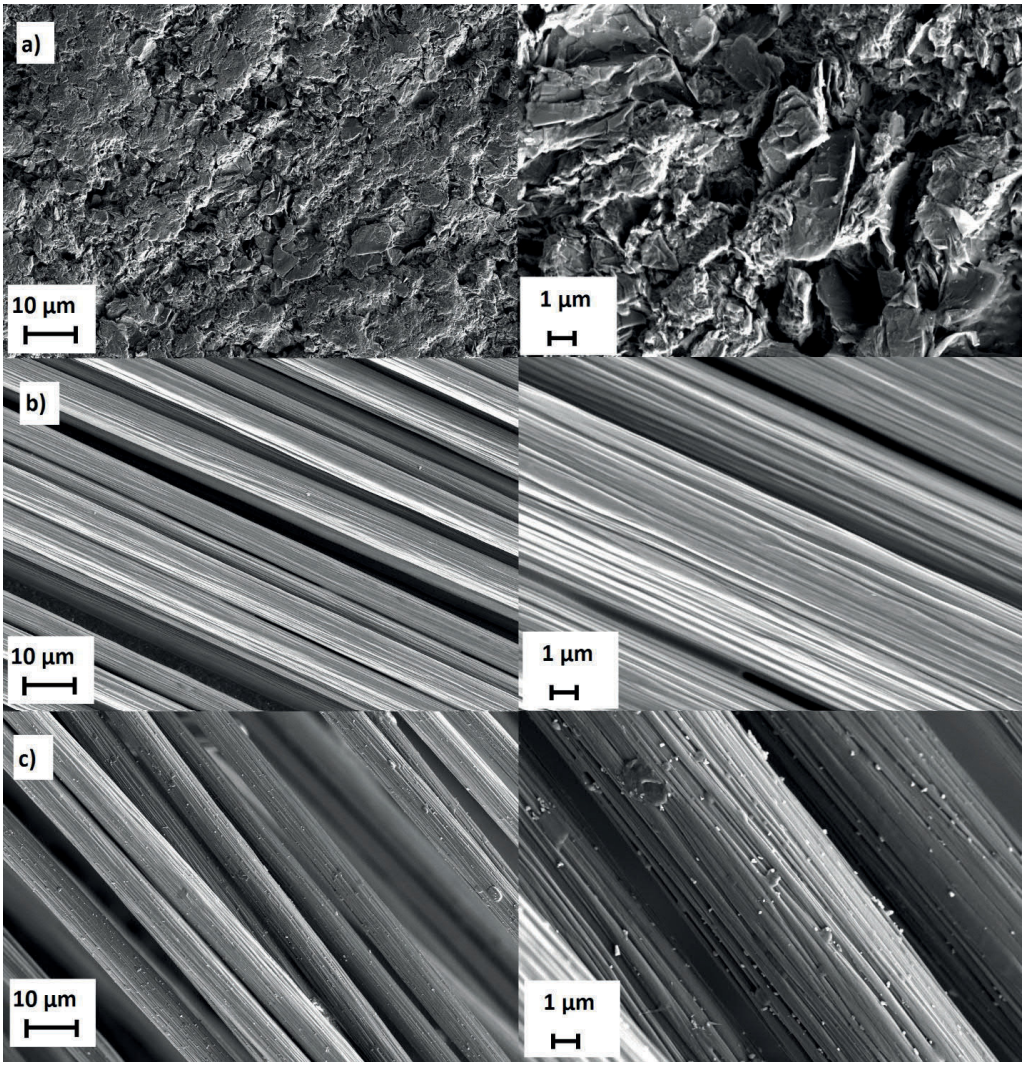
a)
10 µm
1 µm
b)
10 µm
1 µm
c)
10 µm
1 µm

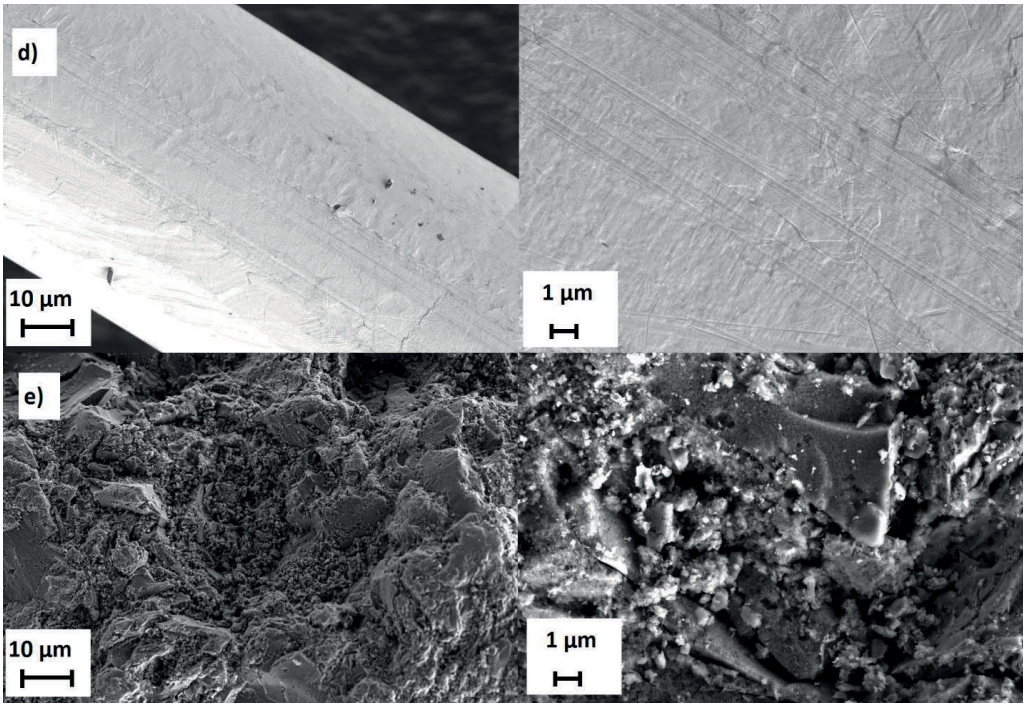


**Figure S2.** SEM images of the clean electrode materials with two different magnifications for each material. Graphite plate (a), carbon cloth (b), zeolite coated carbon cloth (c), tin coated copper (d), and granular activated carbon (e).

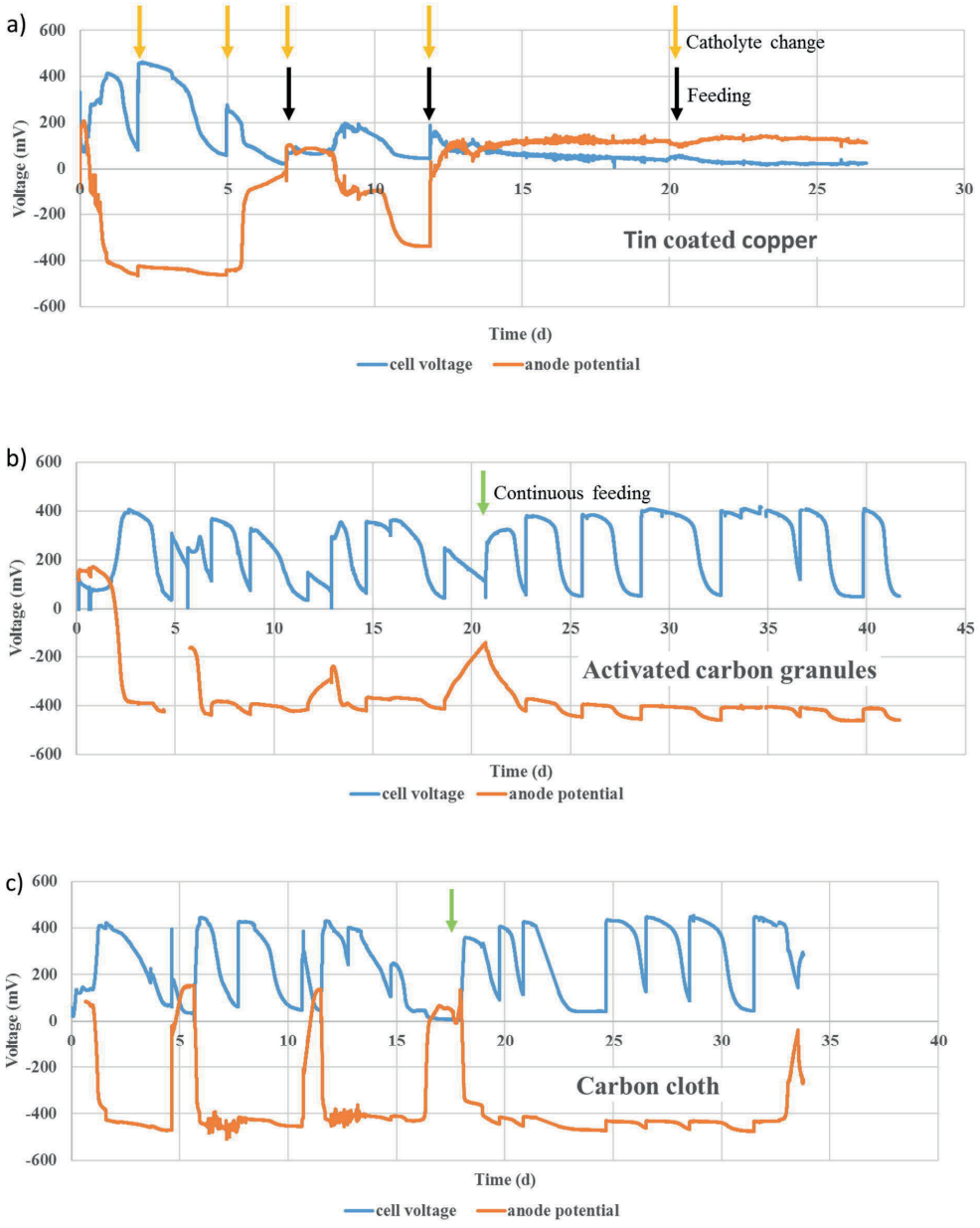
a)
Catholyte change
Feeding
Tin coated copper
Voltage (mV)
Time (d)
cell voltage
anode potential
b)
Continuous feeding
Activated carbon granules
Voltage (mV)
Time (d)
cell voltage
anode potential
c)
Carbon cloth
Voltage (mV)
Time (d)
cell voltage
anode potential

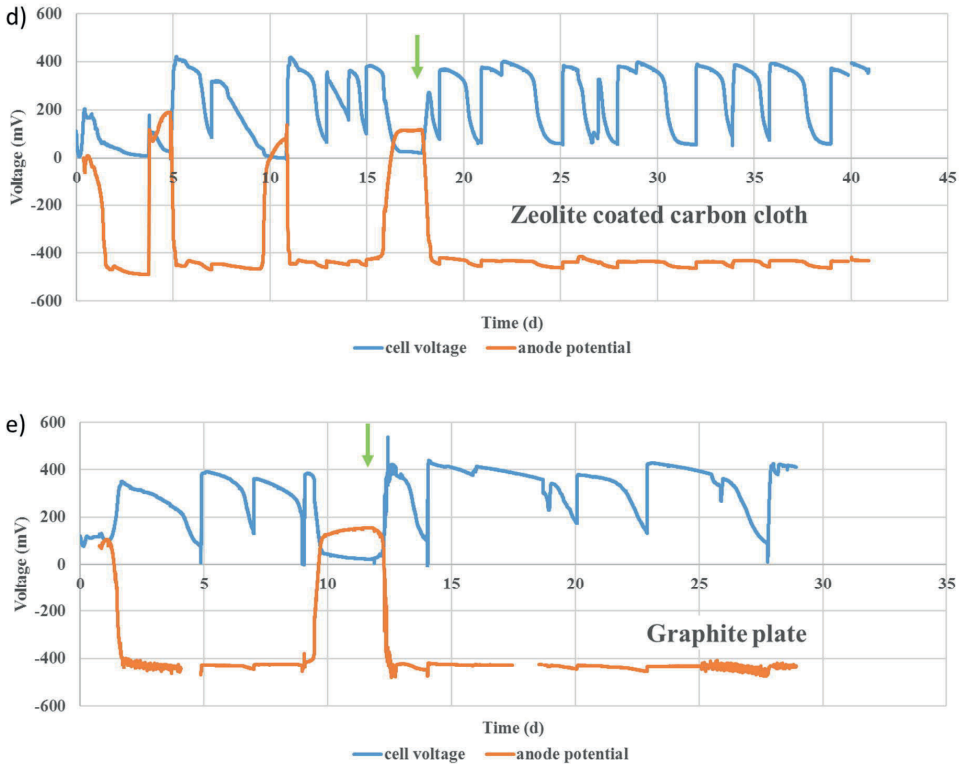


**Figure S3.** Cell voltages and anode potentials as a function of time with the different anode electrodes. The effect of feeding (black arrows) and catholyte changes (yellow arrows) are shown for a) tin coated copper as an example. For b) activated carbon granules, c) carbon cloth, d) zeolite coated carbon cloth, and e) graphite plate the green arrows show the starting point of continuous feeding.

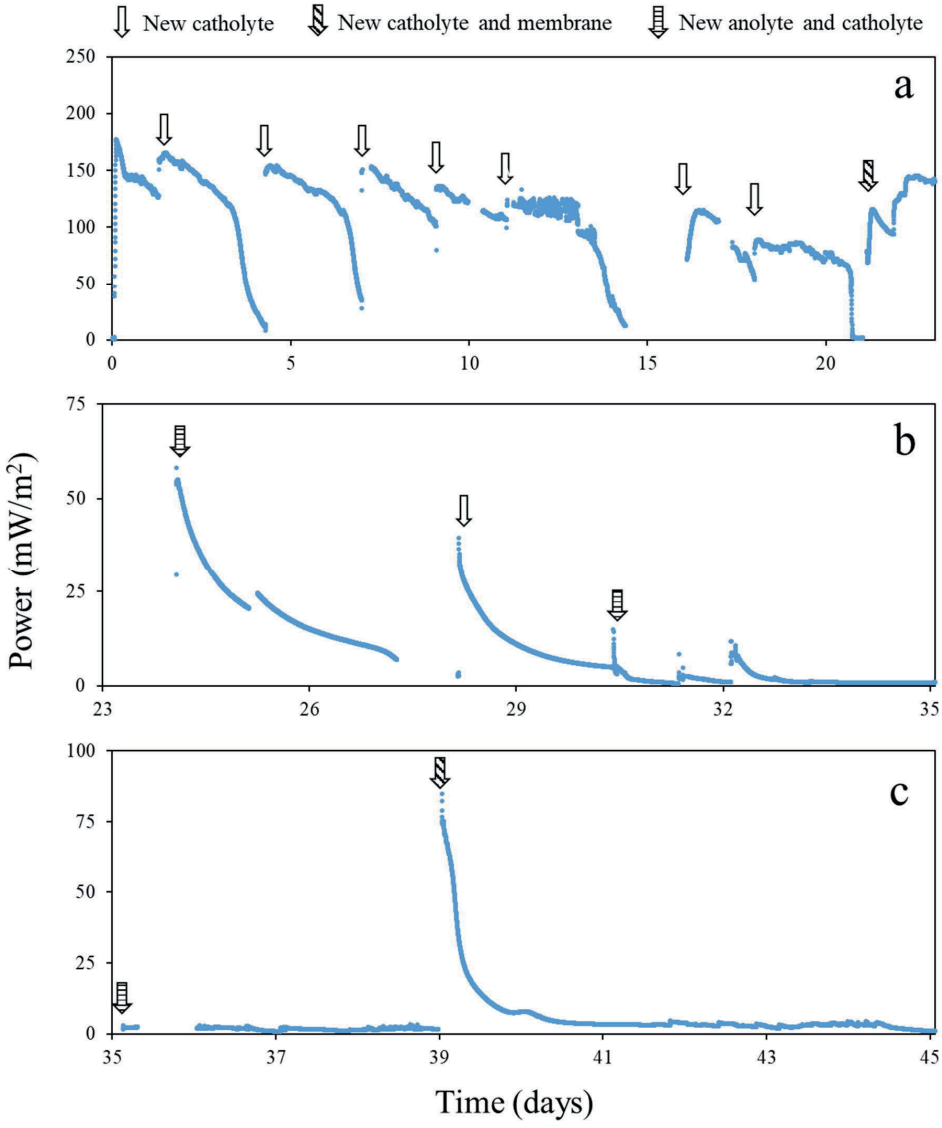


**Figure S4.** Power generated from thermomechanical pulping wastewater in the upflow MFC operated with an AEM and fed in continuous mode with xylose (a), and in semi-continuous (b) or continuous (c) mode with TMP wastewater.

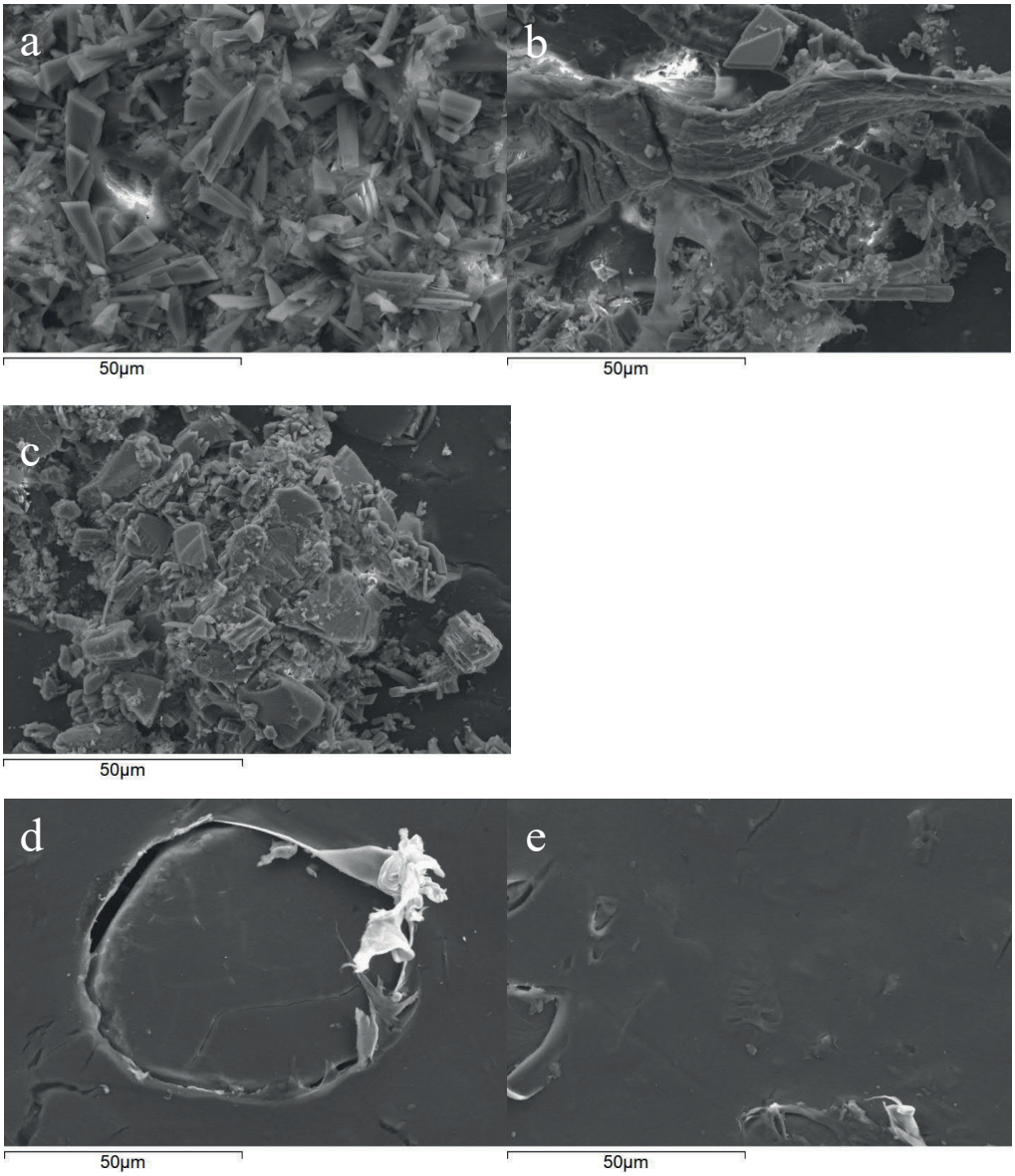


**Figure S5.** SEM images of three different points of the fouled CEM after approximately 30 days of continuous up-flow MFC operation with thermomechanical pulping wastewater (a, b, c), as well as the active site (d) and frame (e) of the fresh CEM.

**Table S1.** Criteria for electrode scalability, which were chosen to evaluate the potential of the anode electrodes for full-scale operation. Short distances between anode and cathode electrodes and high electrode conductivity are required to decrease the internal resistances and good chemical and mechanical strength are required to keep large electrodes intact during long-term operation.

| Anode electrode | Potential for using electrode material in different reactor configurations | Conductivity[a] | Chemical and mechanical strength | Overall evaluation[b] |
|---|---|---|---|---|
| **Carbon cloth** | Thin, flexible material that has been used in various MFC configurations [1–4] | ++ | Low mechanical strength due to loose weaving. Corrosion resistant [5] | ++ |
| **Graphite plate** | Thick, hard material that can be used as flat plate [6,7] | +++ | Relatively high mechanical strength although brittle [8] Corrosion resistant [5] | ++ |
| **GAC in SS cage** | Adaptable to various electrode and MFC configurations [9–11]. 3D structure that can also be fluidized [12]. | ++ for GAC +++ for SS | High mechanical strength due to the stainless steel cage. GAC: corrosion resistant [5] SS: corrosion resistant as MFC anode under anaerobic conditions [13] | +++ |

| | | | | |
|---|---|---|---|---|
| **Zeolite coated carbon cloth** | Thin, flexible material that can be used in various MFC configurations in a similar way to carbon cloth | ++ | Low mechanical strength due to loose weaving. Corrosion resistant [5] | ++ |
| **Tin coated copper** | Thin, flexible material that has been studied in simple MFC configurations [14,15] | +++ | The material was oxidized in only 3 days in this study | + |

[a] Anode material conductivities: carbon cloth 333 S/m [16]; graphite plate $3\times10^5$ S/m [17]; GAC 748 S/m [16], stainless steel and copper >$1x10^6$ S/m [17]. The lower conductivity of GAC compared to graphite plate can be compensated with close contact to SS cage or by frequent collisions to SS in fluidized bed; (>1000 S/m +++, 100-1000 S/m ++, < 100 S/m +)

[b] Overall evaluation is based on the flexibility, conductivity and chemical and mechanical strength of the electrode (all aspects satisfactory +++, at least one aspect challenging ++, at least one aspect failing +)

**Example calculation of the coulombic efficiency in the xylose-fed MFC**

Added xylose concentration in the influent:

Xylose (1.00 g/L)

Measured VFA and xylose concentrations in effluent of the MFC with graphite plate anode:

Xylose 0.017 g/L, Acetate 0.14 g/L, Propionate 0.05 g/L

Theoretical COD per unit mass of $C_xH_yO_z$ was calculated according to the following equation [18]:

$$COD_{theoretical} = \frac{8 * (4x + y - 2z)}{12x + y + 16z} g_{COD}/gC_xH_yO_z.$$

| | Theoretical COD (gCOD/g$C_xH_yO_z$) |
|---|---|
| Xylose ($C_5H_{10}O_5$) | 1.0667 |
| Acetic acid ($CH_3COOH$) | 1.0667 |
| Propionic acid ($CH_3CH_2COOH$) | 1.5135 |

With help of the previous table, the concentrations of xylose, acetate and propionate in the influent and effluent can be given as theoretical COD:

| | Concentration in influent as COD (g/L) | Concentration in effluent as COD (g/L) |
|---|---|---|
| xylose | 1.067 | 0.018 |
| acetic acid | 0 | 0.151 |
| propionic acid | 0 | 0.081 |
| Total | 1.067 | 0.250 |

Theoretical COD removal was:

$\frac{1.067 g_{COD}/L - 0.25 g_{COD}/L}{1.067 g_{COD}/L} = 77\%.$

Coulombic efficiency was calculated according to Logan et al. [19]:

$$\epsilon_C = \frac{MI}{FbqΔCOD},$$

where $M = 32$, the molecular weight of oxygen, $F$ is Faraday's constant, $b = 4$ is the number of electrons exchanged per mole of oxygen, $q$ is the volumetric influent flow rate and $\Delta COD$ is the difference in the influent and effluent COD.

The average current (I) of the MFC with graphite plate anode was 0.004156 A (0.74 A/$m^2$ as shown in Table 2).

With influent flow rate of 0.1 mL/min, the influent COD flow was

$$1.0667\ \mathrm{g_{COD}/L}\frac{0.1\ \mathrm{mL/min}}{60\frac{\mathrm{s}}{\mathrm{min}}*1000\frac{\mathrm{mL}}{\mathrm{L}}}=1.7778*10^{-6}\mathrm{g_{COD}/s}$$

and the CE was

$$\epsilon_C=\frac{MI}{FbqA\Delta COD}=\frac{32\ \mathrm{g/mol}*0.004156\mathrm{A}}{864478\mathrm{C}*4\ \mathrm{e^-/mol}*1.7778*10^{-6}\mathrm{g_{COD}/s}\ *0.77}=28\%.$$

**References**


[1] S. Hays, F. Zhang, B.E. Logan, Performance of two different types of anodes in membrane electrode assembly microbial fuel cells for power generation from domestic wastewater, J. Power Sources. 196 (2011) 8293–8300.

[2] H. Yazdi, L. Alzate-Gaviria, Z.J. Ren, Pluggable microbial fuel cell stacks for septic wastewater treatment and electricity production, Bioresour. Technol. 180 (2015) 258–263. doi:10.1016/j.biortech.2014.12.100.

[3] H. Liu, S. Cheng, L. Huang, B.E. Logan, Scale-up of membrane-free single-chamber microbial fuel cells, J. Power Sources. 179 (2008) 274–279.

[4] S.-H. Chang, B.-Y. Huang, T.-H. Wan, J.-Z. Chen, B.-Y. Chen, Surface modification of carbon cloth anodes for microbial fuel cells using atmospheric-pressure plasma jet processed reduced graphene oxides, RSC Adv. 7 (2017) 56433–56439.

[5] C. Santoro, C. Arbizzani, B. Erable, I. Ieropoulos, Microbial fuel cells: From fundamentals to applications. A review, J. Power Sources. 356 (2017) 225–244.

[6] J.M. Haavisto, M.E. Kokko, C.-H. Lay, J.A. Puhakka, Effect of hydraulic retention time on continuous electricity production from xylose in up-flow microbial fuel cell, Int. J. Hydrogen

Energy. 42 (2017) 27494–27501.

[7] A. Dewan, H. Beyenal, Z. Lewandowski, Scaling up microbial fuel cells, Environ. Sci. Technol. 42 (2008) 7643–7648.

[8] L.G. Borzani Manhani, L.C. Pardini, F.L. Neto, Assessement of tensile strength of graphites by the Iosipescu Coupon test, Mater. Res. 10 (2007) 233–239.

[9] D. Jiang, B. Li, Granular activated carbon single-chamber microbial fuel cells (GAC-SCMFCs): A design suitable for large-scale wastewater treatment processes, Biochem. Eng. J. 47 (2009) 31–37.

[10] S. Wu, H. Li, X. Zhou, P. Liang, X. Zhang, Y. Jiang, X. Huang, A novel pilot-scale stacked microbial fuel cell for efficient electricity generation and wastewater treatment, Water Res. 98 (2016) 396–403.

[11] D. Jiang, M. Curtis, E. Troop, K. Scheible, J. McGrath, B. Hu, S. Suib, D. Raymond, B. Li, A pilot-scale study on utilizing multi-anode/cathode microbial fuel cells (MAC MFCs) to enhance the power production in wastewater treatment, Int. J. Hydrogen Energy. 36 (2011) 876–884.

[12] A. Deeke, T.H.J.A. Sleutels, T.F.W. Donkers, H.V.M. Hamelers, C.J.N. Buisman, A. Ter Heijne, Fluidized capacitive bioanode as a novel reactor concept for the microbial fuel cell, Environ. Sci. Technol. 49 (2015) 1929–1935.

[13] E. Guerrini, P. Cristiani, M. Grattieri, C. Santoro, B. Li, S. Trasatti, Electrochemical behavior of stainless steel anodes in membraneless microbial fuel cells, J. Electrochem. Soc. 161 (2014) H62–H67.

[14] E. Taskan, H. Hasar, Comprehensive comparison of a new tin-coated copper mesh and a graphite plate electrode as an anode material in microbial fuel cell, Appl. Biochem. Biotechnol. 175 (2014) 2300–2308.

[15] E. Taskan, B. Ozkaya, H. Hasar, Comprehensive evaluation of two different inoculums in MFC

with a new tin-coated copper mesh anode electrode for producing electricity from a cottonseed oil industry effluent, Environ. Prog. Sustain. Energy. 35 (2016) 110–116.

[16] U. Karra, S.S. Manickam, J.R. McCutcheon, N. Patel, B. Li, Power generation and organics removal from wastewater using activated carbon nanofiber (ACNF) microbial fuel cells (MFCs), Int. J. Hydrogen Energy. 38 (2013) 1588–1597.

[17] M. Helmenstine, Table of Electrical Resistivity and Conductivity, Https://Www.Thoughtco.Com/Table-of-Electrical-Resistivity-Conductivity-608499. (2019) 1–4.

[18] Van Haandel, A., Van der Lubbe, J., 2012. Handbook of biological wastewater treatment: Design and Optimisation of Activated Sludge Systems. Quist Publishing, Leidschendam, The Netherlands.

[19] Logan, B.E., Hamelers, B., Rozendal, R., Schröder, U., Keller, J., Freguia, S., Aelterman, P., Verstraete, W., Rabaey, K., 2006. Microbial fuel cells: Methodology and technology. Environ. Sci. Technol. 40, 5181–5192.

# PUBLICATION IV

**Effect of hydraulic retention time on continuous electricity production from xylose in up-flow microbial fuel cell**

Haavisto, J.M., Kokko, M.E. Lay, C-H. & Puhakka, J.A.

International Journal of Hydrogen Energy 42:27494-27501
https://doi.org/10.1016/j.ijhydene.2017.05.068

INTERNATIONAL JOURNAL OF HYDROGEN ENERGY 42 (2017) 27494–27501

Available online at www.sciencedirect.com

ScienceDirect

journal homepage: www.elsevier.com/locate/he

# Effect of hydraulic retention time on continuous electricity production from xylose in up-flow microbial fuel cell

*Johanna M. Haavisto* [a,*], *Marika E. Kokko* [a], *Chyi-How Lay* [b,c], *Jaakko A. Puhakka* [a]

[a] *Laboratory of Chemistry and Bioengineering, Tampere University of Technology, Tampere, Finland*
[b] *Green Energy Development Center, Feng Chia University, Taichung, Taiwan, ROC*
[c] *Master's Program of Green Energy Science and Technology, Feng Chia University, Taiwan, ROC*

ARTICLE INFO

*Article history:*
Received 10 February 2017
Received in revised form
9 May 2017
Accepted 10 May 2017
Available online 30 May 2017

*Keywords:*
Microbial fuel cell
Xylose
Continuous operation
Up-flow
Hydraulic retention time
Microbial community

ABSTRACT

Aerobic wastewater management is energy intensive and thus anaerobic processes are of interest. In this study, a microbial fuel cell was used to produce electricity from xylose which is an important constituent of lignocellulosic waste. Hydraulic retention time (HRT) was optimized for the maximum power density by gradually decreasing the HRT from 3.5 d to 0.17 d. The highest power density (430 mW/m$^2$) was obtained at 1 d HRT. Coulombic efficiency decreased from 30% to 0.6% with HRTs of 3.5 d and 0.17 d, respectively. Microbial community analysis revealed that anode biofilm contained known exoelectrogens, including *Geobacter* sp. and fermentative organisms were present in both anolyte and the anode biofilm. The peak power densities were obtained at 1–1.7 d HRTs and xylose degraded almost completely even with the lowest HRT of 0.17 d, which demonstrates the efficiency of up-flow MFC for treating synthetic wastewater containing xylose.



## Introduction

Sustainability in wastewater management requires energy and performance efficiencies. The energy-rich compounds in wastewater should be converted to useful energy. One possibility to recover energy from wastewaters is production of electricity using microbial fuel cells (MFCs) [1,2]. In MFCs, microorganisms oxidize wastewater constituents and convert their chemical energy into electricity with simultaneous wastewater purification [3].

In Finnish paper, cardboard and pulp mills, in 2013, approximately 500 Mm$^3$ of wastewater was produced [4] containing cellulose and hemicellulose. Glucuronoxylans with xylose as the most abundant monomer, are hemicellulose that

*Abbreviations:* CE, Coulombic efficiency (%); COD, chemical oxygen demand; DGGE, denaturing gradient gel electrophoresis; HRT, hydraulic retention time (d); MFC, microbial fuel cell; OLR, organic loading rate (g/L/d); PCR, polymerase chain reaction; SL, sequence length; UV, ultraviolet; VFA, volatile fatty acid.

* *Corresponding author*. Laboratory of Chemistry and Bioengineering, Tampere University of Technology, P.O. Box 541, FI-33101 Tampere, Finland.
E-mail address: johanna.haavisto@tut.fi (J.M. Haavisto).

http://dx.doi.org/10.1016/j.ijhydene.2017.05.068
0360-3199/

is present in high concentrations especially in hardwood [5]. The occurrence of hemicellulose and thus xylose in forest industry wastewaters decreases the cost-effectiveness of the treatment process if xylose is not degraded [6]. For example, a yeast *Saccharomyces cerevisiae* cannot utilize xylose for bioethanol production without gene modification [7]. However, it has been reported that in MFCs xylose can be anaerobically converted to electricity [8–11].

Continuous treatment is a prerequisite for efficient and low-cost wastewater treatment. Only a few studies have reported continuous electricity production from xylose [8,10]. In continuous operation, organic loading rate (OLR) has a remarkable effect on electricity production [12] and the OLR is controlled by the HRT used. By now, several different reactor configurations have been tested for simultaneous electricity production and wastewater treatment, from which up-flow reactors are easily scalable and have comparatively low space requirements and thus have potential for future applications [12–16]. Up-flow reactors can be operated with high OLRs [17], i.e. low HRTs, and to treat wastewaters containing compounds, such as phenol [18]. Recently, granular activated carbon (GAC) has been reported at the MFC anodes to increase the surface area and performance of anodes as well as their wastewater treatment efficiency [19,20]. GAC can be combined with up-flow reactors, i.e. fluidized bed reactors [21], which further highlights the importance of up-flow configuration for bioelectrochemical systems in the future [20]. To make MFCs economically feasible for wastewater treatment, the treatment time should be close to the conventional processes. This makes HRT an important operational parameter [22].

This study examined the effects of HRT and organic loading rate on the ability of an up-flow MFC to convert xylose to electricity by further optimizing the operation parameters reported by Lay et al. [10]. The COD removal efficiencies and microbial communities at the anolytes were determined for each tested HRT. In addition, the microbial community of the biofilm was characterized in the end of the experiment.

## Materials and methods

### MFC construction and operation

The up-flow MFC used was similar to the one used by Lay et al. [10]. Anode and cathode chambers (working volumes 500 mL and 250 mL, respectively) of dual-chambered up-flow MFC (Fig. 1) were separated with an anion exchange membrane (Ø 4.5 cm, AMI-7001, Membranes International Inc., USA). The membrane was changed on days 23, 78, 117, 132, and 159 due to membrane fouling. Flat plate graphite electrodes at the anode and cathode (0.00385 $m^2$, McMaster-Carr, Aurora, OH) and 100 Ω external resistance were used [10]. A reference electrode (Ag/AgCl in 3 M KCl solution, −205 mV vs. standard hydrogen electrode (SHE), SENTEK QM710X) was attached to the anode recirculation tubing on day 15 through a glass capillary (QiS, the Netherlands). Anolyte temperature was maintained at 37 °C with heating coils around the anode chamber. Temperature was measured from the circulated anolyte which had a flow rate of 60 mL/min [10]. Medium was prepared as described by Mäkinen et al. [23] without addition of EDTA, yeast extract, and resazurin. Xylose (0.5 g/L) was used as substrate and pH of the medium was adjusted to 7.0 with NaOH before feeding. During continuous operation, influent container was kept in a cool box (approximately 9 °C) to minimize microbial growth outside the reactor. The catholyte was potassium ferricyanide (50 mM $K_3Fe(CN)_6$) in phosphate buffer (100 mM $Na_2HPO_4$, pH 7.0). Catholyte was circulated after day 83 through a container (500 mL) with a minimum flow rate of 0.2 mL/min. MFC was started as fed-batch where 0.5 $g/L_{anode\ chamber\ volume}$ xylose was added with an interval of 4–7 days. Continuous operation was started on day 43 with 3.5 d HRT, and HRT was gradually decreased to 0.17 d. Inoculum [10] was originally enriched from a compost culture.

### Analyses

#### Electrochemical measurements and calculations

Cell voltage and anode potential were measured at 2 min intervals with an Agilent 34970A data Acquisition/Switch Unit (Agilent, Canada). The current was calculated from cell voltage ($U$) and external resistance ($R$) with ohm's law. Current and power densities were calculated against the projected area of the anode electrode (0.00385 $m^2$) or the volume of the anode chamber ($0.5 \times 10^{-3}$ $m^3$).

Performance analyses were performed at the end of each HRT by measuring cell voltage and anode potential after 30 min of stabilization with different external resistances (1000 Ω, 499 Ω, 240 Ω, 100 Ω, 10 Ω) and at open circuit mode. Power density and polarization curves were drawn from performance analyses results. Internal resistances were further estimated from the slopes of polarization curves according to Ref. [24].

Coulombic efficiency (CE) was calculated at each HRT using the measured cell voltage and the added influent xylose concentration over the periods with stable cell performance according to Equation (1)

$$C_E = \frac{M_s \int_{t_1}^{t_2} \frac{U}{R} dt}{F b_{es} \frac{t_b v_a}{HRT} c}, \quad (1)$$

where $M_s$ = molecular weight of xylose (g/mol), $t_2 - t_1$ = time period of the measurement (d), $F$ = Faraday's constant (96,485 C/mol * e), $b_{es}$ = number of the electrons released per mol of xylose ($20e^-$), $v_a$ = working volume of anode chamber (L), HRT = hydraulic retention time (d) and $c$ = xylose concentration (g/L).

#### Sampling and chemical analysis

Xylose concentration, pH, and volatile fatty acids (VFAs) and alcohols were analyzed 3 times a week. During batch mode operation, samples were taken from sample port a (Fig. 1) before substrate was added. During continuous operation, samples were taken from sample port b (Fig. 1) and from effluent and influent. Samples for VFA, ethanol and xylose analysis were filtered through 0.2 or 0.45 μm PET filter. WTW pH 330 meter was used for measuring pH.

Xylose concentration was measured with phenol-sulfuric acid method [25] using customized sample and reagent volumes (1 mL sample, 0.5 mL 5% phenol solution, and 2.5 mL

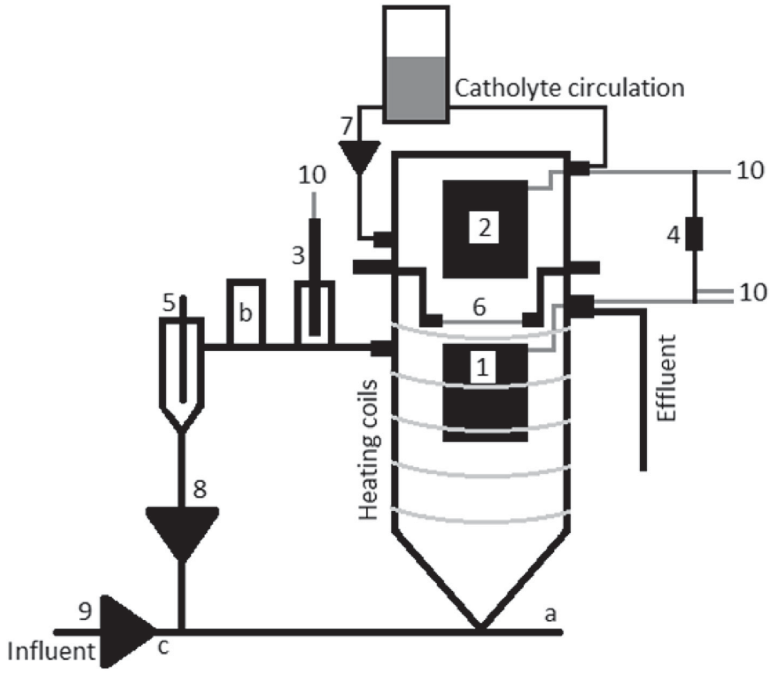


**Fig. 1 – Diagram of MFC construction. 1) Anode electrode, 2) Cathode electrode, 3) Reference electrode, 4) External resistance, 5) Temperature sensor, 6) Anion exchange membrane, 7) to 9) Peristaltic pumps, 10) Electrical wires connected to data logger, a) to c) Sampling ports.**

sulfuric acid) and measuring the absorbance at 485 nm with UV–visible spectrophotometer (Shimadzu UV-1601). VFAs and alcohols were measured with a gas chromatograph (Shimadzu Ordior GC-2010 plus) equipped with ZB-WAXplus column (Phenomenex, USA) and flame ionization detector (FID). The oven temperature was held at 40 °C for 2 min, increased 20 °C/min to 160 °C, and 40 °C/min to 220 °C, where the temperature was held for 2 min. Temperature of injector and detector was 250 °C. The flow of helium (carrier gas) was 30 mL/min. Internal standards were crotonic acid (100 mg/L) and 1-propanol (60 μL/L), and 0.06 M oxalic acid solution was used to acidify the samples.

COD removal was calculated by converting the analysed effluent VFAs and xylose concentrations to COD equivalents according to van Haandel and van der Lubbe [26].

*Microbial community analyses*

Microbial community samples were obtained from the anodic solution at each HRT at stabilized conditions and from the anode biofilm in the end of the experiment. The biofilm sample was removed from the anode electrode by sonicating 5 min in 0.9% NaCl solution, followed by further separation of biomass with a centrifuge (5000 × g, 10 min). DNA was extracted from defrosted pellets with PowerSoil DNA isolation kit (MO BIO Laboratories, Inc., Carlsbad, CA, USA). PCR was used to amplify partial 16S rRNA genes as described by Koskinen et al. [27] using GC-BacV3f [28] and 907r [29] primers. DGGE was performed as described by Lakaniemi et al. [30]. Separated DNA sequences were reamplified according to Koskinen et al. [27] before sequencing at Macrogen Inc. (Seoul, Korea). BioEdit software and BLAST (http://blast.ncbi.nlm.nih.gov/Blast.cgi) were used for analyzing sequence data.

## Results and discussion

*Electricity generation*

Electricity production with the studied up-flow microbial fuel cell was mainly affected by the changes in HRT. The effects of other variables, such as fast reduction of catholyte and changes in internal resistance caused by membrane fouling, were minimized by circulating the catholyte and by changing the membrane periodically, respectively (Fig. A2). During reactor operation, cell voltage increased from 344 mV to the highest value of 408 mV when HRT was decreased from 3.5 d to 1 d. Decreasing HRT to 0.75 d and further to 0.17 d decreased the cell voltage remarkably to 218 mV and 156 mV, respectively (Fig. A2). Similar trend was observed in performance analysis (Fig. 2), which was done at the end of each HRT.

The highest current density of 2460 mA/m$^2$ and the highest voltages with all tested external resistances (10–1000 Ω) were obtained with HRT of 1 d (Fig. 2A). At HRTs above 1 d the current densities and voltages were lower than at HRT of 1 d. The OLR at HRTs above 1 d was below 0.4 g COD/L/d, which may not have provided enough substrate for the

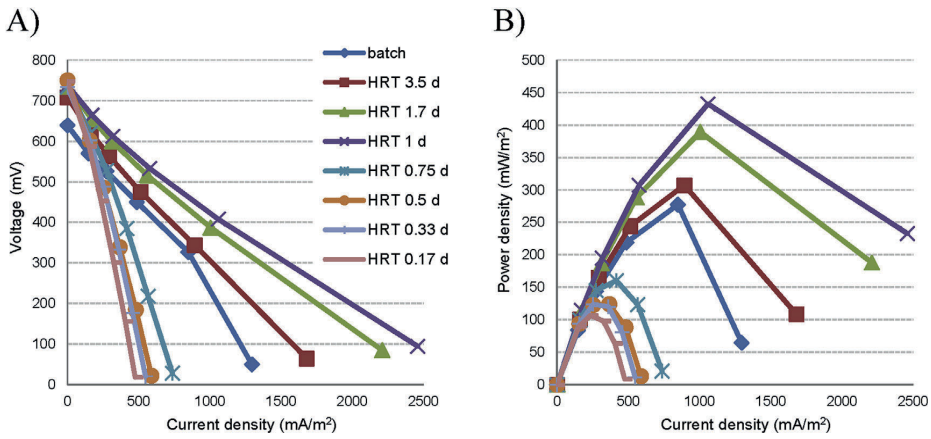


**Fig. 2 – A) Cell voltage and B) power density as a function of current density in the up-flow microbial fuel cell operated with different HRTs.**

microorganisms to sustain higher voltages [8]. Also decreasing HRT below 1 d decreased the current densities, cell voltages (Fig. 2A) and CEs and increased VFA concentrations (Chapter 3.2), which indicates that at lower HRTs the biofilm could not utilize xylose for current production as efficiently as at higher HRTs. Increasing mass transfer or diffusion limitations likely affected the decreasing performance of the cell [31,32].

Internal resistances of the cell were smaller in batch mode (90 Ω) and at HRTs between 1 and 3.5 d (70–90 Ω) and increased remarkably when HRT was decreased below 1 d (270–450 Ω). Ieropoulos et al. [31] and Lee and Oa [17] also found the increase in internal resistance with higher influent flow rates. On reason for this can be insufficient substrate transfer to biofilm and proton transfer into cathode chamber [17] (mass transfer and diffusion limitations), which could be prevented by improving the anode electrode geometry [33] and reactor design. Ieropoulos et al. [31] also suggested that the increase in internal resistance is partly due to the increased microbial growth on anode electrode at lower HRTs resulting in diffusion limitations or due to the changes in microbial community that may have caused mass transfer limitations with higher flow rates. At each HRT of this study, the time reserved for stabilization was at least 10 times the HRT. These periods were long enough for causing changes in biofilm thickness and increasing internal resistance. Although the highest current densities were measured with 1 d HRT, anode potential reached the most negative stable values (with 100 Ω resistance) of −455 ± 2 mV vs. Ag/AgCl with the smallest HRTs of 0.17–0.5 d compared to −416 mV vs. Ag/AgCl at HRT of 1 d (Table 1). This indicates that the performance of the anodic biofilm did not deteriorate with decreasing HRTs. However, at smaller HRTs the high internal resistances decreased power densities.

The internal resistance of the cell was high (70 Ω, Fig. 2) also with the optimal HRT of 1 d indicating that the reactor configuration requires improvements. This could be done, for example, by decreasing the distance between the electrodes [13] and improving the membrane operation, e.g. by increasing the area of the membrane. For example, Sevda et al. [34] reported that the hindered ion flow through a separator between anode and cathode compartments caused more resistance with smaller HRTs in their reactor.

According to the power density curves (Fig. 2B), 1 and 1.7 d HRTs resulted in the highest power densities and 1 d HRT gave 11% higher values than 1.7 d HRT. On the other hand, during the stable operation (Fig. 3, Fig. A2) 1.7 d HRT gave 26% higher power densities than 1 d HRT. When taking into account the variations in cell voltage (Fig. A2) caused by the fast reduction of catholyte, xylose consumption in the feeding tank, and membrane fouling, the cell performance at HRTs 1 and 1.7 d was comparable. Thus, both 1 d and 1.7 d are near the optimal HRT for the studied up-flow MFC in relation to the electricity production from synthetic wastewater containing xylose (Fig. 3). These are in the same range with the HRTs of the existing activated sludge wastewater treatment plants in pulp and paper mill [35].

The peak power density obtained at 1 d HRT is significantly higher than 8.4 ± 0.4 mW/m$^2$ reported by Huang et al. (Table 1) with xylose. They suggested that low power densities were due to non-optimal cultivation conditions. Huang and Logan [8] measured 1093 ± 43 mW/m$^2$ (against projected surface of cathode electrode) for continuous process fed with xylose (3 g/L). This value was 150% higher than the maximum power density in our study, but their estimated anode electrode surface was approximately 300 times higher than the cathode electrode area resulting in unreliable comparison.

CEs (calculated from the stable operational period, Fig. A2) decreased with HRT during the whole experiment (Table 1). The highest CE of 30% measured with 3.5 d HRT was remarkably higher than reported by Lay et al. ([10] in Table 1) in the same reactor configuration as used in this study. Furthermore, power density with 3.5 d HRT measured in this experiment was three times higher compared to the results of Lay et al. [10] with the same HRT. One reason for the better CE and power density in this experiment can be the longer acclimation time, which helps bacteria to adapt to the operational conditions. Also regular membrane changes due to membrane fouling might have improved the results of this

**Table 1 – Maximum power densities and Coulombic efficiencies measured in this study and reported in literature. Maximum power density is normalized to anode electrode area unless otherwise stated.**

| Reactor | Xylose feeding concentration | Max. power density (mW/m$^2$) | CE (%) | Reference |
|---|---|---|---|---|
| Air cathode MFC | 3 g/L (fed-batch) in 100 mM PBS | 673 ± 43[a] | n.g. | [8] |
| Air cathode MFC | 3 g/L (fed-batch) in 200 mM PBS | 944 ± 32[a] | n.g. | [8] |
| Air cathode MFC | 3 g/L (continuous); 0.83 d HRT | 1093 ± 43[a] | 41 | [8] |
| Up-flow; two-chamber | 0.5 g/L (fed-batch) | 107 | 21.3 ± 1.0 | [11] |
| Up-flow; two-chamber | 0.5 g/L (continuous); 3.5 d HRT | 72 | 12.7 ± 0.6 | [11] |
| Up-flow; two-chamber | 0.5 g/L (continuous); 1 d HRT | 430 | 9.2 | This study |
| Two-chamber system | 0.08 g/L (fed-batch) | 2.6 ± 0.2 | 41 ± 1.6 | [31] |
| Two-chamber system with stirring | 1.5 g/L (fed-batch) | 8.4 ± 0.4 | 36 ± 1.2 | [31] |

n.g. = not given.
[a] Normalized to cathode electrode area.

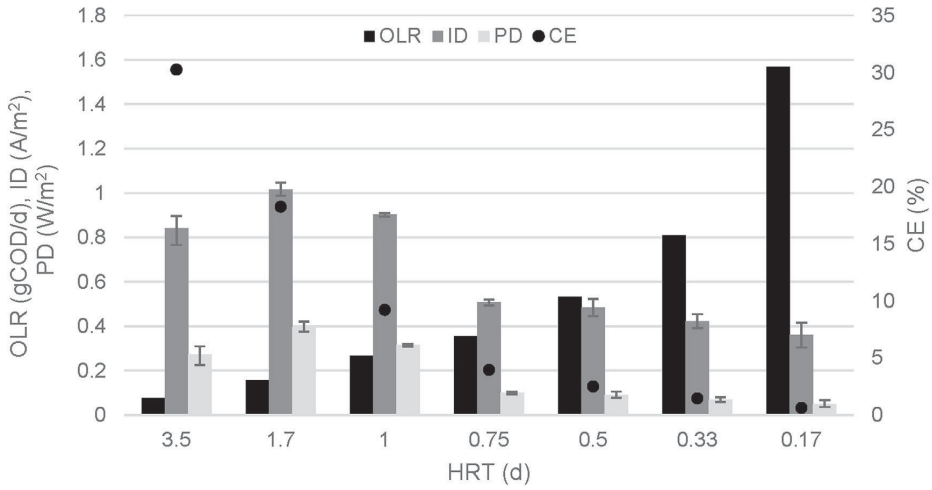


**Fig. 3 – Organic loading rate (OLR, gCOD/d), average current density (ID, mA/m$^2$), power density (PD, mW/m$^2$) and Coulombic efficiency (CE, %) as a function of hydraulic retention time (HRT, d) in up-flow microbial fuel cell. The error bars show the minimum and maximum values in stable conditions.**

experiment, since they decreased the internal resistance. For example, with 1 d HRT, membrane change improved the cell voltage by 17% (measured one day after the membrane change). Later with smaller HRTs the differences were even higher (Fig. A2) indicating that smaller HRT increased membrane fouling. Huang and Logan [8] were able to transform 13–40% of the chemical energy of the removed xylose (initial concentration 20 mM = 3.0 g/L) into electricity with HRTs of 10–38 h. They used graphite fiber brushes as anodes which enabled a larger surface area and lower internal resistance (2–3.4 Ω) than used in this study. Thus, decreasing the internal resistance in the reactor configuration of this study will likely increase CE and power densities.

The purpose of this study was to examine the effects of different HRTs to the performance of the anode. To further optimize the economical feasibility of the process, different anode electrode materials and structures should be tested. Also reactor configuration optimization is needed for more efficient electricity production. Potassium ferricyanide is a very good electron acceptor for studying reactions at anode chamber. For practical application, however, this has to be replaced with an inexpensive and environmental friendly choice, such as efficient cathode based on $O_2$ reduction.

### *Metabolic activity in up-flow MFC*

On average, 99% of the xylose was removed at the anode during the continuous reactor operation. The xylose removal was very efficient even with the lowest HRT of 0.17 d compared to the other MFC studies with continuous xylose feeding. For example, in the studies of Huang and Logan [8] 51–96% of xylose was degraded with HRTs of 5–38 h. However, the influent xylose concentration was lower in our study, which might have affected removal efficiency.

The COD removal calculated from the effluent VFAs and xylose concentrations varied between 57 and 95% due to remaining VFAs in effluent (Table 2). Propionate remained below 0.5 mM during the reactor run, while the acetate increased with decreasing HRT (2.9 ± 0.6 mM at 0.75 d HRT). With lower HRTs than 0.75 d, the acetate concentrations

**Table 2 – Stable anode potentials with different HRTs and electron balance of the added xylose divided to CE and acetate, propionate and xylose measured from the effluent. Detection limit for VFAs was 0.5 mM. CE was calculated for the stable conditions (S1), but concentrations of VFAs and xylose in effluent were calculated over the whole operation period at each HRT. COD removal was calculated based on the effluent composition.**

| HRT | Anode potential (mV vs. Ag/AgCl) | CE (%) | Acetate (%) | Propionate (%) | Xylose (%) | Calculated COD removal (%) |
|---|---|---|---|---|---|---|
| 3.5 | −410 | 30.3 | <6 | <10 | 3.1 ± 2.6 | 95 |
| 1.7 | −383 | 18.2 | 8.3 ± 6.6 | 8.6 ± 5.2 | <2 | 82 |
| 1 | −417 | 9.2 | 21.7 ± 10.1 | 9.4 ± 3.5 | <2 | 69 |
| 0.75 | −444 | 3.9 | 35.1 ± 7.6 | 7.0 ± 2.4 | <2 | 57 |
| 0.5 | −455 | 2.5 | 30.2 ± 10.5 | <10 | <2 | 68 |
| 0.33 | −455 | 1.5 | 22.5 ± 3.1 | n.d. | <2 | 77 |
| 0.17 | −455 | 0.6 | 21.6 ± 8.5 | n.d. | <2 | 78 |

n.d. = not detected.

decreased with HRT. The VFA concentrations fluctuated as indicated by high standard deviations in Table 2.

During batch mode operation, the pH in the reactor decreased to 5.5, at which point it was increased with NaOH to 7.0. During continuous operation, the pH values remained between 6.7 and 7.1 in the reactor and 6.8–7.4 in the effluent.

### *Microbial community analysis*

Decreasing HRT will likely wash out some of the bacteria not attached to the biofilm [36]. Thus, the changes in anolyte microbial community were monitored during the experiment. DGGE was used for community profiling although it was realized that it is a semi-quantitative method at best. However, it enables the detection of main bacterial species present at the anolyte. The anolyte microbial communities changed slightly during the experiments. The intensity of the bands on the DGGE gel [27,37] changed at different HRTs indicating that the share of *Christensenella minuta* increased remarkably after the HRT decreased to 0.5 d (Fig. A1, Table 3). *C. minuta* is a xylose fermenting bacterium [38] and its share likely increased due to increased xylose loading rates at lower HRTs and was related to decreasing power densities and CEs. Fermentative bacteria, being able to degrade xylose, have a role also in electricity production by offering acetate, propionate and butyrate as fermentation end products for exoelectrogenic bacteria [11,39]. However, high substrate concentration increases the growth of fermenting bacteria, thus decreasing power density by overtaking the anolyte and anode electrode biofilm [40]. The share of a nitrate reducing bacterium [41], *Petrobacter* sp., decreased with HRT. With HRTs of 0.17–0.5 d and the most negative anode potentials, the strongest bands belonged to *C. minuta*, *Citrobacter freundii*, *Clostridium indolis*, and *Proteiniphilum acetatigenes*. All of these bacteria are fermenting, but *P. acetatigenes* cannot ferment D-xylose [38,42,43]. *C. indolis* is a sulfate reducer [44] and *C. freundii* is an exoelectrogenic organism [45]. *C. indolis* has also been found from a biofilm sample of a MFC [37].

The reactor was stopped due to a malfunction in temperature controller, which increased the temperature in the reactor causing heat shock. The microbial community of anode biofilm was characterized after this temperature increase, which possibly affected the results. *Geobacter* sp. was identified from biofilm sample as was also an uncultured *spirochete*, *P. acetatigenes* and *Wolinella succinogenes*. *Geobacter* sp. is a well-known exoelectrogenic organism, but also the

**Table 3 – Identified bands on DGGE gel. SL = sequence length of the sample, Sim (%) = similarity (%), Affiliation (acc) = closest species in database and its accession number, and Origin of the sample = Origin of the sample with the closest match.**

| Band label | SL | Sim (%) | Affiliation (acc) | Class/family | Origin of the sample |
|---|---|---|---|---|---|
| 1 | 454–481 | 99.7–100 | *Proteiniphilum acetatigenes* (HQ710548.1) | Bacteroidia/*Porphyromonadaceae* | Crude oil contaminated soil |
| 2 | 421 | 99.5 | *Wolinella succinogenes* (NR_025942.1) | Epsilonproteobacteria/ *Helicobacteraceae* | Rumen |
| 3 | 271–444 | 97.0–99.7 | *Clostridium indolis* (KF611981.1) | Clostridia/*Lachnospiraceae* | Pit mud |
| 4 | 460–538 | 100 | *Geobacter* sp. (KF006333.1) | Deltaproteobacteria/*Geobacteraceae* | MFC, inoculated with wastewater |
| 5 | 461 | 99.3 | *Christensenella minuta* (AB490809.1) | Clostridia/*Christensenellaceae* | Isolated from human faeces |
| 6 | 437 | 99.7 | *Clostridium oroticum* (AB818947.1) | Clostridia/*Lachnospiraceae* | Mud |
| 7 | 262 | 100 | *Enterobacter* sp. (KF934473.1) | Gammaproteobacteria/ *Enterobacteriaceae* | Sediment samples from Prydz Bay and sea area |
| 8 | 437–482 | 100 | *Citrobacter freundii* (AB680434.1) | Gammaproteobacteria/ *Enterobacteriaceae* | Unknown |
| 9 | 475 | 99.5–100 | *Petrobacter* sp. (HM059764.1) | Betaproteobacteria/ *Hydrogenophilaceae* | Aerobic enrichment of biodegraded oil sample |
| 10 | 416 | 100 | Uncultured *spirochete* (JF736651.1) | Spirochaetia/unknown | MFC, inoculated with activated sludge |

uncultured *spirochete* and fermenting *P. acetatigenes* have been found from biofilm of MFC reactors [46–48]. Cord-Ruwisch et al. [49] found syntrophic cooperation between *W. succinogenes* and *Geobacter* where *W. succinogenes* kept hydrogen partial pressure low, thus helping *Geobacter* to ferment acetate. The increase in effluent acetate concentration with 0.17–1 d HRTs indicates that acetate oxidation to electricity was the process limiting factor. This was possibly due to liquid flow bypass and the following diffusion and mass transfer limitations between anode biofilm and anolyte flow, which could be improved with more sophisticated anode electrode design.

Fermentative xylose degraders were present in the anolyte and the biofilm contained a known exoelectrogen, *Geobacter* sp. Thus, syntrophic interaction between fermenting and electricity producing bacteria likely took place. *P. acetatigenes*, *W. succinogenes*, *Petrobacter* sp., uncultured *spirochete*, and *C. freundii* were also present in the anolyte of the reactor from which the inoculum was obtained for this study [10].

## Conclusions

HRT affected xylose conversion to electricity in up-flow microbial fuel cells as follows: 1) The highest power densities were achieved with 1 d and 1.7 d HRTs, while CE decreased with the HRT from 30% to 0.6%; 2) Xylose was almost completely removed with all HRTs, but due to incomplete acetate oxidation at lower HRTs COD removal remained at 59–95% (70% with 1 d HRT); 3) Microbial communities of anolyte and biofilm contained fermentative bacteria and known electricity producers, respectively. This demonstrates synergistic interaction between xylose fermenting bacteria and exoelectrogens in the biofilm. However, the increasing share of fermentative bacteria with HRTs below 0.75 d likely decreased power density by increasing the internal resistance.

## Acknowledgment

The Academy of Finland (New Indigo ERA-Net Energy 2014; Project no. 283013) is gratefully acknowledged for financial support. We would like to thank Dr. Aino-Maija Lakaniemi for assistance during the writing process.

## Appendix A. Supplementary data

Supplementary data related to this article can be found at http://dx.doi.org/10.1016/j.ijhydene.2017.05.068.

## REFERENCES

[1] Kokko M, Mäkinen AE, Puhakka JA. Anaerobes in bioelectrochemical systems. Adv Biochem Eng Biotechnol 2016;156:263–92.
[2] Butti SK, Velvizhi G, Sulonen M, Haavisto J, Köroğlu E, Çetinkaya A, et al. Microbial electrochemical technologies with the perspective of harnessing bioenergy: maneuvering towards upscaling. Renew Sustain Energy Rev 2016;53:462–76.
[3] Logan BE. Simultaneous wastewater treatment and biological electricity generation. Water Sci Technol 2005;52(1–2):31–7.
[4] Finnish Forest Industry Federation. Statistics [WWW]. 2014. Available at: http://www.forestindustries.fi/ [accessed 16.6.15].
[5] Willför S, Sundberg A, Pranovich A, Holmbom B. Polysaccharides in some industrially important hardwood species. Wood Sci Technol 2005;39(8):601–17.
[6] Groves S, Liu J, Shonnard D, Bagley S. Evaluation of hardboard manufacturing process wastewater as a feedstream for ethanol production. J Ind Microbiol Biotechnol 2013;40(7):671–7.
[7] Wei N, Xu H, Kim S, Jin Y-S. Deletion of FPS1, encoding aquaglyceroporin Fps1p, improves xylose fermentation by engineered *Saccharomyces cerevisiae*. Appl Environ Microbiol 2013;79(10):3193–201.
[8] Huang L, Logan BE. Electricity production from xylose in fed-batch and continuous-flow microbial fuel cells. Appl Microbiol Biotechnol 2008;80(4):655–64.
[9] Mäkinen AE, Lay C-H, Nissilä ME, Puhakka JA. Bioelectricity production on xylose with a compost enrichment culture. Int J Hydrogen Energy 2013;38(35):15606–12.
[10] Lay C-H, Kokko ME, Puhakka JA. Power generation in fed-batch and continuous up-flow microbial fuel cell from synthetic wastewater. Energy 2015;91:235–41.
[11] Huang L, Zeng R, Angelidaki J. Electricity production from xylose using a mediator-less microbial fuel cell. Bioresour Technol 2008;99(10):4178–84.
[12] Hashemi J, Samimi A. Steady state electric power generation in up-flow microbial fuel cell using the estimated time span method for bacteria growth domestic wastewater. Biomass Bioenergy 2012;45:65–76.
[13] He Z, Minteer SD, Angenent LT. Electricity generation from artificial wastewater using an upflow microbial fuel cell. Environ Sci Technol 2005;39(14):5262–7.
[14] He Z, Wagner N, Minteer S, Angenent L. An upflow microbial fuel cell with an interior cathode: assessment of the internal resistance by impedance spectroscopy. Environ Sci Technol 2006;40(17):5212–7.
[15] Zhao L, Song T. Simultaneous carbon and nitrogen removal using a litre-scale upflow microbial fuel cell. Water Sci Technol 2014;69(2):293–7.
[16] Salar-García MJ, Ortiz-Martínez VM, Baicha Z, de los Ríos AP, Hernández-Fernández FJ. Scaled-up continuous up-flow microbial fuel cell based on novel embedded ionic liquid-type membrane-cathode assembly. Energy 2016;101:113–20.
[17] Lee Y, Oa SW. High speed municipal sewage treatment in microbial fuel cell integrated with anaerobic membrane filtration system. Water Sci Technol 2014;69(12):2548–53.
[18] Jayashree C, Sweta S, Arulazhagan P, Yeom P, Iqbal M, Banu J. Electricity generation from retting wastewater consisting of recalcitrant compounds using continuous upflow microbial fuel cell. Biotechnol Bioprocess Eng 2015;20(4):753–9.
[19] Jiang D, Li B. Granular activated carbon single-chamber microbial fuel cells (GAC-SCMFCs): a design suitable for large scale wastewater treatment processes. Biochem Eng J 2009;47:31–7.
[20] Jiang D, Curtis M, Troop E, Scheible K, McGrath J, Hu B, et al. A pilot-scale study on utilizing multi-anode/cathode microbial fuel cells (MAC MFCs) to enhance the power production in wastewater treatment. Int J Hydrogen Energy 2011;36:876–84.
[21] Li J, Ge Z, He Z. A fluidized bed membrane bioelectrochemical reactor for energy-efficient wastewater treatment. Bioresour Technol 2014;167:310–5.

[22] Kim K-Y, Yang W, Logan B. Impact of electrode configurations on retention time and domestic wastewater treatment efficiency using microbial fuel cells. Water Res 2015;88:41–6.
[23] Mäkinen AE, Nissilä ME, Puhakka JA. Dark fermentative hydrogen production from xylose by a hot spring enrichment culture. Int J Hydrogen Energy 2012;37(17):12234–40.
[24] Logan BE, Hamelers B, Rozendal R, Schröder U, Keller J, Freguia S, et al. Microbial fuel cells: methodology and technology. Environ Sci Technol 2006;40(17):5181–92.
[25] Dubois M, Gilles KA, Hamilton JK, Rebers PA, Smith F. Colorimetric method for determination of sugars and related substances. Anal Chem 1956;28(3):350–6.
[26] van Haandel A, van der Lubbe J. Handbook biological wastewater treatment. Design and optimization of activated sludge systems. Leidschendam: Quist Publishing; 2007.
[27] Koskinen PEP, Kaksonen AH, Puhakka JA. The relationship between the instability of $H_2$ production and compositions of bacterial communities within a dark fermentation fluidized-bed bioreactor. Biotechnol Bioeng 2007;97(4):742–58.
[28] Muyzer G, de Waal EC, Uitterlinden AG. Profiling complex microbial populations by denaturing gradient gel electrophoresis analysis of polymerase chain reaction-amplified genes coding for 16S rRNA. Appl Environ Microbiol 1993;59(3):695–700.
[29] Muyzer G, Hottenträger S, Teske A, Waver C. Denaturing gradient gel electrophoresis of PCR-amplified 16S rRNA – a new molecular approach to analyse the genetic diversity of mixed microbial communities. In: Akkermans ADL, van Elsas JD, de Bruijn F, editors. Molecular microbial ecology manual. Dordrecht: Kluwer; 1996. p. 1–23.
[30] Lakaniemi A-M, Hulatt CJ, Thomas DN, Tuovinen OH, Puhakka JA. Biogenic hydrogen and methane production from *Chlorella vulgaris* and *Dunaliella tertiolecta* biomass. Biotechnol Biofuels 2011;4:34.
[31] Ieropoulos I, Winfield J, Greenman J. Effects of flow-rate, inoculum and time on the internal resistance of microbial fuel cells. Bioresour Technol 2010;101:3520–5.
[32] Shen L, Ma J, Song P, Lu Z, Yin Y, Liu Y, et al. Anodic concentration loss and impedance characteristics in rotating disk electrode microbial fuel cells. Bioprocess Biosyst Eng 2016;39(10):1627–34.
[33] Kim J, Boghani H, Amini N, Aguey-Zinsou K-F, Michie I, Dinsdale R, et al. Porous anodes with helical flow pathways in bioelectrochemical systems: the effect of fluid dynamics and operating regimes. J Power Sources 2012;213:382–90.
[34] Sevda S, Chayambuka K, Sreekrishnan TR, Pant D, Dominguez-Benetton X. A comprehensive impedance journey to continuous microbial fuel cells. Bioelectrochemistry 2015;106:159–66.
[35] Kostamo A, Holmbom B, Kukkonen J. Fate of wood extractives in wastewater treatment plants at kraft pulp mills and mechanical pulp mills. Water Res 2004;38:972–82.
[36] Requeiro L, Lema J, Carballa M. Key microbial communities steering the functioning of anaerobic digesters during hydraulic and organic overloading shocks. Bioresour Technol 2015;197:208–16.
[37] Beecroft NJ, Zhao F, Varcoe JR, Slade RCT, Thumser AE, Avignone-Rossa C. Dynamic changes in the microbial community composition in microbial fuel cells fed with sucrose. Appl Microbiol Biotechnol 2012;93(1):423–37.
[38] Morotomi M, Nagai F, Watanabe Y. Description of *Christensenella minuta* gen. nov., sp. nov., isolated from human faeces, which forms a distinct branch in the order *Clostridiales*, and proposal of *Christensenellaceae* fam. nov. Int J Syst Evol Microbiol 2012;62:144–9.
[39] Lin C-Y, Cheng C-H. Fermentative hydrogen production from xylose using anaerobic mixed microflora. Int J Hydrogen Energy 2006;31(7):832–40.
[40] Wei L, Yan Z, Cui M, Han H, Shen J. Study on electricity-generation characteristic of two-chambered microbial fuel cell in continuous flow mode. Int J Hydrogen Energy 2012;37(1):1067–73.
[41] Salinas MB, Fardeau M-L, Cayol J-L, Casalot L, Patel B, Thomas P, et al. *Petrobacter succinatimandens* gen. nov., sp. nov., a moderately thermophilic, nitrate-reducing bacterium isolated from an Australian oil well. Int J Syst Evol Microbiol 2004;54:645–9.
[42] Chen S, Dong X. *Proteiniphilum acetatigenes* gen. nov., sp. nov., from a UASB reactor treating brewery wastewater. Int J Syst Evol Microbiol 2005;55:2257–61.
[43] Keevil CW, Hough JS, Cole JA. Prototrophic growth of *Citrobacter freundii* and the biochemical basis for its apparent growth requirements in aerated media. J Gen Microbiol 1977;98:273–6.
[44] Biddle A, Leschine S, Huntemann M, Han J, Chen A, Kyrpides N, et al. The complete genome sequence of *Clostridium indolis* DSM 755 T. Stand Genomic Sci 2014;9:1089–104.
[45] Huang L, Zhu N, Cao Y, Peng Y, Wu P, Dong W. Exoelectrogenic bacterium phylogenetically related to *Citrobacter freundii*, isolated from anodic biofilm of a microbial fuel cell. Appl Biochem Biotechnol 2015;175(4):1879–91.
[46] Sun D, Wang A, Cheng S, Yates M, Logan B. *Geobacter anodireducens* sp. nov., an exoelectrogenic microbe in bioelectrochemical systems. Int J Syst Evol Microbiol 2014;64:3485–91.
[47] Sun Y, Wei J, Liang P, Huang X. Electricity generation and microbial community changes in microbial fuel cells packed with different anodic materials. Bioresour Technol 2011;102(23):10886–91.
[48] Wang S, Huang L, Gan L, Quan X, Li N, Chen G, et al. Combined effects of enrichment procedure and non-fermentable or fermentable co-substrate on performance and bacterial community for pentachlorophenol degradation in microbial fuel cells. Bioresour Technol 2012;120:120–6.
[49] Cord-Ruwisch R, Lovley D, Schink B. Growth of *Geobacter sulfurreducens* with acetate in syntrophic cooperation with hydrogen-oxidizing anaerobic partners. Appl Environ Microbiol 1998;64(6):2232–6.

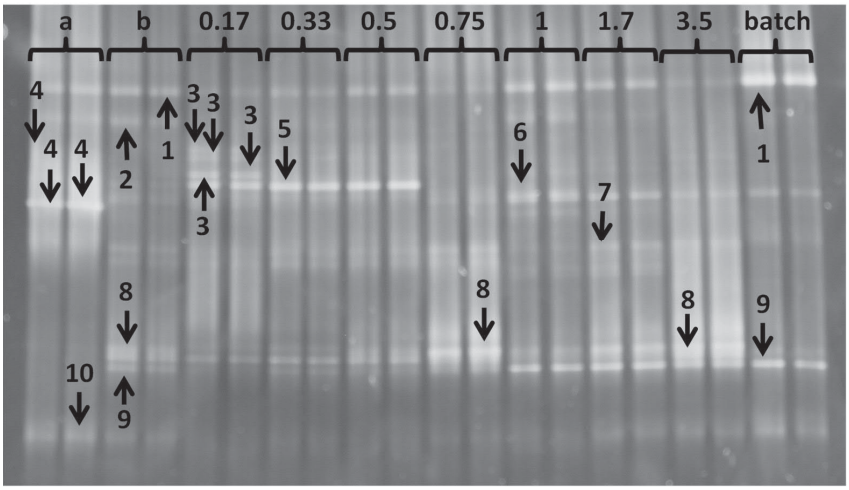


**Figure A1.** DGGE gel with band labels. Sample a was taken from the anode biofilm in the end of the experiment and the others are microbial community samples taken from the anolyte at each HRT (from 3.5 to 0.17 d) and during fed-batch feeding (batch). Sample b was taken from the anolyte 1 d after the heat shock (with 0.17 d HRT). Anolyte samples b and 0.17-3.5 were taken from port b, and sample batch from port a.

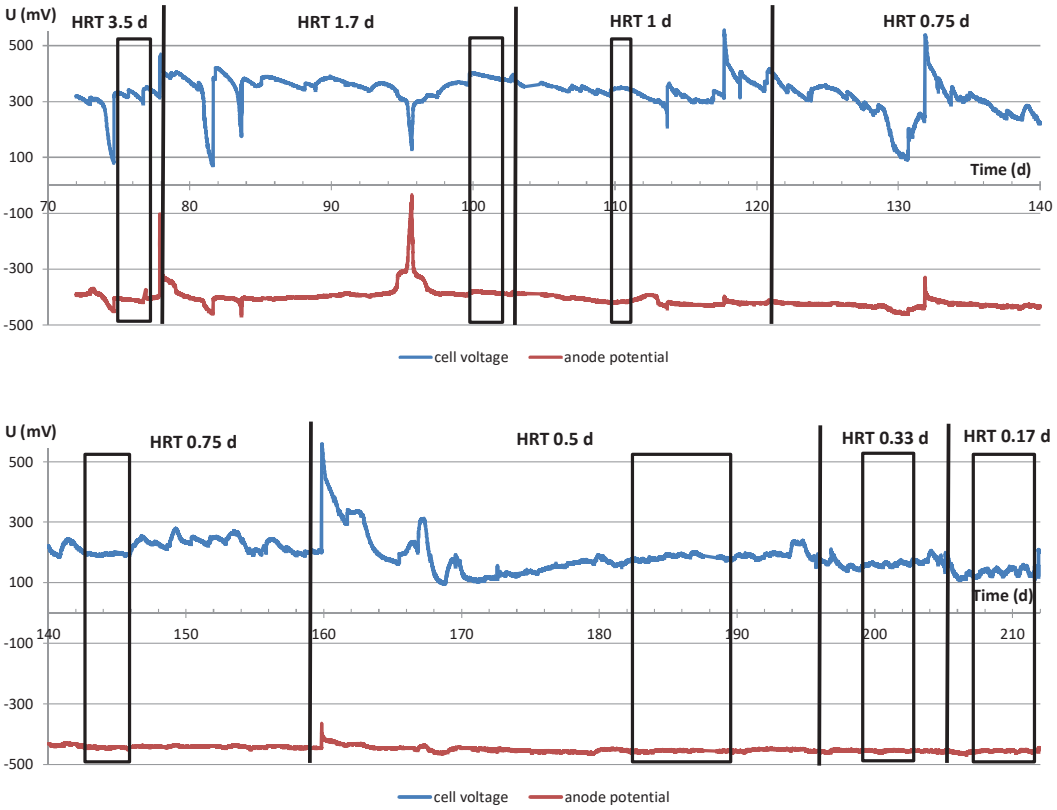


**Figure A2.** Cell voltage and anode potential between days 72 and 212. Changes in HRT are shown in the figure. Time frames used for CE calculations are shown with boxes. Catholyte circulation was started on day 83 which enabled more stable cell voltage. Membrane was changed on days 78, 117, 132, and 160. On day 95, influent tube was clogged and on day 130 gas accumulation under the membrane disturbed the performance. Disturbances in influent flow occurred between days 160 and 170.